

AD-A252 061



WATER QUALITY
RESEARCH PROGRAM

2

TECHNICAL REPORT W-92-1



US Army Corps
of Engineers

MODELING WATER QUALITY OF RESERVOIR TAILWATERS

by

Mark S. Dortch, Dorothy H. Tillman, Barry W. Bunch

Environmental Laboratory

DEPARTMENT OF THE ARMY

Waterways Experiment Station, Corps of Engineers
3909 Halls Ferry Road, Vicksburg, Mississippi 39180-6199



DTIC
ELECTE
JUN 25 1992
S B D



May 1992

Final Report

Approved For Public Release; Distribution Is Unlimited

92-16438



92 6 22 064

Prepared for DEPARTMENT OF THE ARMY
US Army Corps of Engineers
Washington, DC 20314-1000

Under WQRP Work Unit 32368



**Destroy this report when no longer needed. Do not return
it to the originator.**

**The findings in this report are not to be construed as an official
Department of the Army position unless so designated
by other authorized documents.**

**The contents of this report are not to be used for
advertising, publication, or promotional purposes.
Citation of trade names does not constitute an
official endorsement or approval of the use of
such commercial products.**

REPORT DOCUMENTATION PAGE

Form Approved
OMB No. 0704-0188

Public reporting burden for this collection of information is estimated to average 1 hour per response, including the time for reviewing instructions, searching existing data sources, gathering and maintaining the data needed, and completing and reviewing the collection of information. Send comments regarding this burden estimate or any other aspect of this collection of information, including suggestions for reducing this burden, to Washington Headquarters Services, Directorate for Information Operations and Reports, 1215 Jefferson Davis Highway, Suite 1204, Arlington, VA 22202-4302, and to the Office of Management and Budget, Paperwork Reduction Project (0704-0188), Washington, DC 20503.

1. AGENCY USE ONLY (Leave blank)		2. REPORT DATE May 1992	3. REPORT TYPE AND DATES COVERED Final report	
4. TITLE AND SUBTITLE Modeling Water Quality of Reservoir Tailwaters			5. FUNDING NUMBERS WU 32368	
6. AUTHOR(S) Mark S. Dortch, Dorothy H. Tillman, Barry W. Bunch				
7. PERFORMING ORGANIZATION NAME(S) AND ADDRESS(ES) USAE Waterways Experiment Station Environmental Laboratory 3909 Halls Ferry Road, Vicksburg, MS 39180-6199			8. PERFORMING ORGANIZATION REPORT NUMBER Technical Report W-92-1	
9. SPONSORING/MONITORING AGENCY NAME(S) AND ADDRESS(ES) US Army Corps of Engineers, Washington, DC 20314-1000			10. SPONSORING/MONITORING AGENCY REPORT NUMBER	
11. SUPPLEMENTARY NOTES Available from National Technical Information Service, 5285 Port Royal Road, Springfield, VA 22161				
12a. DISTRIBUTION/AVAILABILITY STATEMENT Approved for public release; distribution is unlimited.			12b. DISTRIBUTION CODE	
13. ABSTRACT (Maximum 200 words) Results from field studies of water quality downstream of reservoirs are analyzed to obtain an improved understanding of the mechanisms and chemical transformations occurring in reservoir tailwaters. The research focuses on the poor water quality (e.g., low dissolved oxygen and increased concentrations of reduced substances, such as iron, manganese, and sulfide) associated with deep, anoxic releases from hydropower and nonhydropower dams. In some cases, the analyses confirmed kinetic models that describe the change in constituent concentration with time and resulted in relationships to estimate kinetic rate coefficients. Results were used to develop a model of tailwater quality, and the model was validated with data from the field studies. A description of the model and a model user guide are also included.				
14. SUBJECT TERMS Kinetics Modeling Reduced substances			15. NUMBER OF PAGES 145	
			16. PRICE CODE	
17. SECURITY CLASSIFICATION OF REPORT UNCLASSIFIED		18. SECURITY CLASSIFICATION OF THIS PAGE UNCLASSIFIED	19. SECURITY CLASSIFICATION OF ABSTRACT	
20. LIMITATION OF ABSTRACT				

PREFACE

The work reported herein was conducted as part of the Water Quality Research Program (WQRP), Work Unit 32368. The WQRP is sponsored by the Headquarters, US Army Corps of Engineers (HQUSACE), and is assigned to the US Army Engineer Waterways Experiment Station (WES) under the purview of the Environmental Laboratory (EL). Funding was provided under Department of the Army Appropriation No. 96X3121, General Investigation. The WQRP is managed under the Environmental Resources Research and Assistance Programs (ERRAP), Mr. J. L. Decell, Manager. Mr. Robert C. Gunkel was Assistant Manager, ERRAP, for the WQRP. Technical Monitors during this study were Messrs. Pete Juhle and James Gottesman and Dr. John Bushman, HQUSACE.

Principal Investigators for the study were Dr. Mark S. Dortch and Ms. Dorothy H. Tillman of the Water Quality Modeling Group (WQMG), Ecosystem Research and Simulation Division (ERSD), EL. This report was prepared by Dr. Dortch, Ms. Tillman, and Dr. Barry Bunch of the WQMG under the direct supervision of Dr. Dortch, Chief, WQMG, and under the general supervision of Mr. Donald L. Robey, Chief, ERSD, and Dr. John Harrison, Director, EL. The report was reviewed by Mr. Tom Cole of WQMG; Drs. Robert Kennedy and James Brannon of the Aquatic Processes and Effects Group, ERSD; and Dr. Joe Nix, Department of Chemistry, Ouachita Baptist University, Arkadelphia, AR.

At the time of publication of this report, Director of WES was Dr. Robert W. Whalin. Commander and Deputy Director was COL Leonard G. Hassell, EN.

This report should be cited as follows:

Dortch, Mark S., Tillman, Dorothy H., and Bunch, Barry W. 1992. "Modeling Water Quality of Reservoir Tailwaters," Technical Report W-92-1, US Army Engineer Waterways Experiment Station, Vicksburg, MS.



Accession For	
NTIS GRA&I	<input checked="" type="checkbox"/>
DTIC TAB	<input type="checkbox"/>
Unannounced	<input type="checkbox"/>
Justification	
By _____	
Distribution/	
Availability Codes	
Dist	Avail and/or Special
A-1	

CONTENTS

	<u>Page</u>
PREFACE	1
CONVERSION FACTORS, NON-SI TO SI (METRIC) UNITS OF MEASUREMENT . .	3
PART I: INTRODUCTION	4
Background	4
Objectives	4
Approach	5
PART II: DESCRIPTIONS OF TAILWATER QUALITY PROCESSES	8
Model Basis	8
Manganese	9
Iron	11
Sulfide	13
Other Water Quality Constituents	16
PART III: DATA ANALYSES	22
Reduced Manganese Removal	22
Reduced Iron Removal	31
Sulfide Removal	34
Nitrification	35
PART IV: NUMERICAL MODEL	38
Description	38
Application	51
PART V: CONCLUSIONS AND RECOMMENDATIONS	68
REFERENCES	71
APPENDIX A: 1989 NIMROD TAILWATER DATA	A1
APPENDIX B: MODEL OPERATION	B1
APPENDIX C: KINETIC RATE REGRESSIONS	C1
APPENDIX D: NOTATION	D1

CONVERSION FACTORS, NON-SI TO SI (METRIC)
UNITS OF MEASUREMENT

Non-SI units of measurement used in this report can be converted to SI
(metric) units as follows:

<u>Multiply</u>	<u>By</u>	<u>To Obtain</u>
cubic feet	0.02831685	cubic meters
feet	0.3048	meters
miles (US statute)	1.609347	kilometers

PREDICTING WATER QUALITY OF
RESERVOIR TAILWATERS

PART I: INTRODUCTION

Background

1. Thermal stratification in reservoirs is often accompanied by depletion of dissolved oxygen (DO) in the bottom waters (hypolimnion). Oxygen depletion and the establishment of reducing conditions in the hypolimnion increase mobilization from the sediments of dissolved nutrients (i.e., ammonium and inorganic phosphorus), sulfide, reduced metals (e.g., iron and manganese), and organic substances (i.e., simple organic acids and methane). These substances can accumulate in the hypolimnion, thus impacting in-pool and release water quality. Reservoir releases that are low in DO and high in reduced substances can threaten aquatic life, cause water treatment problems for downstream water supply, and can be obnoxious to downstream recreational users.

2. When water is released to the downstream environment, stream reaeration occurs and reduced substances begin to oxidize (Stumm and Morgan 1981). Water quality improves as the water moves downstream, eventually recovering to a more natural stream condition. The recovery distance, which depends on site-specific physical, chemical, and biological processes, is often on the order of tens of miles (Nix et al. 1991).

3. A better understanding of the recovery mechanisms and chemical transformations in tailwaters is needed to be able to address issues concerning reservoir tailwater quality and to better manage tailwater quality problems. As a result of this need, a research work unit, entitled "Techniques for Evaluating Water Quality of Reservoir Tailwaters," was initiated in the Water Quality Research Program. Since surface releases generally contain DO and are void of troublesome reduced substances, this research focused on degraded water quality downstream of dams with deep, anoxic releases.

Objectives

4. The objectives of this research were to:

- a. Develop an improved understanding of chemical transformations in reservoir tailwaters.
- b. Provide guidance on sampling and analysis of tailwater quality.
- c. Develop an easy-to-use personal computer (PC) model to predict water quality of reservoir tailwaters given in-pool or release concentrations.

This report is the second of two reports produced from this research work unit and addresses Objectives a and c above. Objective b was addressed in a report by Nix et al. (1991). Nix et al. (1991) present field study results for four study sites. One of the study sites, Nimrod tailwater, was revisited in 1989 to gain additional information. Those data are presented in Appendix A. Results from the four field study sites are analyzed herein to obtain an improved capability for predicting the time-dependent changes in reduced substances (e.g., reduced iron and manganese) in reservoir tailwaters. A numerical water quality model for reservoir tailwaters was developed and is presented in Part IV and Appendix B. Appendix C presents the kinetic rate regressions.

Approach

5. Effective water quality management of reservoir tailwaters requires assessment of existing conditions and prediction of future conditions resulting from structural and/or operational modifications of the dam or tailwater system. For example, the conversion of a nonhydropower, deep release to a hydropower release can lead to water quality problems. Releases through hydropower turbines are not subjected to the usually high degree of reaeration to which nonhydropower releases are subjected (Bohac, Harshbarger, and Lewis 1983); thus, low DO may persist for a number of miles downstream, which is detrimental to downstream aquatic habitat.

6. Mathematical water quality modeling is a cost-effective tool for predicting future conditions resulting from human actions (McCutcheon 1989). A model can be used to estimate downstream water quality for a proposed release condition at a dam. However, water quality models are limited in the context of process descriptions. For example, consider a first-order loss or decay of a substance (e.g., biochemical oxygen demand). First-order loss or decay occurs when the time rate of change of a constituent concentration C is directly proportional to the concentration, which is mathematically stated as

$$\frac{dC}{dt} = -KC \quad (1)$$

where t is time.* Equation 1 has been successfully used to describe the kinetics of numerous water quality constituents. The difficulty in applying Equation 1 in practice is estimating or calibrating the reaction coefficient, K . The modeler usually tries to fit the model to observed concentrations by varying K during calibration. In reality, K can vary with environmental conditions, such as temperature, pH, DO, etc. One of the greatest difficulties of water quality modeling is that information on the processes that affect K is limited. Therefore, empirical observations are required to develop K values for site-specific conditions. Improved understanding of the physicochemical processes is required for more general application of water quality models.

7. An improved understanding of water quality processes can be obtained through carefully designed field study because laboratory studies may fail to include all environmental factors that affect water quality kinetics. Short-term intensive field studies were conducted at four reservoir tailwater sites where physical and water quality conditions were measured to quantify chemical transformations. The study sites were Little Missouri River, Arkansas, below Lake Greeson; Fourche La Fave River, Arkansas, below Nimrod Reservoir; Rough River, Kentucky, below Rough River Reservoir; and Guadalupe River, Texas, below Canyon Reservoir. Narrows Dam (i.e., Lake Greeson) has hydropower; Canyon Dam was retrofitted for non-Federal hydropower shortly after this study. The other sites are nonhydropower. All sites had deep releases characterized by the presence of reduced substances with low DO. The study sites provided a range of physical and environmental conditions, such as varying stream slope, substrate, and pH.

8. Samples were collected for water quality analyses at a number of stations extending over the tailwater reaches. The study reaches extended from the dam to about 10 to 36 river kilometers downstream, depending on flow conditions and stream characteristics, both of which impact particle travel time. Particle travel time is the time required for a parcel of water to move

* For convenience, symbols and abbreviations are listed in the Notation (Appendix D).

from the release point to a given distance downstream. The study reaches were generally limited to a travel time of about 2 days, because most of the chemical reactions occurred within this time period.

9. The release flow rate from the dam was held constant during each field study to provide steady flow and nearly steady-state conditions (with the exception of diel effects). This approach greatly simplifies interpretation of results. Lagrangian sampling, which tracks a water parcel as it moves downstream, and snapshot sampling, in which samples are collected at all stations at or near the same point in time, yielded similar results for steady flows (Nix et al. 1991), which means the systems were approximately at steady state. Dye studies were conducted to determine the travel time to each station. With concentrations measured at the stations and with known travel time to the stations, it is possible to evaluate the reaction kinetics of Equation 1 for various processes, such as the loss of reduced manganese. Part II of this report describes tailwater quality processes based upon literature review. Part III presents the analyses of the field studies for use in model development, and Part IV presents the numerical model and its application to the field study sites.

PART II: DESCRIPTIONS OF TAILWATER QUALITY PROCESSES

Model Basis

10. It is useful to first present the fundamental model that will be used to model water quality of reservoir tailwaters. The mathematical model is based on the one-dimensional (1-D) mass conservation equation for streams

$$\frac{\partial C}{\partial t} + U \left(\frac{\partial C}{\partial x} \right) = D \left(\frac{\partial^2 C}{\partial x^2} \right) \pm S \quad (2)$$

where

U - stream mean velocity

x - distance downstream

D - longitudinal dispersion

S - rate of change in concentration resulting from transformation or chemical reactions

Equation 2 assumes completely mixed conditions over the depth and width of the stream. The dispersion term, which is the first term on the right side of Equation 2, is usually much less than advection (second term on the left side of Equation 2) for streamflow (Fischer et al. 1979). Neglecting dispersion, assuming steady-state conditions, and changing from an Eulerian to a Lagrangian reference frame, where $U = dx/dt$ is the velocity of a parcel of water, Equation 2 can be simplified to

$$\frac{dC}{dt} = \pm S \quad (3)$$

If S in Equation 3 is a first-order loss rate (i.e., $-KC$), Equation 3 is identical to Equation 1.

11. The Eulerian viewer observes concentrations at multiple stream stations as the water flows by; the Lagrangian viewer follows a parcel of water as it flows downstream and observes its concentration. The analyses in the following sections use the Lagrangian view because it conveniently relates results from all field study sites to a common variable, travel time of a parcel of water. However, the numerical model discussed in Part IV uses the

Eulerian view, but assumes steady flow and steady-state conditions. Therefore, the two views are still equivalent.

Manganese

12. Anoxic conditions in the hypolimnion of deep reservoirs induce the formation of dissolved, reduced manganese, Mn^{+2} or Mn(II). Reduced manganese can accumulate in the reservoir, affecting in-pool as well as release water quality. Mn^{+2} accumulates in the water column from sediment release and reduction of Mn(IV) in the water column under anoxic conditions, and Mn^{+2} is mostly in the dissolved state with particulate Mn^{+2} being negligible (Wilson 1980).

13. Little work has been conducted to evaluate the fate of reduced substances after they are released to the tailwater system (Gordon 1983). The oxidation of reduced manganese in the tailwater can be influenced by many environmental factors such as temperature, pH, presence of DO, electron acceptors, degree of mixing, etc. (Gordon 1989). In an effort to observe the fate of reduced manganese spatially in the Duck River, Gordon conducted a field study below Normandy Dam, near Tullahoma, TN (Gordon 1989). Gordon found from the Duck River field data that the manganese removal rate was first-order with time of travel, and the reaction rate was much faster than that typically found in laboratory studies. He also found that the removal rate was a function of river discharge.

14. The removal of reduced Mn^{+2} from reservoir tailwaters can involve physical processes (i.e., adsorption) as well as oxidation. Nix (1986), Gordon (1989), and Gordon and Burr (1989) have found that a primary removal process of Mn^{+2} can involve adsorption of Mn^{+2} onto an oxide-coated substrate. Stumm and Morgan (1981) suggest that once the Mn^{+2} is adsorbed onto the substrate, oxidation on the manganese oxide surface is a slow process. Hsiung (1987) reported that reduced manganese is removed primarily by oxidation for pH above 9.0 and by surface catalysis at lower pH. Wilson (1980) also suggests that the removal of Mn^{+2} during the turnover of lakes is probably through adsorption onto particulate matter and co-precipitation followed by slow oxidation.

15. Work by Nix (1986) showed that gravel coated with hydrous manganese oxides from the tailwater of Narrows Dam (Lake Greason) effectively removed reduced manganese in the laboratory, whereas removal without the gravel was

slow. Data from the study sites report by Nix et al. (1991) indicate that total and dissolved manganese both consistently decrease in the downstream direction, suggesting an adsorption removal mechanism. If only water column oxidation was occurring without adsorption onto the bottom, one would think that the stream turbulence would be sufficient to keep particulate (i.e., oxidized) manganese suspended, thus holding the total manganese concentrations relatively constant rather than decreasing as observed.

16. Gordon (1989) found through laboratory experiments that reduced manganese removal was associated with a "slime" found on rock surfaces in the Duck River below Normandy Dam. Gordon and Burr (1989) were able to effectively remove reduced manganese using columns packed with glass marbles acclimated with the slimy black coating characteristic of the Duck River stones. The results of these studies all indicate the need to consider the substrate as a primary removal mechanism of Mn^{+2} in the tailwater.

17. During some earlier work, Dortch and Hamlin (1988) hypothesized that flow rate impacted the manganese removal rate in the Lake Greeson tailwater. The reasoning behind this hypothesis was that if adsorption onto the substrate is a primary removal mechanism, then altering the streamflow rate changes the ratio of bottom contact area to cross-sectional flow area, which is equivalent to altering the hydraulic depth. Thus, higher flow rates, with greater depths, should be less effective in removing dissolved manganese; this was found to be true for the Greeson tailwater.

18. Hess, Byung, and Roberts (1989) developed a manganese model using the Duck River data and subsequently applied the model to the Chattahoochee River below Buford Dam, Georgia. This model contained two removal mechanisms, homogeneous and heterogeneous oxidation. Homogeneous oxidation is direct oxidation of Mn^{+2} in the water, and heterogeneous removal involves catalytic activity (i.e., sorption and oxidation) with available surfaces (i.e., hydrous manganese oxides and suspended particulates). The Hess model for manganese reaction is based on the work of Morgan (1967), which states

$$\frac{d[Mn(II)]}{dt} = - \left(k_0[OH^-]^2[DO] + k[OH^-]^2[DO][Mn(IV)] \right) [Mn(II)] \quad (4)$$

where

[Mn(II)] = dissolved (reduced) manganese concentration, moles/l

k_0 = homogeneous reaction rate, $\text{day}^{-1} (\text{moles/l})^{-3}$

[OH⁻] = hydroxide ion concentration, moles/l

[DO] = dissolved oxygen concentration, moles/l

k = heterogeneous reaction rate, $\text{day}^{-1} (\text{moles/l})^{-4}$

[Mn(IV)] = particulate (oxidized) manganese concentration, moles/l

Morgan (1967) found that the rate constants are temperature dependent. Hess, Byung, and Roberts (1989) reported that pH has a much greater effect on the manganese oxidation rate than dissolved oxygen concentration.

19. The major limitation of the Hess model is that it does not include sorption of manganese onto the channel bottom (substrate). The ideas developed in Equation 4 provide a good starting point for analyzing the data obtained within the present study, provided that the effects of substrate adsorption are included.

Iron

20. The rate of oxidation of reduced iron (i.e., ferrous iron, Fe⁺⁺, Fe(II)) is first-order with respect to concentrations of Fe(II) and O₂ and inverse second-order with respect to the H⁺ concentration (i.e., [H⁺] in moles/l where [H⁺] = 10^{-pH}) in solutions of pH > 5 (Stumm and Morgan 1981). This rate law is expressed as

$$\frac{d[\text{Fe(II)}]}{dt} = -k_{\text{Fe}} \frac{[\text{Fe(II)}][\text{DO}]}{[\text{H}^+]^2} \quad (5)$$

where [Fe(II)] is the concentration in moles/l of ferrous iron and $k_{\text{Fe}} = 3.0 \times 10^{-12} \text{ moles/l min}^{-1}$ at 20 °C. Equation 5 is in the form of Equation 1 with the overall reaction rate for ferrous iron described as

$$K_{\text{Fe}} = k_{\text{Fe}} \frac{[\text{DO}]}{[\text{H}^+]^2} \quad (6)$$

The reaction rate increases with temperature; using an activation energy of 23.0 kcal/mole in the Arrhenius equation (Stumm and Morgan 1981), the temperature dependence can be described with

$$K_T = K_{20} (1.14)^{(T-20)} \quad (7)$$

where

K_T - reaction rate at temperature T, °C

K_{20} - reaction rate at 20 °C

Sung and Morgan (1980) concluded that temperature dependence is primarily a result of the change in the H^+ concentration due to the temperature dependence of the ionization constant of water.

21. Sung and Morgan (1980) also reported that the rate constant (i.e., k_{Fe} of Equation 5) is inversely proportional to ionic strength and individual anions (e.g., Cl^- and SO_4^{-2}). For example, in the pH range of 6.5 to 7.2, sulfate ions have a significant retarding influence on the oxygenation rate. For pH of about 7 or greater, data indicate an autocatalytic rate expression, i.e., homogeneous and heterogeneous oxidations with the latter involving adsorption of ferrous iron by ferric hydroxide (Sung and Morgan 1980). Sarikaya (1990) proposed recycling of ferric sludge at treatment plants to provide effective catalytic removal of ferrous iron, thus reducing volumes required for aeration tanks.

22. As reducing conditions progress in anoxic reservoir bottom sediments, sulfate reduction follows iron reduction, and iron sulfide forms (Stumm and Morgan 1981, Wetzel 1975). Although iron sulfide is insoluble at the pH conditions typically found in reservoir waters, iron sulfide may be temporarily suspended in the water column and released to the tailwater.

23. The presence of iron sulfide in the tailwater can complicate the understanding of ferrous iron and sulfide reactions. Generally, not enough H_2S is available for pyrite (FeS_2) formation; thus, iron sulfide should exist as FeS in fresh water (Berner 1980). The oxidation of FeS is rapid. Connell (1966) showed that 120 ppm total sulfides in a soil was reduced to 5 ppm after 2 hr of exposure to air; this translates into an oxidation rate of about 38.0 day^{-1} .

24. The reactions for FeS_2 should be somewhat similar to those that occur in streams subjected to acid mine drainage as explained by Stumm and

Morgan (1981). The sulfide of FeS_2 is oxidized to sulfate-releasing dissolved ferrous iron and acidity (i.e., H^+). Subsequently, ferrous iron is oxidized to ferric iron, which hydrolyzes to form insoluble ferric hydroxide, releasing more acidity. Ferric iron can be rapidly reduced by FeS_2 to oxidize sulfide, releasing more dissolved ferrous iron and acidity.

25. Because iron sulfide reactions in acid mine drainage usually occur with very low pH, one would expect the oxidation of ferrous iron to ferric iron to be slow. In fact, the rate of oxidation of ferrous iron for low pH (i.e., pH below 4 to 5) is controlled primarily by the action of autotrophic iron-oxidizing bacteria rather than chemical oxidation (Stumm and Morgan 1981; Noike, Kanji, and Jun'Ichiro 1983). However, Noike, Kanji, and Jun'Ichiro (1983) found ferrous iron oxidation rates between 25.9 and 49.0 day^{-1} in a low-pH stream (pH 1.5 to 2.9) receiving acid mine drainage. These rates are comparable to those that occur at the higher pH values found in natural waters. The oxidation of sulfide by oxygen or hydroxides also occurs rapidly. Stumm and Morgan (1981) report half-times on the order of 20 to 1,000 min for oxidation of iron sulfide by ferric hydroxide; this corresponds to reaction rates of 50 day^{-1} to 1 day^{-1} .

Sulfide

26. Dissolved sulfide, $\text{S}[-\text{II}]$, can exist as hydrogen sulfide (H_2S), bisulfide ion (HS^-), and S^{-2} . Negligible amounts (less than 0.5 percent) of dissolved sulfide exist as S^{-2} for the pH range of most streams and lakes; the distribution between HS^- and H_2S varies with pH, with high pH favoring HS^- and low pH favoring H_2S (American Public Health Association et al. 1981). At a pH of 7.0, sulfide exists as about half hydrogen sulfide and half bisulfide ion. Hydrogen sulfide can be removed from the water through volatilization and oxidation, although oxidation of H_2S occurs very slowly compared with oxidation of HS^- (Millero 1986). HS^- is removed primarily by oxidation.

27. The general consensus from the literature is that oxidation kinetics of sulfide in natural waters is very complex and poorly understood (Chen and Morris 1972a, Stumm and Morgan 1981, Millero 1986). Based upon the review by Millero (1986), the oxidation of sulfide can be described as first-order with respect to HS^- with a rate that increases with increasing temperature, pH, and concentrations of DO, metal ions, and initial sulfide. There is also general agreement that sulfur bacteria play an important role in sulfide

oxidation in natural and waste waters. These influencing factors help to explain why the first-order sulfide oxidation rates reported vary between 0.26 and about 55.0 day⁻¹, which correspond to half-lives between 65.0 and 0.3 hr (Millero 1986).

28. The oxidation rate of sulfide is strongly dependent on pH. For an increase in pH from about 6.0 to 8.0, there is an eightfold increase in the rate (Chen and Morris 1972b). Millero (1986) attributes this to the shift in sulfide concentration from predominantly nonreactive H₂S to predominantly reactive HS⁻ with increasing pH. This reasoning suggests that HS⁻ concentration, based on pH, should be used in the kinetic equation.

29. Almgren and Hagstrom (1974) found a second-order rate dependence with the oxidation dependent on [S(-II)] and [O₂]. However, Wilmot et al. (1988) reported that the order of reaction with respect to [O₂] was only 0.2 rather than 1.0; they preferred to use the Michaelis-Menton law to describe the influence of DO, which is stated as

$$\frac{dS}{dt} = -k_s S \frac{DO}{DO_{1/2} + DO} \quad (8)$$

where

S = sulfide concentration in the form of HS⁻, mg/l

k_s = sulfide oxidation rate, day⁻¹

DO = dissolved oxygen concentration, mg/l

DO_{1/2} = dissolved oxygen half-saturation constant, mg/l

A value of 3.0 was recommended by Wilmot et al. (1988) for DO_{1/2}. O'Brien and Birkner (1977) reported that the order of reaction with respect to [O₂] was about 0.8. Chen and Morris (1972a) also found that the variation of rate with DO was less than first-order (e.g., order of about 0.5). These discrepancies are probably related to the different experimental conditions and methods used (Millero 1986). In the absence of better information, Equation 8 is appealing from a modeling standpoint.

30. Ions present in natural waters can enhance sulfide oxidation rates. Almgren and Hagstrom (1974) found fairly high rates of sulfide oxidation for seawater (k_s on the order of 25.0 day⁻¹). O'Brien and Birkner (1977) reported that sulfide oxidation increases with increasing ionic strength. Paschke, Hwang, and Johnson (1977) found that the use of manganese salts as catalysts

and adjusting the pH to 8.5 were effective in removing approximately 90 percent of the sulfide within 1 to 2 hr for wastewater from a cellulose sponge-making operation. This result translates into sulfide oxidation rates between about 27 and 55 day⁻¹. Chen and Morris (1972a) also found strong catalytic effects of metal ions, e.g., orders of magnitude reduction in oxidation rates.

31. Sulfide-oxidizing bacteria are also considered to increase the oxidation rate (Chen and Morris 1972a, Wilmot et al. 1988). Wilmot et al. (1988) reported oxidation rates between about 14 and 130 day⁻¹ for wastewaters with as much as half of the oxidation attributed to bacteria. Wilmot et al. (1988) also determined that larger initial sulfide concentrations resulted in greater oxidation rates.

32. The sulfide oxidation rate approximately doubles for a 15.0 °C temperature increase (Wilmot et al. 1988). This dependency on temperature can be represented as

$$(k_s)_T = (k_s)_{20} (1.05)^{(T - 20)} \quad (9)$$

where $(k_s)_{20}$ is the oxidation rate at 20 °C.

33. Hydrogen sulfide (H₂S) is a highly volatile dissolved gas that oxidizes very slowly (Chen and Morris 1972a, 1972b). Therefore, the major loss mechanism is through volatilization from the water. Methods described by Lyman et al. (1982) were used for determining volatilization rates of H₂S. Henry's constant at 25 °C for H₂S is 1.01 × 10⁻² atm m³/mol. Therefore, the transfer is liquid phase controlled, and volatilization can be computed with a first-order rate constant from information on the dissolved oxygen reaeration rate in streams,

$$K_s = K_2 \frac{D^s}{D^o} = K_2 \sqrt{\frac{M^o}{M^s}} \quad (10)$$

where

K_s - volatilization rate of H₂S, day⁻¹

K_2 - DO stream reaeration rate, day⁻¹

D^s - molecular diffusivity of H₂S, cm²/sec

D^o - molecular diffusivity of DO, cm^2/sec

M^o - molecular weight of DO, g/mole

M^s - molecular weight of H_2S , g/mole

Since the molecular weights of hydrogen sulfide and DO are about equal, K_2 is approximately equal to K_1 . With little or no H_2S in the atmosphere, the volatilization ($\text{mg}/\ell/\text{day}$) is computed as

$$J = -K_2 C_s \quad (11)$$

where C_s is the concentration of H_2S in the stream. The stream reaeration rate can be estimated from a variety of mathematical formulations as noted in Appendix B.

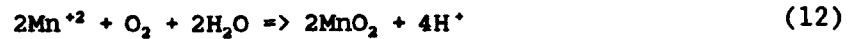
Other Water Quality Constituents

34. Other water quality constituents that are of primary interest in reservoir tailwaters are temperature, dissolved oxygen, and nutrients. Heat exchange mechanisms are relatively well understood, and the capability to accurately model stream temperature is well established (Dortch and Martin 1989). Therefore, there was no emphasis in this research on predicting stream temperature. Dissolved oxygen is required for aquatic life; thus, it is of prime importance in reservoir tailwaters, and the sources and sinks of oxygen must be considered. The nutrients nitrogen and phosphorus can exist in various forms: organic, inorganic, particulate, and dissolved. The only nutrient form that presents an immediate potential problem for tailwaters dominated by anoxic hypolimnetic releases is ammonia. Ammonia is important because oxygen is used during nitrification to nitrate. The photosynthesis, respiration, and nutrient uptake of phytoplankton and macrophytes were not considered in this work because of the relatively minor influence on tailwater quality processes at the sites studied (Nix et al. 1991).

35. Oxidation of reduced substances in the tailwater is a major sink, or loss mechanism, of oxygen (Nix et al. 1991). The primary source of oxygen is stream reaeration. The reactions and their products must be known in order to determine how much oxygen is taken up during oxidation. Once this is known, the stoichiometry for the amount of DO taken up per unit of substance

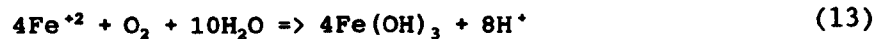
oxidized can be specified within the model. Each of the reduced substances discussed above, plus ammonia, is considered below.

36. The oxidation of Mn(II) may be represented (Benefield, Judkins, and Weand 1982) by



This reaction requires 0.29 mg/l of DO to oxidize 1.0 mg/l of Mn. However, Stumm and Morgan (1981) point out that experimental findings indicate the extent of Mn(II) removal is not accounted for by the stoichiometry of the oxidation reaction alone, and the products of oxygenation are nonstoichiometric, showing various degrees of oxidation ranging from about 30 to 90 percent oxidation to MnO₂. Thirty percent oxidation requires about 0.10 mg/l of DO per 1.0 mg/l Mn. A DO uptake stoichiometry of 0.29 mg/l per mg/l of Mn removed can be used as a worst case for modeling.

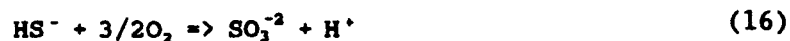
37. The oxidation of Fe(II) may be represented (Stumm and Morgan 1981; Benefield, Judkins, and Weand 1982) by



This reaction requires 0.14 mg/l of DO to oxidize 1.0 mg/l of Fe(II). Based on stoichiometry, the total oxidation of FeS to ferric iron and sulfate requires about 0.73 mg/l of DO per 1.0 mg/l of FeS, and FeS₂ requires about 1.0 mg/l of DO per 1.0 mg/l of FeS₂.

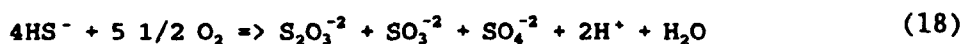
38. Oxidation of sulfide can produce sulfur (S), thiosulfate (S₂O₃⁻²), sulfite (SO₃⁻²), or sulfate (SO₄⁻²) according to the following reactions (Chen and Morris 1972b):





The above reactions (i.e., Equations 14-17) require 0.5, 1.0, 1.5, and 2.0 mg/l DO per 1.0 mg/l S⁻², or 0.48, 0.97, 1.45, and 1.94 mg/l DO per 1.0 mg/l HS⁻, respectively. Equation 16 is an intermediate step for sulfate production, where another half molecule of O₂ is required to complete the reaction. However, the oxidation of sulfite to sulfate has been observed to occur slowly (O'Brien and Birkner 1977, Chen and Morris 1972b). Thiosulfate is considered a relatively stable oxidation product (O'Brien and Birkner 1977) that is slowly oxidized to sulfate with an observed half time of 8 days (Avrahami and Golding 1968). At low pH, elemental sulfur has been observed as a precipitate (i.e., Equation 14), whereas for high pH, thiosulfate (Equation 15) is the primary product (Chen and Morris 1972a). At neutral pH, a high ratio of sulfide to oxygen results in precipitation of sulfur, while a low ratio results in direct oxidation to thiosulfate (Chen and Morris 1972b).

39. A literature review by O'Brien and Birkner (1977) indicated that most experiments observed sulfite, thiosulfate, and sulfate as oxidation products of sulfide. They proposed the hypothetical reaction model

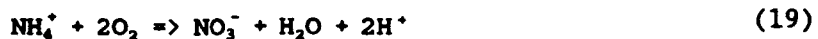


This reaction requires 1.38 mg/l O₂ per 1.0 mg/l S⁻², or 1.33 mg/l O₂ per 1.0 mg/l HS⁻. Experimental results of O'Brien and Birkner (1977) indicated an average stoichiometric value of 1.36 mg/l O₂ per 1.0 mg/l S⁻² at pH = 7.55. Respirometric studies by Chen and Morris (1972a) showed that about one molecule of oxygen was required per atom of sulfur oxidized, indicating a net oxidation primarily to thiosulfate for a pH range of 6.7 to 13.5. In view of the variation in results and the complications of sulfide reactions, the value of 1.38 mg/l O₂ per 1.0 mg/l S⁻² is recommended to provide a reasonable yet conservative estimate of DO uptake requirements.

40. Ammonia can exist in un-ionized form, NH₃, or in ionized form, NH₄⁺ (ammonium). Models usually consider total ammonia and do not distinguish the two forms. The distribution between ionized and un-ionized ammonia

concentration varies with temperature and pH, where un-ionized ammonia increases with temperature and pH. However, un-ionized ammonia usually exists in small quantities in most natural waters. For example, for a pH of 8.0 and a temperature of 20.0 °C, less than 4.0 percent of the total ammonia is NH₃ (Bowie et al. 1985).

41. Nitrifying bacteria convert ammonium (NH₄⁺) to nitrate (NO₃⁻) where the overall reaction is described as follows (Wetzel 1975)



thus requiring 4.57 mg/l O₂ per 1.0 mg/l ammonium nitrogen (i.e., NH₄⁺ as N). Nitrite (NO₂⁻) is an intermediate product that is highly labile to oxidation. Field studies of reservoir tailwaters (Nix et al. 1991) indicate that almost all of the loss in ammonia can be accounted for by nitrification to nitrate, i.e., loss in ammonia nitrogen approximately equaled gain in nitrate nitrogen with some loss of nitrate due to denitrification.

42. The rate of nitrification, or the oxidation of ammonium, can vary widely and is considered to be first-order dependent on ammonium concentration and dependent on temperature, DO, pH, and stream hydraulics, such as wetted perimeter and depth (Bowie et al. 1985). Measured nitrification rates between 0.1 and 0.5 day⁻¹ are typical for the deeper, larger water bodies, and rates greater than 1.0 day⁻¹ are not uncommon for shallow streams (Thomann and Mueller 1987). A temperature correction is usually used in the form of Equation 7 with a value of 1.08 for the base of the power term. Much work remains to be done before there exists a capability to predict the nitrification rate.

43. Nitrification is a source for nitrate nitrogen, and denitrification and algal uptake are sinks. Most stream water quality models, such as QUAL2E (Brown and Barnwell 1987), do not provide for denitrification when the stream is aerated (e.g., DO greater than about 0.5 to 2.0 mg/l). However, it is well established that denitrification can still occur in the bottom sediments of well-oxygenated streams, thus removing nitrate from the water column (Hill 1979). If proper representation of the nitrate balance is desired, then the model should include nitrification and denitrification, regardless of the DO concentration of the water column.

44. Sediment oxygen demand (SOD) can have a significant impact on DO in surface waters (Hatcher 1986). Benthic respirometers were used at several of

the tailwater study sites in this research. SOD values of about 1.0 to 2.0 g/m²/day were measured in the Nimrod and Rough River tailwaters where the bed consisted predominantly of fine sediments (Nix et al. 1991). These rates exert an oxygen demand that is comparable to the demands caused by the oxidation of reduced substances and on the same order of magnitude as reaeration for sluggish streams. Therefore, SOD should be considered for a tailwater DO model.

45. Most surface waters experience oxygen uptake due to the decomposition of organic matter (i.e., organic carbon), in addition to the other oxygen sinks discussed above. There was an attempt to quantify this demand during the tailwater field studies of Nix et al. (1991). Standard, seeded 5-day biochemical oxygen demand (BOD) measurements indicated that BOD in the tailwaters ranged from 0.8 to greater than 7.0 mg/l. However, this measurement includes any nitrogen demand and/or chemical oxidation, such as oxidation of iron and iron sulfide. Therefore, these measurements were of little use for determining organic carbon oxygen demand.

46. Ten-day, unseeded BOD studies were also conducted where multiple bottles were analyzed at 1- to 2-day intervals for each sample location (Nix et al. 1991). During these studies, various constituents that can exert an oxygen demand (ammonium, iron, etc.) were measured, in addition to DO and total organic carbon (TOC). The hope was to stoichiometrically account for the various components of known oxygen demand and calculate the organic carbon demand by difference. Although there was a definite oxygen demand in each 10-day BOD study, the TOC did not show any trend, and the studies failed to reveal any definitive quantification of the organic carbon demand.

47. The QUAL2E model has carbonaceous BOD (i.e., CBOD) in it as a modeled state variable. This variable can be used to represent the organic carbon demand since the other oxygen demands will be accounted for directly through modeled state variables. The problem remains of how to estimate a value for CBOD released from the reservoir that properly represents the organic carbon oxygen demand.

48. Reaeration is considered to be the primary source of DO in reservoir tailwaters fed by deep releases because production of oxygen through photosynthesis decreases with temperature, and deep releases tend to be cold. Additionally, deep releases tend to be void of phytoplankton. Light and dark bottle DO studies indicated that this is a good assumption (Nix et al. 1991). Numerous stream reaeration models have been developed (Bowie et al. 1985), and

most stream water quality models allow the user to select from a number of these models. Although this area of stream water quality modeling is well developed, there is still not a unified theory or equation to predict reaeration for a variety of stream conditions. It was beyond the scope of this research to investigate improved methods for modeling stream reaeration. Existing formulae are used for the model.

PART III: DATA ANALYSES

49. A list of water quality constituents collected during the field studies of Nix et al. (1991) is provided in Table 1. The analyses discussed herein do not address each constituent but are limited to those of interest for the water quality model. Presently, the model focuses on DO, the variables that impact DO, and the most problematic substances (i.e., reduced iron, reduced manganese, and sulfide). Eventually, the model may be expanded to include other processes, such as pH dynamics, and the analysis of other data collected during the field studies may become necessary. The sections that follow in Part III describe analyses of field data to support development of the kinetic algorithms of the numerical model discussed in Part IV.

Table 1
Water Quality Constituents Measured
During Field Studies

Temperature
Dissolved oxygen
Specific conductance
pH
Free carbon dioxide
Alkalinity
Total organic carbon
Carbonaceous biochemical oxygen demand
Iron (total and dissolved)
Manganese (total and dissolved)
Sulfate
Sulfide
Nitrate-nitrogen
Ammonia-nitrogen
Total Kjeldahl nitrogen
Total phosphorus
Soluble reactive phosphorus
Chloride
Turbidity

Reduced Manganese Removal

50. Data taken from the four tailwater study sites (Nix et al. 1991; Appendix A) plus data from the earlier Greeson tailwater study (Nix 1986) and Duck River (Gordon 1989) were analyzed for dissolved manganese removal rate.

A general equation to calculate the first-order removal rate (K_{Mn}) for Mn^{+2} was developed based on stream characteristics. The procedure for development of an equation to predict K_{Mn} was accomplished in several steps.

51. The first step was to determine the observed dissolved manganese loss rate K_{Mn} from the field data of dissolved manganese and travel time. The SAS procedure PROC REG (SAS Institute, Inc. 1988) was used to obtain the least squares best fit of the natural logarithm transform of the observed concentrations versus time. This regression equation form, which is shown in Equation 20, is the natural logarithm of Equation 1, where the slope of the line is K_{Mn} , or

$$\ln C = \ln C_0 - K_{Mn} t \quad (20)$$

where

C = Mn^{+2} observed at a downstream station with travel time, t , mg/l

C_0 = initial (release) Mn^{+2} concentration, mg/l

K_{Mn} = Mn^{+2} loss rate for a specific field condition, 1/day

t = travel time to station, days

The regression models developed from each observed data set to predict concentration of Mn^{+2} versus time (including regression coefficients, equation significance values, and correlation coefficients) are listed in Table 2. The initial concentration C_0 was a free parameter to be estimated (i.e., the intercept of the regression). If the significance probability of the equation was greater than 0.05, an estimated K_{Mn} was not accepted. Thus, unacceptable K_{Mn} values were not used further in the determination of a general equation for K_{Mn} . All the data sets (i.e., observed dissolved manganese concentration versus time) and the regression lines are plotted in Appendix C. It should be noted that the manganese data for Rough River were separated and analyzed as upper (i.e., the Falls of Rough pool caused by the mill dam) and lower (i.e., free-flowing stream) reaches since the data showed different slopes with a change in slope at the Falls of Rough Dam.

52. The next step was to try to relate the observed (through regression) K_{Mn} values to other variables, such as stream-average ambient water quality conditions. The initial approach used stepwise, multiple linear regression analysis (PROC STEPWISE, SAS Institute, Inc. 1988) to identify

Table 2

Regression Results for Mn²⁺ Concentration Versus Time from Observed Data

<u>Location</u>	<u>Data Set Number*</u>	<u>Independent Variables</u>	<u>Regression Coefficients</u>	<u>Equation Significance</u>	<u>R²</u>
Duck River	1	Intercept Time	0.45 -1.19	0.0001	0.98
Duck River	2	Intercept Time	0.44 -1.65	0.0001	0.96
Duck River	3	Intercept Time	0.63 -1.72	0.0001	0.96
Little Missouri River	1	Intercept Time	-1.38 -0.87	0.2810	0.36
Little Missouri River	2	Intercept Time	-1.36 -2.09	0.0177	0.79
Little Missouri River	3	Intercept Time	-1.35 -2.34	0.0002	0.92
Little Missouri River	4	Intercept Time	-0.88 -4.37	0.0002	0.95
Little Missouri River	5	Intercept Time	-1.13 -2.27	0.0746	0.86
Little Missouri River	6	Intercept Time	-2.52 -1.56	0.0007	0.92
Little Missouri River	7	Intercept Time	-2.43 -2.89	0.0001	0.97
Little Missouri River	8	Intercept Time	-1.67 -3.94	0.0051	0.94
Little Missouri River	9	Intercept Time	-1.76 -4.18	0.0146	0.97
Fourche La Fave River	1	Intercept Time	1.05 -1.52	0.0014	0.94
Fourche La Fave River	2	Intercept Time	0.82 -0.70	0.1136	0.79

(Continued)

* The data set number is shown on the plots in Figure C1.

Table 2 (Concluded)

<u>Location</u>	<u>Data Set Number*</u>	<u>Independent Variables</u>	<u>Regression Coefficients</u>	<u>Equation Significance</u>	<u>R²</u>
Fourche La Fave River	3	Intercept Time	1.21 -0.71	0.0001	0.99
Fourche La Fave River	4	Intercept Time	0.12 -1.79	0.0001	0.99
Fourche La Fave River	5	Intercept Time	0.21 -1.81	0.0004	0.97
Rough River (upper)	1	Intercept Time	0.75 -0.05	0.0855	0.56
Rough River (lower)	2	Intercept Time	0.60 -0.30	0.2178	0.89
Rough River (upper)	3	Intercept Time	0.72 -0.03	0.1801	0.40
Rough River (lower)	4	Intercept Time	0.67 -0.43	0.0142	0.99
Guadalupe River (Canyon)		Intercept Time	-2.08 -4.45	0.0066	0.87

independent variables that were the best predictors of K_{Mn} . Many of the variables tested (i.e., pH, [DO], [OH⁻], [C_o], temperature, etc.) have been cited by other researchers as affecting manganese oxidation (Stumm and Morgan 1981, Hess 1984, Hsiung 1987). Table 3 lists the variables and combinations of variables tested using PROC STEPWISE. Average values for the tailwater reach were used for each variable in Table 3. Hess' equation (Equation 4) was the first equation examined since it had been used to describe manganese oxidation in tailwaters. However, the Hess equation produced unrealistic relationships (i.e., negative coefficients) for some of the independent variables, thus incorrectly describing the processes. As a result, variations of this equation and many others were examined to try to explain the mechanisms driving the oxidation and loss of Mn⁺². As with the Hess equation, unrealistic relationships were obtained for many of the independent variables examined in the other equation forms. The PROC STEPWISE analysis did not produce an equation that adequately described the rate coefficients for Mn⁺² removal.

Table 3
Variables Tested in K_m Regression Analysis

<u>Variable</u>	<u>Variable Description</u>
$[\text{OH}^-]^2$	Hydroxide ion concentration squared
$[\text{H}^+]^2$	Hydrogen ion concentration squared
$[\text{C}_o]$	Initial Mn^{+2} concentration, moles/l
Ratio	Top width (W) over hydraulic depth (H), ft/ft
[DO]	Dissolved oxygen concentration, moles/l
P_o	Partial pressure of oxygen, atm
1/H	Inverse of hydraulic depth (H), 1/ft
u_* / H	Ratio of shear velocity (u_*) to H, 1/sec
$[\text{C}_o] / H$	Ratio of $[\text{C}_o]$ to H, moles/l-ft
COMB1	Combination of $[\text{OH}^-]^2 * \text{Ratio} * \text{C}_o$
COMB2	Combination of $[\text{OH}^-]^2 * \text{Ratio} * \text{C}_o * [\text{DO}]$
COMB3	Combination of $[\text{OH}^-]^2 * [\text{DO}]$
COMB4	Combination of $\text{Ratio} * \text{C}_o$
COMB5	Combination of $[\text{OH}^-]^2 * P_o$
COMB6	Combination of $[\text{OH}^-]^2 * [\text{DO}] * \text{C}_o$
COMB7	Combination of $[\text{OH}^-]^2 * \text{C}_o$
COMB8	Combination of $[\text{C}_o][\text{DO}]$
COMB7/H	Ratio of $[\text{OH}^-]^2 * \text{C}_o$ to H
COMB6/H	Ratio of $[\text{OH}^-]^2 * [\text{DO}] * \text{C}_o$ to H
COMB8/ $[\text{H}^+]^2$	Ratio of $[\text{C}_o][\text{DO}]$ to $[\text{H}^+]^2$
$[\text{C}_o] / [\text{H}^+]^2$	Ratio of $[\text{C}_o]$ to $[\text{H}^+]^2$
$1 / [\text{H}^+]^2$	Inverse of $[\text{H}^+]^2$

Note: All variables are averages for the tailwater reach.

53. As discussed in Part II, many researchers suggest that the primary removal mechanism for dissolved manganese is adsorption which occurs rapidly, followed by slow oxidation on particulates or the substrate. If adsorption onto the substrate is a primary removal mechanism for dissolved manganese, it makes sense that variables describing the rate of oxidation would have little meaning in explaining the observed loss rate. Consider the mass balance of dissolved manganese in a control volume of fixed volume V and bottom planar area A . The rate of decrease in dissolved manganese through adsorption onto the bottom can be described by

$$V \frac{dMn}{dt} = -V_s A (Mn - Mn_b) \quad (21)$$

where

Mn = dissolved (i.e., reduced) manganese concentration, mg/l

V_s = mass transfer velocity across diffusive sublayer separating water and substrate, L/T

Mn_b = reduced manganese concentration in sediment pore water, mg/l

Assuming that the manganese in the pore water is rapidly adsorbed onto sediment particles, Mn_b can be assumed to be insignificant, and Equation 21 becomes

$$\frac{dMn}{dt} = -\frac{V_s}{H} Mn \quad (22)$$

where H is the hydraulic depth, i.e., V/A .

54. Equation 22 looks like Equation 1 where the loss rate K_{th} is V_s/H . This reasoning helps to explain why observed data indicate that dissolved manganese is rapidly removed in streams according to a first-order rate law. From the PROC STEPWISE regressions, $1/H$ was found to be the most significant independent variable, having a coefficient of determination (i.e., R^2) of 0.62, or accounting for 62 percent of the variation in the dependent variable.

55. The next step was to find a way to estimate V_s . This led to an approach based on the results published by Boudreau and Guinasso (1982) that relate the mass transfer of dissolved substances across the diffusive sublayer of the ocean bed. Several relationships from Boudreau and Guinasso (1982) were used to compute V_s . These computed V_s values for each equation were graphically compared with *measured* (i.e., based on observed manganese data) V_s values, which were calculated from $V_s = K_{th} H$, where K_{th} values were taken from the slope of the manganese versus time regressions (Table 2).

56. All of the relationships from Boudreau and Guinasso (1982) require water viscosity ν and molecular diffusivity of the solute D for computing V_s . Therefore, V_s values were computed using values of ν and D corresponding to the observed average stream temperature, T . The value for D_T (i.e., at temperature T) can be computed (Thibodeaux 1979) from

$$D_T = D_{25} \frac{T\nu_{25}}{25\nu_T} \quad (23)$$

where

D_T - molecular diffusion coefficient of Mn^{+2} at stream temperature T , cm^2/sec

D_{25} - molecular diffusion coefficient of Mn^{+2} at 25 °C, $6.88 \times 10^{-6} cm^2/sec$

T - ambient stream temperature, °C

ν_{25} - kinematic viscosity of water at 25 °C, $0.93 \times 10^{-6} cm^2/sec$

ν_T - kinematic viscosity at stream temperature T , cm^2/sec

A regression for viscosity (ν_T) versus temperature was developed from tabulated values, resulting in

$$\nu_T = 0.000001674 - 3.061667 \times 10^{-8} T \quad (24)$$

57. The following equation was chosen to calculate (i.e., predict) V_s since its absolute mean error (i.e., mean |predicted - measured|) was less than the absolute mean error of the other relationships in Boudreau and Guinasso (1982):

$$V_s = \frac{D u_* Sc^{1/3}}{24\nu} \quad (25)$$

where

u_* - shear velocity (\sqrt{gHs}), L/T

g - gravitational acceleration, L/T²

s - water surface or streambed slope, nondimensional

Sc - Schmidt Number (ν/D), nondimensional

and values for D and ν are taken at ambient stream temperature T .

58. Graphs of predicted versus measured V_s indicated that the data could be divided into two groups, one representing cobble bed streams and the other representing sediment (i.e., fine grain, silt and clay) bed streams. A two-tailed mean analysis was performed on both groups to see if there was enough difference between the mean V_s for each group to justify having

separate equations for V_s for the two streambed types. To perform the two-tailed mean analysis, the assumption had to be verified that the variances of V_s for the two streambed types were equal. This assumption was verified using the F test analysis at the significance level of $\alpha = 0.02$. Upon verification that the variances were equal, the two-tailed mean analysis was tested at a significance level of $\alpha = 0.05$. It was concluded from the analysis that the mean V_s values for the two streambed types were different enough to develop separate equations for V_s . It is not known how a sandy substrate would impact the manganese removal rate since none of the tailwaters studied here had significant quantities of sandy material.

59. Linear regression analysis with PROC REG (SAS Institute, Inc. 1988) was used to relate the measured and computed (i.e., computed with Equation 25) V_s values for both streambed types, or

$$V_{s_m} = a V_{s_c} \quad (26)$$

where

V_{s_m} = measured mass transfer rate, L/T

a = regression coefficient, dimensionless

V_{s_c} = mass transfer coefficient computed with Equation 25, L/T

Figure 1 shows the regression lines fitting the computed versus measured V_s for the cobble and sediment streambed types, respectively. Regression coefficients, significance value, and R^2 for the Equation 26 model are listed in Table 4 for both streambed types. It is reasonable that the cobble bed regression results in larger values for V_s since larger roughness elements associated with cobbles would tend to increase turbulence, thus increasing the diffusive sublayer mass transfer velocity.

60. The general method to predict K_{Mn} can be summarized as follows. Equations 23 and 24 are first used to obtain D and ν for the ambient water temperature. Next, V_s is estimated with Equation 25 using the previously corrected values for D and ν and the stream hydraulics to obtain u_* . Equation 26 is used to obtain an improved estimate for V_s using the value computed by Equation 25. Finally, the result obtained with Equation 26 is divided by H to obtain K_{Mn} . A plot of predicted versus observed K_{Mn} using this methodology is shown in Figure 2. The line in Figure 2 is the

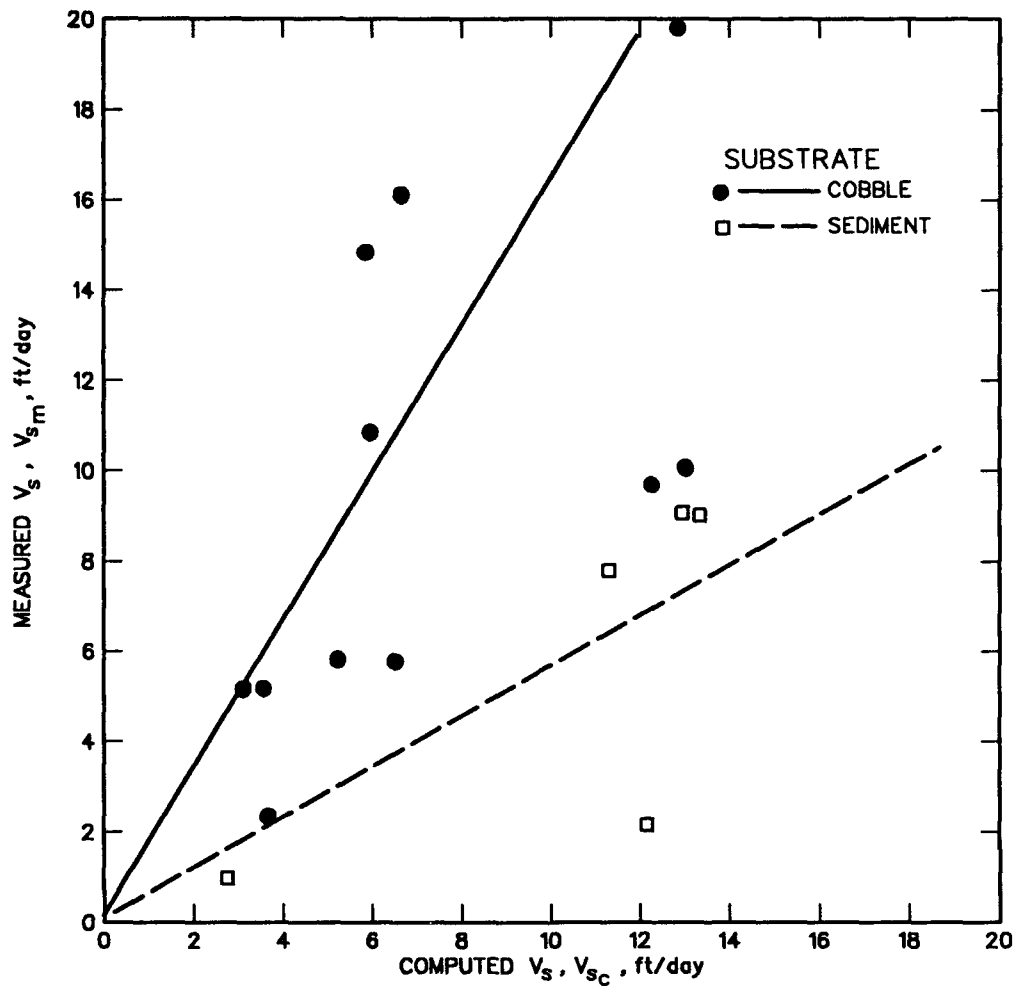


Figure 1. Measured versus computed V_s for Mn data divided into cobble and sediment substrates

Table 4

Regression Results for Equation 26

<u>Streambed Type</u>	<u>Independent Variable</u>	<u>Regression Coefficients</u>	<u>Equation Significance</u>	<u>R²</u>
Cobble	V_s	1.654	0.0001	0.89
Sediment	V_s	0.579	0.0057	0.88

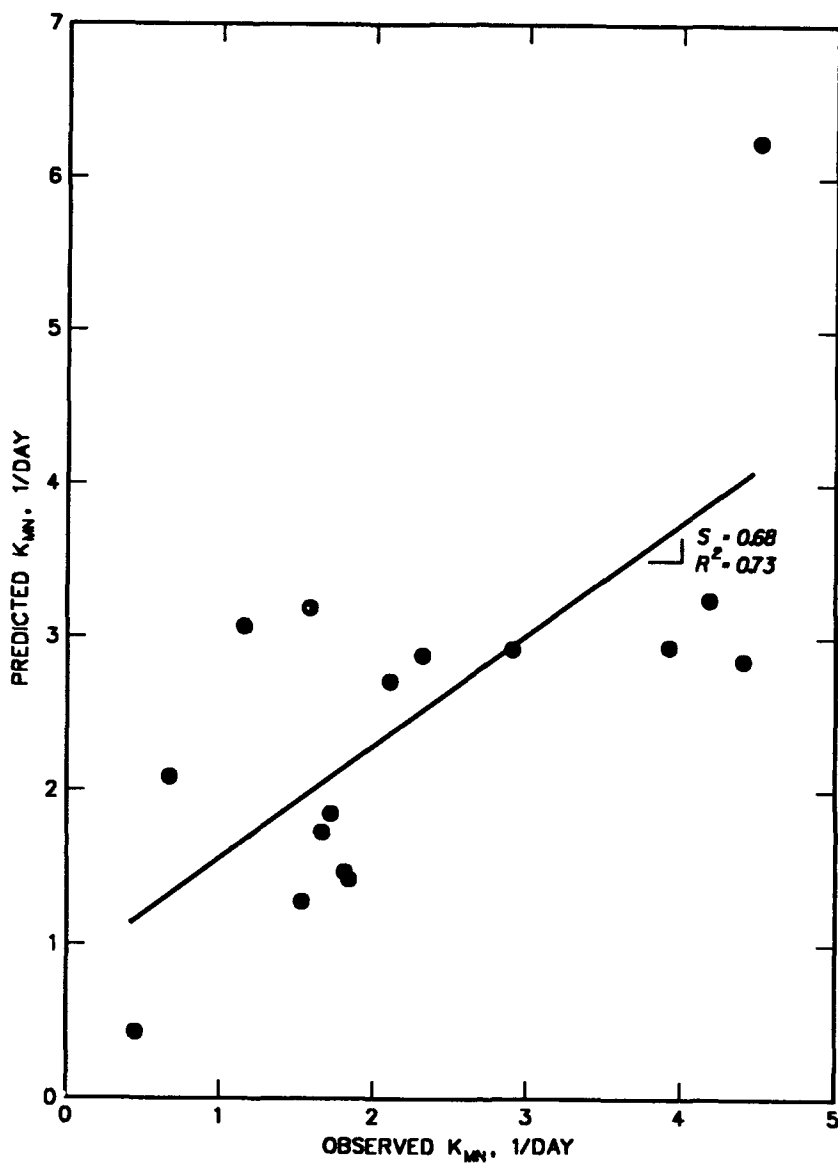


Figure 2. Predicted versus observed dissolved manganese removal rate, K_{Mn}

least squares best fit. The slope of this line is .68 and has an R^2 value of 0.74. The regression slope is not significantly different ($\alpha = 0.05$) from a perfect correlation slope of 1.0.

Reduced Iron Removal

61. It was difficult to interpret the reduced iron data taken at the four study sites. Reduced iron, i.e., ferrous iron, was defined as dissolved

iron, or the iron that passed through a 0.45- μ filter. The dissolved iron data from the Greeson and Canyon tailwaters were very low (less than 0.1 mg/l) and showed little change downstream. Higher concentrations of total and dissolved iron were measured at Nimrod and Rough River tailwaters. The dissolved iron showed little change in the downstream direction of the Nimrod tailwater, whereas at Rough River there was a downstream decline. Nix et al. (1991) speculated that fine floc of ferric iron could have passed the 0.45- μ filter, yielding artificially high dissolved iron concentrations in the downstream reaches of the tailwaters. Gordon, Bonner, and Milligan (1984) recommended that a 0.10- μ filter be used to filter particulate and colloidal iron. Gordon, Bonner, and Milligan (1984) did not detect sulfides below Normandy Dam, but found total iron to be considerably higher than dissolved, indicating the possible presence of iron sulfide. At Nimrod and Rough River tailwaters, the total iron was about two to three times greater than the dissolved iron, and there was an increase in sulfate in the downstream direction. Therefore, it was concluded that iron sulfide was probably released into both tailwaters, thus complicating the iron dynamics (Nix et al. 1991).

62. The information yielded from the iron data was far less than desirable for evaluation of iron oxidation (i.e., removal) rates. However, three of the data sets that clearly showed a downstream decline in dissolved iron concentration were analyzed for order of magnitude rates of oxidation and were compared with predicted values. These three data sets were Greeson, September 1983 (Nix 1986); Greeson, October 1987 (Nix et al. 1991); and Rough River, August 1988 (Nix et al. 1991). The observed changes in dissolved iron concentration and travel time were used to estimate an "observed" oxidation rate of dissolved iron using the first-order rate law (Equation 1). The "predicted" oxidation rate at 20 °C was computed with Equation 6 using the average DO and pH observed throughout the tailwater reach from which the "observed" oxidation rate was estimated. The predicted rates were then corrected for the temperature observed in the reach using Equation 7.

63. The following results were obtained for the three data sets:

<u>Study</u>	<u>Date</u>	<u>Observed K_F, day⁻¹</u>	<u>Predicted K_F, day⁻¹</u>
Greeson	Sep 1983	0.54	0.12
Greeson	Oct 1987	6.65	1.16
Rough River	Aug 1988	1.25	150.

The fact that the predicted rates of iron oxidation do not agree with those observed is not surprising considering the complex interactions surrounding iron and iron sulfide dynamics, as discussed in Part II. These results at least show that Equation 6 can provide the proper order of magnitude estimate for K_{Fe} , as it did for the Greeson site. Gordon, Bonner, and Milligan (1984) measured dissolved iron below Normandy Dam that exhibited removal rates between about 1.8 and 18.0 day⁻¹.

64. The observed rates were higher than the predicted rates at the Greeson site, which might be explained by the presence of other trace metals (Stumm and Morgan 1981, Nix 1986). Higher rates were observed and predicted for the October 1987 Greeson study than for the earlier Greeson study; this may be partially due to the higher pH observed in the later study. A high oxidation rate was predicted for the Rough River study because of much higher pH (i.e., pH = 7.5 versus about 5.6 and 6.2 for the Greeson studies). The relatively low oxidation rate observed at Rough River may not be a true indication of the actual oxidation rate due to the suspected presence of iron sulfide and the associated sampling/analysis problems discussed above. If colloidal iron had passed the filter during the dissolved iron measurements, the dissolved iron measurements would be artificially high, thus lowering estimates for the oxidation rates. Additionally, the sulfate concentrations at Rough River were about three times higher than those at Greeson. As mentioned in Part II, high sulfate concentrations can have a retarding influence on the iron oxidation rate. There was simply not enough information to allow definitive analysis of iron sulfide dynamics.

Sulfide Removal

65. Very little information could be extracted from the field studies for sulfide removal. Sulfide was detected in small quantities at Greeson tailwater in 1983 (Nix 1986), Nimrod tailwater in 1989 (Appendix A), and Canyon tailwater in 1988 (Nix et al. 1991). Analyses of these three data sets are discussed below.

66. The 1983 Greeson data indicate that sulfide decreased from about 0.3 mg/l to 0.04 mg/l over the first 10 km of the tailwater. The travel time for this reach and flow rate reported by Nix (1986) are now considered to be in error; the correct travel time is approximately 3.8 hr. This decrease in sulfide over 3.8 hr translates into a loss rate of about 12.7 day⁻¹. The pH

during this study was approximately 5.5, which means that most (i.e., about 95 percent) of the sulfide existed as H_2S and was lost by volatilization. A hydrogen sulfide volatilization rate of 12.7 day^{-1} is of the same order of magnitude as the reaeration rate of about 7.0 day^{-1} that was measured (Dortch and Hamlin 1988). Recall from Part II that the reaeration rate can be used to estimate the hydrogen sulfide volatilization rate.

67. Sulfide was found to decrease at Nimrod in 1989 from about 0.017 mg/l just below the dam to about 0.012 mg/l at the next downstream sampling station, which is about 1.8 hr travel time at the high-flow discharge. About 75 percent of the measured sulfide was H_2S for the observed pH of 6.5. Therefore, HS^- decreased from 0.0043 to about 0.0030 mg/l . This decrease results in an overall sulfide oxidation rate of about 4.6 day^{-1} . Correcting for DO and temperature (see Equations 8 and 9, respectively) provides an estimated k_a in Equation 8 of about 4.9 day^{-1} at $20 \text{ }^\circ\text{C}$. This rate is on the low side of the range of reported rates discussed in Part II.

68. Nix et al. (1991) reported that the sulfide at Canyon tailwater decreased from about 0.04 mg/l just below the dam to background levels at the next downstream station. The travel time to the first station was 70 min. Based on the data, it was assumed that background levels were about 0.01 mg/l . For the observed pH of 7.6, 80 percent of the sulfide is HS^- . This translates into an overall oxidation rate for HS^- of about 24.0 day^{-1} . Correcting for temperature and DO as above, k_a at $20 \text{ }^\circ\text{C}$ is 36.7 day^{-1} . This value falls about in the middle of the reported ranges.

Nitrification

69. The ammonia data reported by Nix et al. (1991) were analyzed in a manner similar to the manganese data. Ten data sets (Table 5) that clearly showed a downstream decrease in ammonia were used in the analysis. Linear regressions were developed for the natural log of the ammonia concentrations versus travel time so that the overall ammonium loss (i.e., nitrification rate K_a , day^{-1}) could be determined from the slope of the regression. Plots of the data and the regression lines are presented in Appendix C. The K_a value obtained from the regressions (i.e., measured K_a), the correlation coefficient, and significance of the regression are shown in Table 5. Data were excluded from further analysis if the significance probability of the equation was greater than 0.05. Separation of the ammonia data into upper and lower

Table 5

Regression Results for NH⁺ Concentration Versus Time from Measured Data

<u>Location</u>	<u>Data Set Number*</u>	<u>Independent Variables</u>	<u>Regression Coefficients</u>	<u>Equation Significance</u>	<u>R²</u>
Little Missouri River		Intercept Time	-2.69 -4.33	0.2194	0.61
Fourche La Fave River	1	Intercept Time	-0.46 -1.35	0.0007	0.96
Fourche La Fave River	2	Intercept Time	-0.86 -0.77	0.1587	0.71
Fourche La Fave River	3	Intercept Time	-0.57 -0.66	0.0097	0.92
Fourche La Fave River	4	Intercept Time	-1.32 -1.79	0.0001	0.99
Fourche La Fave River	5	Intercept Time	-1.25 -1.32	0.0007	0.96
Rough River	1	Intercept Time	0.13 -0.84	0.0029	0.74
Rough River	2	Intercept Time	0.08 -0.13	0.0116	0.62
Rough River	3	Intercept Time	0.09 -0.15	0.0012	0.80
Guadalupe River		Intercept Time	-2.18 -2.39	0.0003	0.90

* The data set number is shown on the plots in Figure C2.

reaches for Rough River resulted in insignificant regression; thus, the ammonia data were not separated.

70. As discussed in Part II, nitrification is considered to be affected by stream hydraulics, i.e., contact with the substrate. Therefore, the methods outlined earlier for computing the diffusive sublayer mass transfer velocity V_s were used here, with the exception that D_{20} for ammonia is 1.76×10^{-5} cm²/sec, and a reference temperature of 20 °C rather than 25 °C is used in Equation 23. The quantity V_s/H was correlated with the measured K_a , yielding a regression coefficient of 0.136 with an R² value of 0.83 and a

significance of 0.0006. Thus, ammonia is modeled with a first-order removal, with the removal (nitrification) rate prescribed by

$$K_a = 0.136 \frac{V_s}{H} \quad (27)$$

71. A plot of predicted (with Equations 23-25 and 27) versus observed K_a is shown in Figure 3. The slope of the least squares best fit regression line shown in Figure 3 is 0.65 and has an R^2 value of 0.77. This slope is not significantly different ($\alpha = 0.05$) from the perfect correlation slope of 1.0. A temperature correction was applied to K_a with an equation of the same form as Equation 7 and a value of 1.08 for the base of the power term.

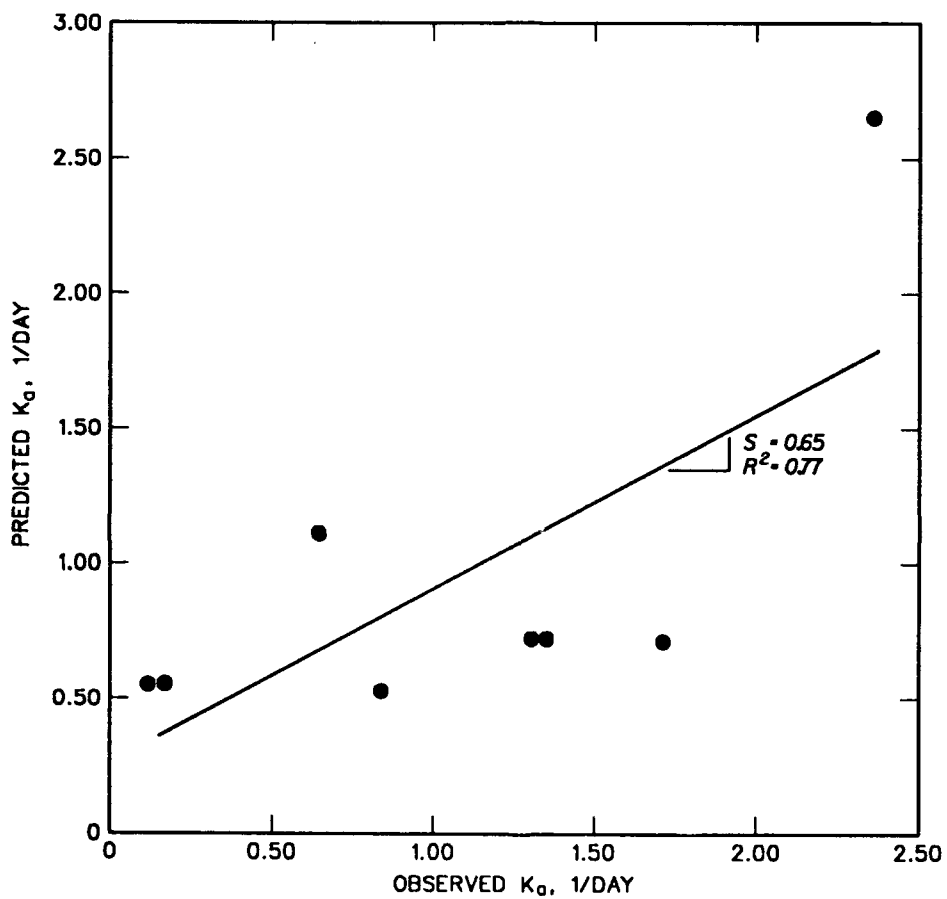


Figure 3. Predicted versus observed ammonia-N removal rate, K_d

PART IV: NUMERICAL MODEL

Description

General

72. The focus of the Tailwater Quality Numerical Model (TWQM) is to predict the downstream transformation of problem constituents, such as DO and several of the reduced substances (i.e., iron, manganese, sulfide, and ammonia). It is intended that the model require as little input data as possible, allowing modest resources for application. The obvious way to reduce input requirements is to restrict the model dimensionality; the model is 1-D in the streamwise direction. Another way to reduce input requirements is to restrict the model to steady-state applications so that time-varying input files are not required. Therefore, TWQM does not allow time-varying flow or water quality inputs, and a steady-state solution is performed.

73. Steady-state solutions for 1-D problems can often be performed analytically, rather than numerically (Dortch and Martin 1989). However, a numerical modeling approach was selected for the TWQM to allow flexibility in interactions of state variables. Additionally, with the microcomputer resources available today, numerical solutions are easily and rapidly attainable.

74. TWQM is based on the US Environmental Protection Agency (EPA) 1-D stream water quality model, QUAL2E (Brown and Barnwell 1987). The major modification to QUAL2E was to include subroutines to model the reduced substances in tailwaters and a user interface to provide easier model application. QUAL2E was selected for several reasons: (a) the model is widely used and accepted, (b) the model provides for steady-state solutions, (c) the model contains other water quality processes that could be used if desired, and (d) the most recent version of QUAL2E had been developed for microcomputers with simpler input requirements.

75. The TWQM combines several components within a user-friendly interface that utilizes menus for selecting alternatives. In addition to the QUAL2E-based tailwater component, there is a reservoir release component. Reservoir release water quality is required for the upstream boundary condition of the stream component. The user may specify this information from observations or can predict the release concentrations based upon observed in-pool concentrations using the SELECT model (Davis et al. 1987). Given the

in-pool temperature stratification, the outlet features, release flow rate, and vertical distribution of water quality constituents, SELECT computes the release concentrations. Also included in SELECT is a structural reaeration component that predicts uptake of dissolved oxygen as flow passes through the release structure. Release concentrations are provided by SELECT to the tailwater component for predicting downstream concentrations. Except for DO, neither SELECT nor the tailwater model alters concentrations of water quality variables as flow passes through the outlet structure; in other words, variables are treated as conservative as they pass through the structure because of the short residence time in the structure. SELECT does allow the option of structural reaeration.

76. The combination of SELECT with the tailwater model allows the user to evaluate the impact on downstream water quality of various release schemes, such as hydropower retrofit or moving the vertical location of the intakes of the outlet structure.

77. TWQM has the capability of simulating up to 17 water quality constituents. Constituents, which can be modeled in any combination by the user, are:

- a. DO.
- b. CBOD.
- c. Temperature.
- d. Algae as chlorophyll a.
- e. Total organic nitrogen.
- f. Ammonia nitrogen.
- g. Nitrite and nitrate nitrogen.
- h. Total organic phosphorus.
- i. Dissolved inorganic (orthophosphate) phosphorus.
- j. Dissolved (reduced) iron.
- k. Dissolved (reduced) manganese.
- l. Total dissolved sulfide (HS^- and H_2S).
- m. Iron sulfide.
- n. Arbitrary nonconservative constituent.
- o. Two conservative constituents.

Most of the above constituents were originally in QUAL2E; the reduced substances iron, manganese, sulfide, and iron sulfide were added. The model's compartmental diagram (Figure 4) illustrates the various state variables and how they interact. The model solves the steady-state mass balance equation

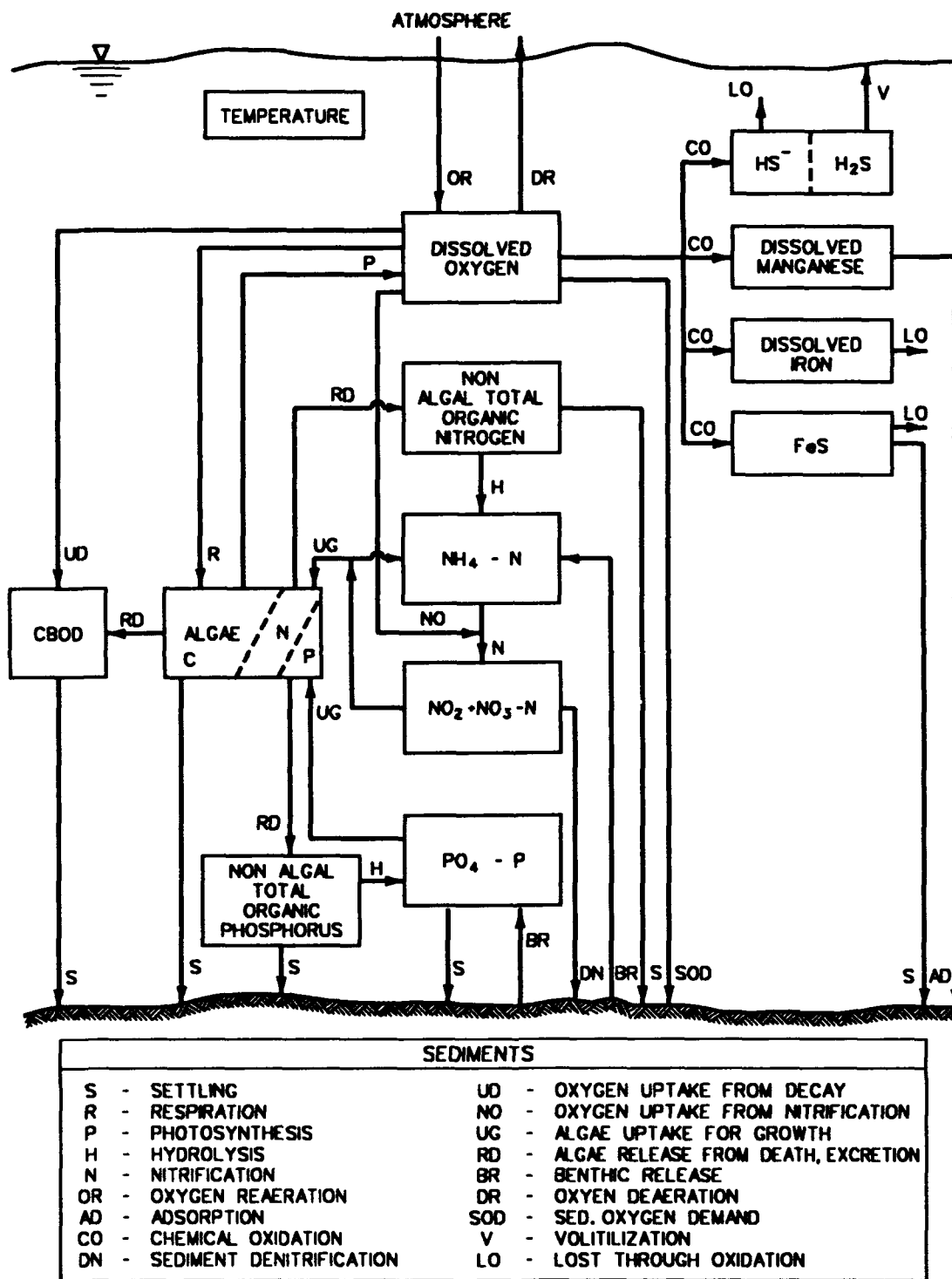


Figure 4. Tailwater quality model compartmental diagram

(i.e., mass transport equation or advection-diffusion equation with mass sources/sinks) for each state variable. The mass balance equation is referred to as the energy equation when temperature is the state variable.

78. The tailwater is physically described by subdividing the stream system into reaches (the basic division of the model). Reaches represent portions of the river having similar channel geometry, hydraulic characteristics, and chemical/biological coefficients. Reaches are further divided into equally spaced units called computational elements, or nodes. An example schematic of a modeled tailwater system is illustrated in Figure 5. Each computational element has inputs, outputs, and reaction terms. The energy and mass balance equations are solved simultaneously (implicitly) for all computational elements. This solution is repeated in an iterative fashion, using the previous solution results, until convergence for the steady-state solution is reached (i.e., the concentrations quit changing within a small tolerance).

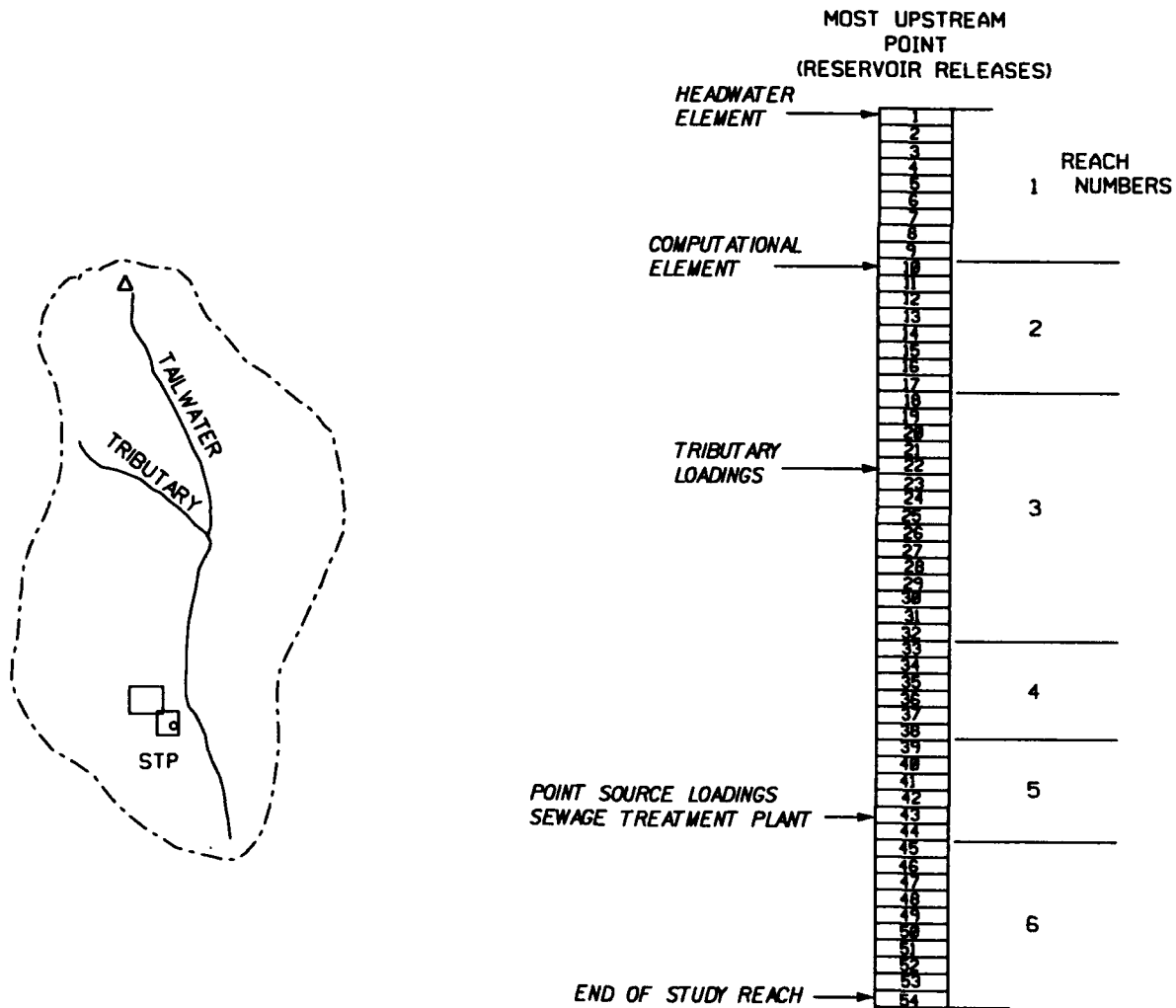


Figure 5. Example schematic of a model stream system

79. The model assumes steady, nonuniform flow. Hydraulic conditions (velocity and depth) used within the energy and mass balance equations are entered for each reach and assumed uniform throughout the reach. Steady flow implies that the flow rate, velocity, width, and depth at any point in the stream are constant with time. Nonuniform flow is allowed, which means flow rate, velocity, width, and depth can change in the longitudinal direction from reach to reach.

80. Model processes of state variables that were added or kinetics that were modified are described in the sections that follow. As with any numerical solution, errors can be associated with the solution scheme. A description of the numerical error inherent in this model and the remedy are discussed in the next section on numerical diffusion.

Numerical diffusion

81. The version of QUAL2E from which TWQM was developed required the user to specify the number of computational elements that a reach would be divided into. QUAL2E allows a maximum of 20 elements per reach, which is not always adequate. Computational element length can affect the results of a simulation. Computational element lengths that are too long can result in numerical diffusion.

82. Numerical diffusion occurs when the mathematical solution scheme used in a model incorrectly contributes to the diffusion of modeled substances. For a model to be representative, predicted movement of substances should be a function of the advective velocity of the water and the dispersion characteristics of the stream (Fischer et al. 1979). For example, if the movement of a tracer in a river is to be modeled, the computational elements should have a length that causes the advective velocity (i.e., displacement velocity or displacement distance divided by elapsed time) of the tracer mean concentration to be the same as the mean flow velocity of the stream. Also, the variance of this tracer cloud should increase at a rate of about two times the dispersion coefficient for a normally distributed cloud. When these conditions are not met, the distribution of the tracer is not only a function of the dispersion coefficient but also of the numerical solution used.

83. To decrease the effects of numerical diffusion in TWQM, the computational element length was determined by equating the estimated longitudinal dispersion of the stream with numerical dispersion. The stream dispersion can be estimated from Fischer et al. (1979).

$$D_n = 0.011 \frac{u^2 W^2}{Hu_*} \quad (28)$$

where

u = average stream velocity, m/sec

W = top width of stream, m

Numerical dispersion for steady-state conditions can be computed (Roache 1972) from

$$D_n = \frac{u \Delta x}{2} \quad (29)$$

where Δx is the computational element length (meters). Variables in Equations 28 and 29 are shown with the appropriate metric units. TWQM has an option that allows expression of distances, flows, velocities, and temperature in non-metric units. Solving Equations 28 and 29 yields a value for Δx of

$$\Delta x = \frac{2(0.011)u^2 W^2}{uHu_*} \quad (30)$$

Substituting for u_* and expressing W in terms of flow rate (Q), depth, and average velocity yields Equation 31,

$$\Delta x = \frac{2(0.011)Q^2}{uH^{3.5}g^{0.5}s^{0.3}} \quad (31)$$

84. The total reach length is divided by the value of Δx determined from Equation 31 to determine the total number of elements per reach. This number is rounded to the nearest integer so as not to have a fraction of an element within a reach. The integer number of elements is divided into the reach length to define the computational element length for that reach. The maximum allowable number of computational elements per reach was increased in TWQM to 100, which limits the minimum length of any computational element to 1/100 of the reach length. This limit was arbitrarily set to restrict storage

requirements of TWQM, but the user can easily increase this limit through a parameter statement in the source code.

85. To test the effectiveness of these changes, simulations were performed in which a nonconservative tracer was continuously injected at the dam and its steady-state concentration was predicted at distances downstream. In the case where the computational element length was determined (Figure 6a), the predicted concentrations were very close to those obtained using the analytical solution (Fischer et al. 1979).

$$C = C_0 \exp \left[\frac{-kx}{u} \left(\frac{2}{\alpha} (\sqrt{\alpha + 1} - 1) \right) \right] \quad (32)$$

where

C_0 = release concentration at $x = 0$, mg/l

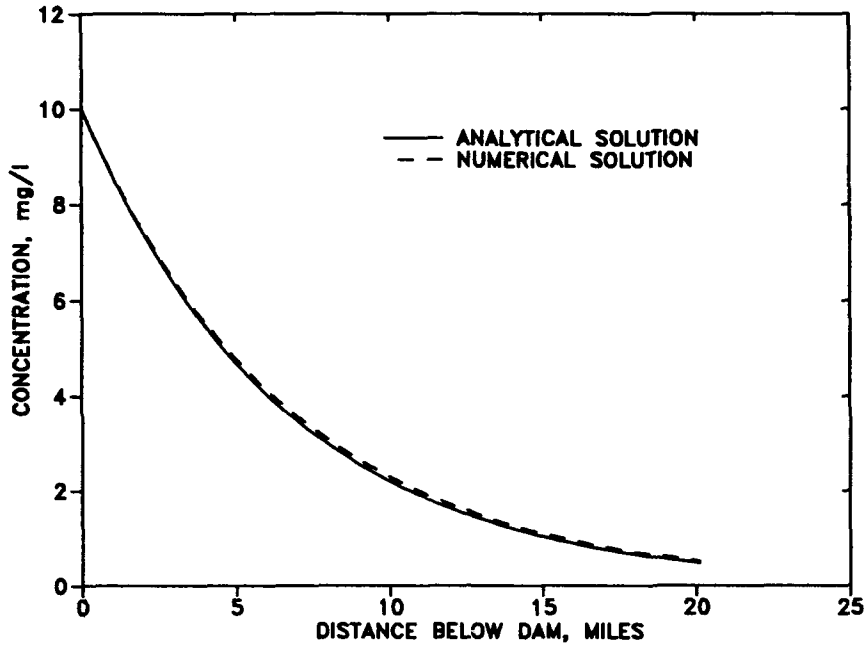
k = reaction rate constant, day⁻¹

$$\alpha = \frac{4Dk}{u^2}$$

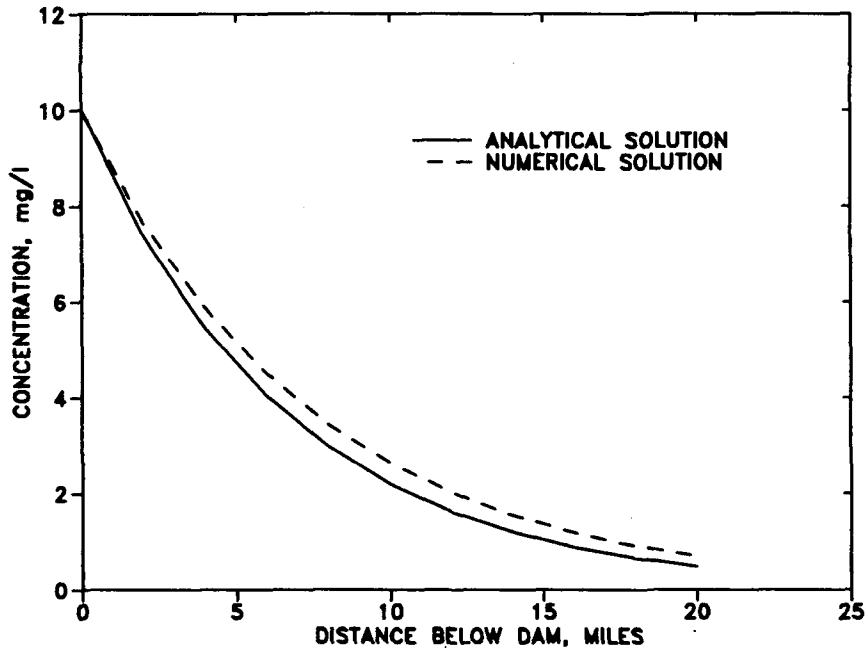
For the simulation in which the computational element length was set at an arbitrary length of 2 miles (Figure 6b), the predicted concentration is not as close to the analytical solution. Both simulations were performed using the same initial concentrations, velocities, and channel geometry. The only difference between the two simulations was the computational element length.

86. QUAL2E, and therefore TWQM, require that the length of computational elements be the same in all reaches. In simulations performed using multiple reaches, the minimum computational element length determined in any reach is used for all reaches. In this case the reach length of the other reaches might be increased or decreased slightly to prevent a reach from containing a fraction of an element.

87. QUAL2E requires the user to input the element type (headwater, standard, point load, end) for each computational element. In TWQM this process has been automated due to the potentially large number of elements used per reach. The only user input requirements of this type are the locations in river miles of point loads (including waste discharges and tributaries) or withdrawals within a reach.



a. Term Δx computed to reduce model numerical diffusion



b. Term Δx equals 2.0 miles in the numerical model

Figure 6. Results of stream transport test

Dissolved manganese

88. Dissolved (i.e., reduced) manganese removal is modeled as a first-order reaction using the equation

$$\frac{dMn}{dt} = -K_{Mn}Mn \quad (33)$$

where

Mn - Mn^{+2} concentration, mg/l

K_{Mn} - Mn^{+2} loss rate, day⁻¹

The manganese loss mechanism is assumed to be predominantly through adsorption onto the bed as discussed in Part III. The user has a choice of having the model calculate the loss rate K_{Mn} as described in the Reduced Manganese Removal section of Part III (i.e., Equations 23-26), or specifying K_{Mn} . A default K_{Mn} value is used if the user does not elect to have the model predict K_{Mn} or does not specify K_{Mn} . If the user elects to model the removal rate, the streambed type (i.e., cobble or sediment) of the tailwater must be specified. If a K_{Mn} value is specified or the default value is used, the value entered is assumed to be at 20 °C, and the following equation is used to correct for temperature dependence:

$$K_T = K_{20}\theta^{(T - 20)} \quad (34)$$

where

K_T - Mn^{+2} removal rate at stream temperature T

K_{20} - Mn^{+2} removal rate at 20 °C

θ - temperature correction constant

Hess, Byung, and Roberts (1989) recommend a value of 1.054 for θ for temperatures below 25 °C. Evaluation of data reported by Hsiung (1987) suggested a value of 1.105 for θ for temperatures above 25 °C.

Dissolved iron

89. Dissolved (i.e., reduced) iron removal/oxidation is also modeled as a first-order reaction with respect to dissolved iron concentration. The loss rate K_{Fe} can be calculated by the model (i.e., using Equations 6 and 7) or specified by the user. Again, if the user does not specify a value or does not elect to let the model compute the loss rate, a default value will be used. When the default value is used or a value is specified, the temperature dependence is taken into account using Equation 7.

Dissolved sulfide

90. Total dissolved sulfide is a modeled state variable composed of HS^- and H_2S . The fractions of H_2S and HS^- present are estimated based on the pH-dependent relationship in Standard Methods (American Public Health Association et al. 1981). For the pH range of 5 to 7, the fraction of total dissolved sulfide as H_2S (FRACT) can be calculated as

$$\text{FRACT} = \frac{-8.3813X^3 + 135.898X^2 - 742.31X + 1,461.46}{100} \quad (35)$$

where X is the pH of the stream. For the pH range of 7 to 9, the fraction of total dissolved sulfide as H_2S is calculated as

$$\text{FRACT} = \frac{-8.25406X^3 + 213.821X^2 - 1.852.79X + 5,374.11}{100} \quad (36)$$

The fraction of dissolved sulfide as HS^- is then calculated as 1-FRACT. If pH is less than 5 or greater than 9, FRACT is set to 1 or 0, respectively. An insignificant amount of dissolved sulfide is made up of S^{2-} (American Public Health Association et al. 1981).

91. Removal of HS^- through oxidation is modeled using Equation 8. The oxidation rate k_s can be specified by the user; otherwise, a default value of 25.0 day^{-1} is used. The temperature correction for k_s is made with Equation 9.

92. Loss of H_2S gas through volatilization is modeled using Equation 11 where the volatilization rate K_s is set equal to the reaeration coefficient K_2 , as discussed in Part II. The reaeration coefficient is modeled according to the formula selected by the user, as discussed in Appendix B.

Iron sulfide

93. Although the oxidation and loss of iron sulfide may be complex, a simple approach for modeling is proposed here, considering the lack of better information and supporting data at this time. The loss of iron sulfide from the tailwater is accounted for by two mechanisms, first-order oxidation (i.e., Equation 1) in the water column and settling to the bottom. Thus, the kinetic equation for iron sulfide is

$$\frac{d(\text{FeS})}{dt} = - \left(K_{\text{FeS}} + \frac{W_s}{H} \right) (\text{FeS}) \quad (37)$$

where

(FeS) - iron sulfide concentration, mg/l

K_{FeS} - first-order oxidation rate, day⁻¹

W_s - settling rate of FeS, m/day

The settling and oxidation rates are either specified by the user or set to the default values of 1.0 m/day and 38.0 day⁻¹, respectively.

Nitrification and denitrification

94. QUAL2E contains algorithms for the nitrogen cycle, including mineralization of organic nitrogen to ammonium nitrogen, nitrification from ammonium to nitrite and from nitrite to nitrate nitrogen, and denitrification. These algorithms were retained for use in the TWQM with some minor modifications. The method for computing the nitrification rate discussed earlier in Part III (i.e., Equation 27) was included as a user option. Additionally, nitrite nitrogen was removed as a state variable since it oxidizes rapidly and its presence only further complicates the model. Therefore, ammonium nitrogen is oxidized directly to nitrate nitrogen. A first-order removal mechanism for nitrate nitrogen was added to represent denitrification by sediments. This denitrification mechanism is independent of DO concentration, and the user can specify the first-order rate or use the default value.

Dissolved oxygen

95. The equation for dissolved oxygen in QUAL2E had to be modified to allow proper representation of the various DO sinks caused by the oxidation of reduced substances in the tailwater. The sinks of DO are:

- a. Algal respiration.
- b. Decomposition of organic carbon (i.e., CBOD decay).
- c. Nitrification of ammonium nitrogen to nitrate nitrogen.
- d. Oxidation of reduced manganese sorbed onto the bed.
- e. Oxidation of reduced (i.e., dissolved) iron.
- f. Oxidation of iron sulfide, both in the water column and in the bed.
- g. Oxidation of HS⁻.
- h. Sediment oxygen demand (SOD).

96. CBOD is used to represent the oxygen uptake due to decomposition of organic carbon. The kinetics and oxidation of CBOD decay and algal respiration in QUAL2E were not modified. The oxygen uptake associated with nitrification was altered to reflect that the intermediate step of nitrification to nitrite was eliminated. Oxygen uptake due to oxidation of dissolved iron, iron sulfide in the water column, and HS^- were included by subtracting the three corresponding stoichiometric sink terms from the right side of the oxygen mass balance equation. QUAL2E contained a loss mechanism of DO through SOD. The SOD for TWQM is considered to be caused by the decomposition of organic material in the bottom sediments.

97. The oxidation of inorganic matter on the bottom (i.e., sorbed, reduced manganese and iron sulfide that settles to the bottom) must also be included in the DO balance. Matter lost from the water column accumulates in the bed for subsequent oxidation. The concentration of manganese and iron sulfide in the bed can be derived from the steady-state mass balance of these two substances in a bed control volume

$$C_b = \frac{wA_s C}{K_b V_b} \quad (38)$$

where

C_b = concentration of reduced manganese or iron sulfide in bed, mg/l

w = loading rate (i.e., mass transfer rate or settling rate) to bed, m/day

A_s = surface area of bed control volume, m^2

C = concentration of reduced manganese or iron sulfide in water column, mg/l

K_b = oxidation rate of reduced manganese or iron sulfide in bed, 1/day

V_b = volume of bed control volume, m^3

The oxidation of these substances creates an additional sediment oxygen demand that can be calculated by

$$\Delta\text{SOD} = \frac{\alpha K_b C_b V_b}{A_s} = \alpha w C \quad (39)$$

where

ΔSOD = additional SOD resulting from manganese or iron sulfide oxidation in bed, g $O_2/(m^2/day)$

α = stoichiometric conversion for mg/l of O_2 uptake per mg/l of substance oxidized, nondimensional

Therefore, the steady-state additional SOD depends on the loading rate from the water column to the bed. Water column oxygen uptake resulting from SOD is accomplished in the DO balance by multiplying the SOD by the surface area of the bed and dividing by the volume of the water column, which is the same as SOD/H . Therefore, the water column DO sink arising from Equation 39 is computed by $\alpha(w/H)C$, where w for reduced manganese is actually V_s computed from Equations 25 and 26.

98. The additional sink terms arising from oxidation reactions of reduced substances that were included in the DO balance are summarized as follows:

$$\begin{aligned} \text{Dissolved iron} &= \alpha_{Fe} K_{Fe} (Fe^{++}) \\ \text{Dissolved sulfide} &= \alpha_{HS} K_{HS} (HS^-) \\ \text{Reduced manganese} &= \alpha_{Mn} K_{Mn} (Mn^{++}) \\ \text{Iron sulfide} &= \alpha_{FeS} \left(K_{FeS} + \frac{W_s}{H} \right) (FeS) \end{aligned} \tag{40}$$

where the substance quantities in parentheses are concentrations in milligrams per liter. The default values for the parameters in the above relations are shown in Table 6. The sources of DO, reaeration and algal photosynthesis, were not modified. It will be necessary to model algae in many tailwater applications of TWQM.

Table 6
Default Values for Stoichiometry and Kinetics

<u>Parameter</u>	<u>Default Value</u>
α_{Fe} , DO uptake conversion for Fe^{++} oxidation	0.14 mg/l O_2 per mg/l Fe^{+2}
α_{HS} , DO uptake conversion for HS^- oxidation	1.38 mg/l O_2 per mg/l S^{-2}
α_{Mn} , DO uptake conversion for Mn^{++} oxidation	0.29 mg/l O_2 per mg/l Mn^{+2}
α_{FeS} , DO uptake conversion for FeS oxidation	0.73 mg/l O_2 per mg/l FeS
K_{Fe} , oxidation rate of Fe^{++}	(day ⁻¹)*
K_{HS} , oxidation rate of HS^-	(day ⁻¹)*
K_{Mn} , loss rate of Mn^{++} from water column	(day ⁻¹)*
K_{FeS} , oxidation rate of FeS in water column	38.0 day ⁻¹
W_s , settling rate of FeS from water column	1.0 m/day

* Parameter predicted by the model for default.

Application

General

99. TWQM was applied to one data set for each of the four field sites (Lake Greeson, September 1987; Nimrod Reservoir, August 1989; Rough River Reservoir, August 1988; and Canyon Reservoir, September 1988) discussed in Nix et al. (1991). All four data sets were obtained with the steady-state method of sampling (Nix et al. 1991). Water quality constituents modeled during each application were DO, CBOD, ammonium nitrogen, organic nitrogen, nitrate nitrogen, dissolved iron (i.e., Fe^{+2}), dissolved manganese (i.e., Mn^{+2}), and total dissolved sulfide (if measured). Iron sulfide was also modeled for Rough River. Temperature and pH were not modeled but were input for each reach. One data set from each site was selected for model verification.

100. Reaction rates for Mn^{+2} , Fe^{+2} , and NH_4 removal were initially modeled using equations discussed in previous sections of this report. Concentrations of Mn^{+2} , Fe^{+2} , and NH_4 were compared with observed results to determine how well removal of the reduced species was predicted throughout the tailwater. If predictions did not compare well with observations, the reaction rate was changed to yield concentrations similar to those observed. All other reaction rates (e.g., organic nitrogen hydrolysis) were set to values recommended by Brown and Barnwell (1987). Table 7 contains final values used

for the input parameters, such as hydraulic data, headwater boundary conditions, ambient constants, and reaction rates, for each field site.

101. The following section presents application results. The order of presentation is to discuss the results for each water quality constituent as modeled for all sites (e.g., results of modeling Mn^{+2} for all sites), rather than to discuss the results of all water quality constituents for each site.

Results

102. Final calibration results for all four sites are shown in Figures 7-10. Final results for Mn^{+2} are shown in Figures 7b (Greeson), 8b (Nimrod), 9b (Rough River), and 10b (Canyon). Mn^{+2} removal was successfully modeled at three of the sites using the predictive equations for K_{Mn} (i.e., Equations 22-26), resulting in acceptable estimations of Mn^{+2} concentrations compared with observed values. However, for the Rough River application, the predictive equations for K_{Mn} caused Mn^{+2} to be removed too quickly, especially in the upper reaches. The first four reaches (approximately the upper 10.0 km) of the modeled Rough River tailwater are in the pool created by the mill dam, referred to as Falls of Rough. Conditions within this pool are much different from the downstream reach below Falls of Rough. By specifying low K_{Mn} values that are consistent with those estimated within the mill dam pool, much better results were obtained (Figure 9b). During data analysis (Part III), it was observed that the K_{Mn} values measured in the pooled reaches of Rough River were much less than those measured at the other sites. A higher value of K_{Mn} , similar to values observed at the other sites, was used in the free-flowing reach below the mill dam.

103. The predictive equations for the manganese removal rate K_{Mn} probably did not perform well for the pooled reaches of the Rough River tailwater because of the conditions that normally exist during the summer months at this site. The releases from Rough River Dam are usually quite low (e.g., 20 cfs*). A low-flow and a high-flow condition were sampled in this study. The results presented here are for the high flow of 200 cfs. For this flow, the water in the pool was well mixed from surface to bottom. However, at the normal low flows, the Fall of Rough pool slightly stratifies, and the release water plunges under a warmwater wedge. This plunging phenomenon prevents the release water, which is rich in reduced substances (e.g., dissolved

* A table of factors for converting non-SI units of measurement to SI (metric) units is presented on page 3.

Table 7
Input Data for Each Application*

Field Site	Data Type	Parameter	Reach No.					
			1	2	3	4	5	6
Greeson	Hydraulic	Depth (ft)	3.11	2.50	2.80	2.63		
		Velocity (ft/sec)	1.65	1.50	0.88	0.75		
		Start of reach (km)	170.27	166.41	161.26	159.65		
		Slope	0.0016					
	Headwater	Flow (cfs)	500.00					
		DO (mg/l)	4.40					
		CBOD (mg/l)**	2.00					
		Fe ⁺² (mg/l)	0.04					
		Mn ⁺² (mg/l)	0.09					
		pH	6.15					
		Org-N (mg/l)	0.18					
		NH ₄ -N (mg/l)	0.02					
		NO ₃ -N (mg/l)	0.17					
	Ambient constants	Temperature (°C)	14.04	15.40	16.00	15.50		
		pH	6.15	6.40	6.30	6.80		
	Reaction rates	CBOD (1/day)	0.10	0.10	0.10	0.25		
		SOD (g/m ² day ⁻¹)	0.00	0.00	0.00	2.0		
		K ₂ value	6.24	7.03	5.62	0.62		
		Org-N hydrolysis (1/day)	0.20					
		Org-N settling (1/day)	0.10					
		NH ₄ -N (1/day)	Modeled					
		Fe ⁺² oxidation (1/day)	Modeled					
		Mn ⁺² oxidation (1/day)	Modeled					
		Denitrification (1/day)	0.00					
	Nimrod	Hydraulic	Depth (ft)	2.00	2.56	3.57		
			Velocity (ft/sec)	0.56	0.45	0.27		
			Start of reach (km)	100.74	97.85	96.08		
			Slope	0.001				
		Headwater	Temperature (°C)	25.88				
			Flow (cfs)	200.00				
DO (mg/l)			7.00					
CBOD (mg/l)			1.00					
Sulfide (mg/l)			0.016					
Fe ⁺² (mg/l)			1.00					
Mn ⁺² (mg/l)			1.20					
pH			6.50					
Org-N (mg/l)			0.32					
NH ₄ -N (mg/l)		0.28						
NO ₃ -N (mg/l)		0.03						
Ambient constants	Temperature (°C)	25.88	26.60	27.00				
	pH	6.50						
Reaction rates	CBOD (1/day)	0.15						
	SOD (g/m ² day ⁻¹)	2.00						
	K ₂ option	3.00						
	Org-N hydrolysis (1/day)	0.2						
	Org-N settling (1/day)	0.1						
	NH ₄ -N (1/day)	1.75						

(Continued)

* Parameters were constant throughout reaches unless otherwise indicated.
 ** CBOD is 5 day CBOD.

Table 7 (Continued)

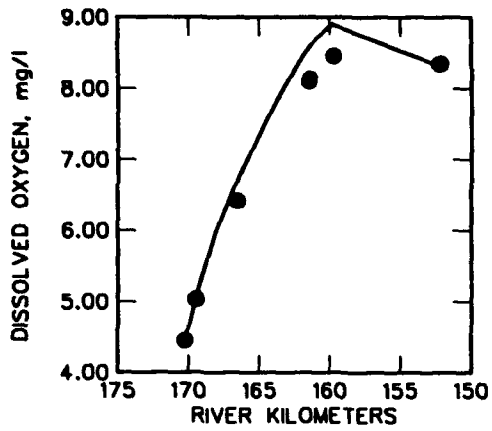
Field Site	Data Type	Parameter	Reach No.						
			1	2	3	4	5	6	
Nimrod (Cont.)		Fe ⁺² (l/day)	Modeled						
		Mn ⁺² (l/day)	Modeled						
		Sulfide (l/day)	1.00	0.50	0.10				
		Denitrification (l/day)	2.25						
Rough River	Hydraulic	Depth (ft)	5.50	6.00	9.00	10.70	3.00		
		Velocity (ft/sec)	0.57	0.30	0.26	0.33	0.62		
		Start of reach (km)	143.88	141.14	138.89	135.67	133.58		
		Slope	0.0023						
	Headwater	Flow (cfs)	200.00						
		DO (mg/l)	8.60						
		CBOD (mg/l)	1.00						
		Fe ⁺² (mg/l)	0.89						
		FeS (mg/l)	2.50						
		Mn ⁺² (mg/l)	2.03						
		pH	7.30						
		Org-N (mg/l)	0.64						
		NH ₄ -N (mg/l)	1.06						
NO ₃ -N (mg/l)		0.01							
Ambient constants	Temperature (°C)	15.20	15.30	15.40	16.50	17.30			
	pH	7.30	7.30	7.20	7.30	7.20			
Reaction rates	CBOD (l/day)	0.20							
	SOD (g/m ² day ⁻¹)	1.80							
	K ₂ option	3.00							
	Org-N hydrolysis (l/day)	0.20							
	Org-N settling (l/day)	0.10							
	NH ₄ -N (l/day)	0.20	0.20	0.20	0.20	0.70			
	Fe ⁺² (l/day)	Modeled							
	FeS (l/day)	2.00							
	FeS settling (m/day)	0.00							
	Mn ⁺² (l/day)	0.05	0.05	0.05	0.03	0.50			
	Denitrification (l/day)	3.50							
Canyon	Hydraulic	Depth (ft)	1.30						
		Velocity (ft/sec)	1.04						
	Start of reach (km)	487.63	486.02	484.73	482.32	477.65	473.15		
	Slope	0.00144							
Headwater	Flow (cfs)	114.00							
	DO (mg/l)	8.80							
	CBOD (mg/l)	1.00							
	Sulfide (mg/l)	0.04							
	Fe ⁺² (mg/l)	0.012							
	Mn ⁺² (mg/l)	0.168							
	pH	7.50							
	Org-N (mg/l)	0.00							
	NH ₄ -N (mg/l)	0.11							
	NO ₃ -N (mg/l)	0.04							
Ambient constants	Temperature (°C)	17.20	17.70	19.10	20.60	22.50	23.10		
	pH	7.50	7.70	7.80	7.80	7.90	7.90		

(Continued)

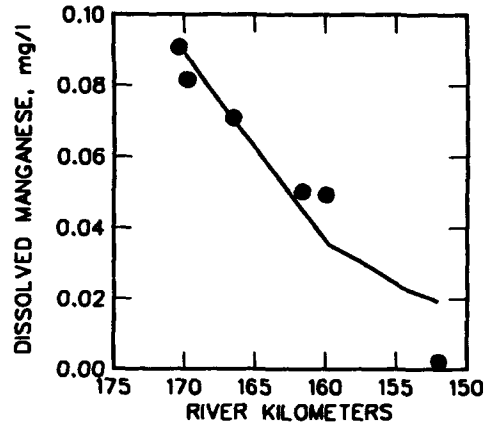
(Sheet 2 of 3)

Table 7 (Concluded)

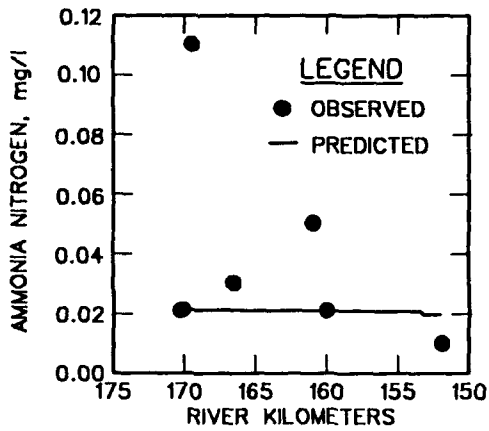
Field Site	Data Type	Parameter	Reach No.					
			1	2	3	4	5	6
Canyon (Cont.)	Reaction rates	CBOD (1/day)	0.15					
		SOD ($\text{g/m}^2 \text{ day}^{-1}$)	2.00					
		K_2 option	3.00					
		Org-N hydrolysis (1/day)	0.20					
		Org-N settling (1/day)	0.10					
		$\text{NH}_4\text{-N}$ (1/day)	1.80					
		Fe^{+2} (1/day)	Modeled					
		Mn^{+2} (1/day)	Modeled					
		Sulfide (1/day)	25.00					
Denitrification (1/day)	0.00							



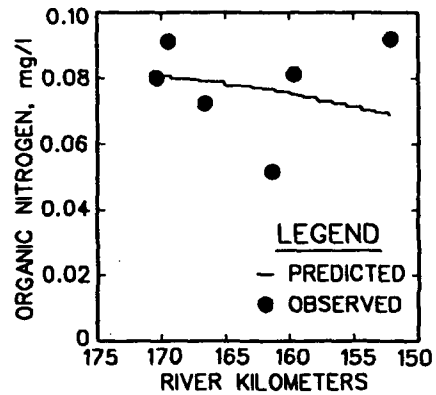
a. Dissolved oxygen



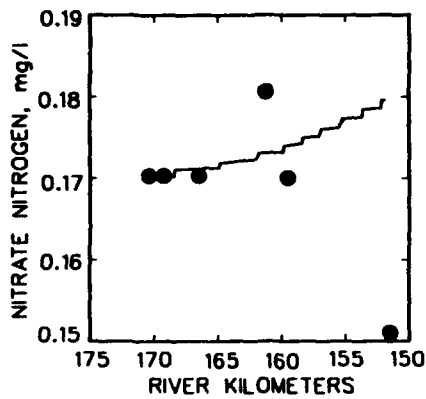
b. Dissolved manganese



c. Ammonium nitrogen

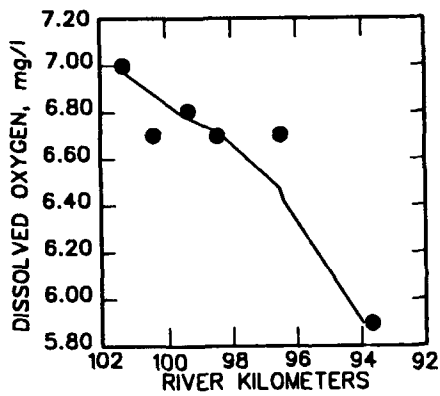


d. Organic nitrogen

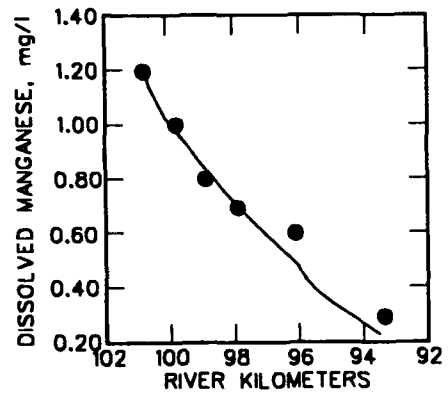


e. Nitrate nitrogen

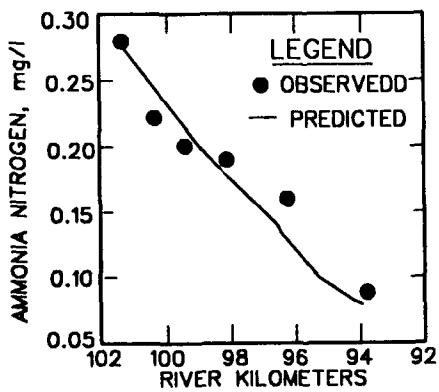
Figure 7. Predicted and observed water quality, Greeson Dam tailwater



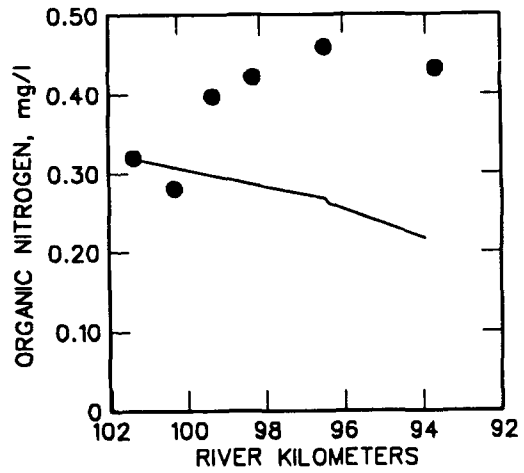
a. Dissolved oxygen



b. Dissolved manganese

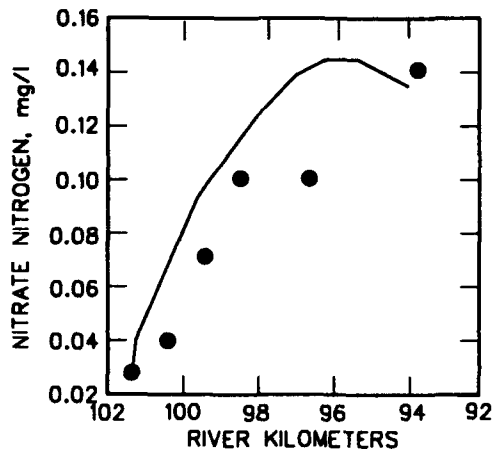


c. Ammonium nitrogen

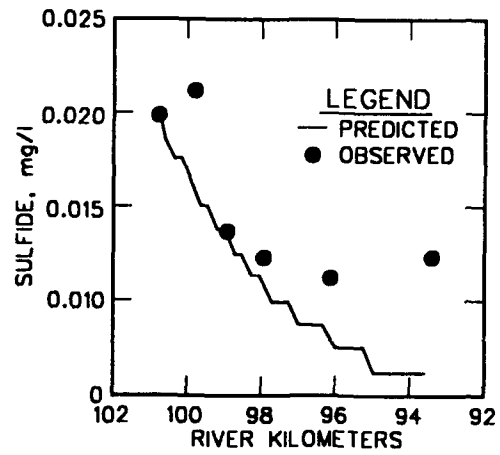


d. Organic nitrogen

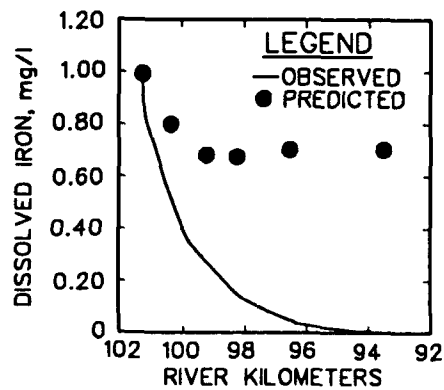
Figure 8. Predicted and observed water quality, Nimrod Dam tailwater (Continued)



e. Nitrate nitrogen

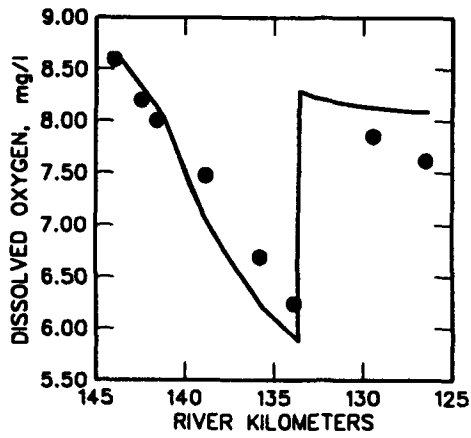


f. Dissolved sulfide

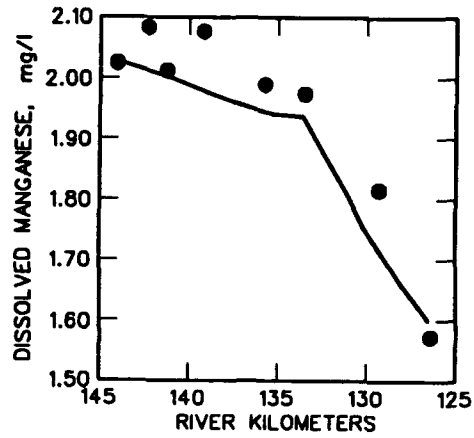


g. Dissolved iron

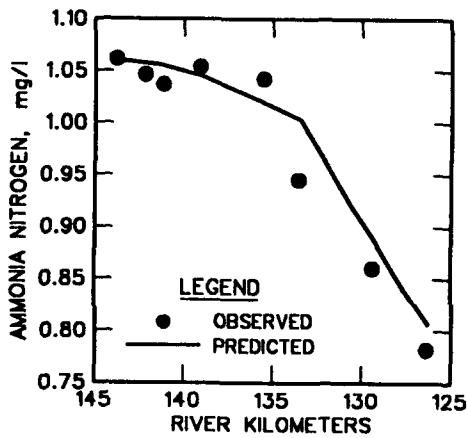
Figure 8. (Concluded)



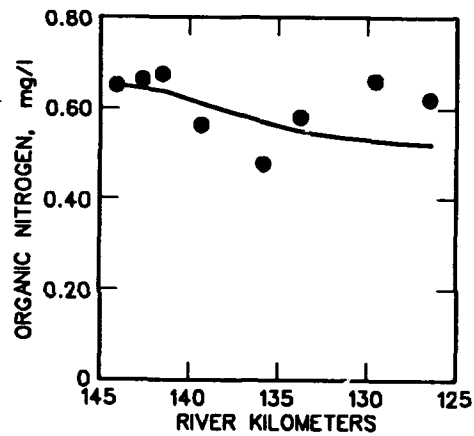
a. Dissolved oxygen



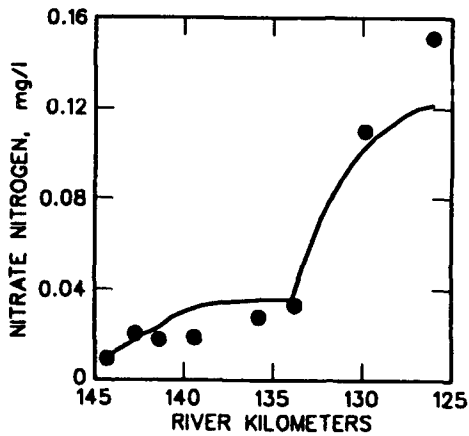
b. Dissolved manganese



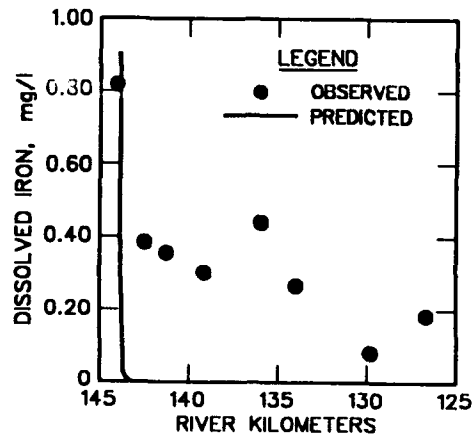
c. Ammonium nitrogen



d. Organic nitrogen

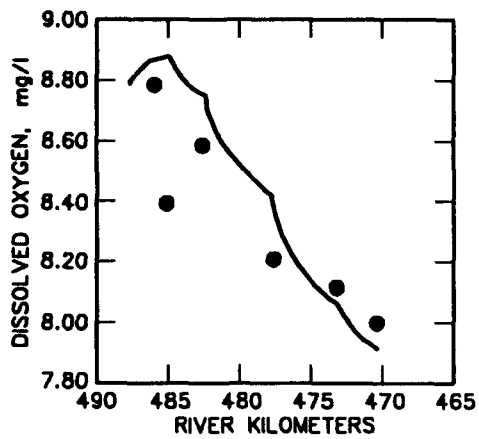


e. Nitrate nitrogen

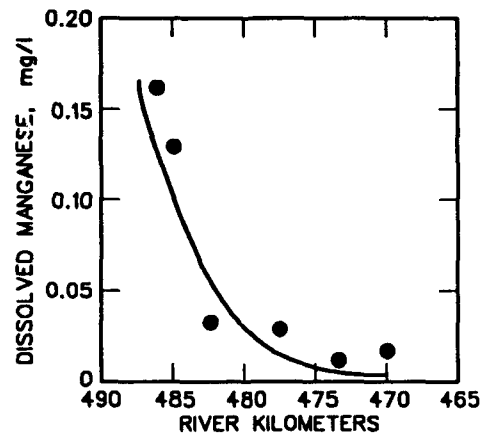


f. Dissolved iron

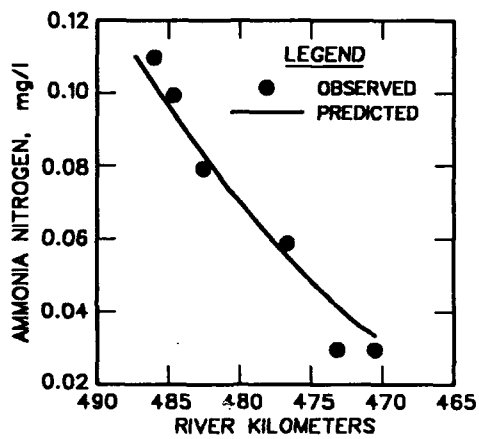
Figure 9. Predicted and observed water quality, Rough River tailwater



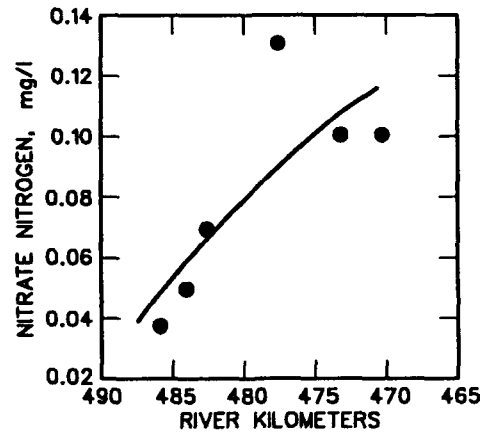
a. Dissolved oxygen



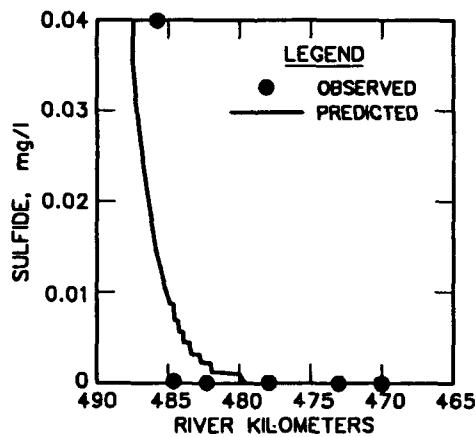
b. Dissolved manganese



c. Ammonium nitrogen



d. Nitrate nitrogen



e. Dissolved sulfide

Figure 10. Predicted and observed water quality, Canyon Dam tailwater

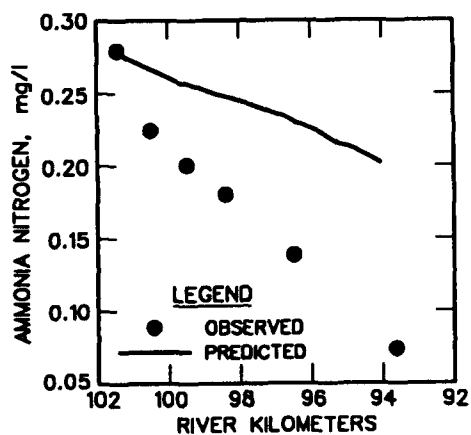
manganese), from being reaerated through the air-water interface. For these conditions, it seems reasonable to expect that there is less opportunity for hydrous oxides of manganese to accumulate on the substrate, thus lowering the capacity of the pooled reaches to remove manganese.

104. Final results for ammonium are shown in Figures 7c (Greeson), 8c (Nimrod), 9c (Rough River), and 10c (Canyon). The ammonia oxidation rate (i.e., nitrification rate) was initially modeled using Equation 27 for all four sites. However, results at Nimrod, Rough River, and Canyon (Figures 11a, 12c, and 13, respectively) showed that the nitrification rate was calculated to be too high (Rough River) or too low (Nimrod and Canyon). Modeled nitrification rates (i.e., Equation 27) were retained at the Greeson site, which had low concentrations (Figure 7c). The nitrification rates were calibrated against observed ammonia nitrogen data, yielding the rates shown in Table 7 and the concentrations shown in Figures 7c, 8c, 9c, and 10c. The low rates used for the pooled reaches of Rough River are probably related to the reasons discussed above for manganese.

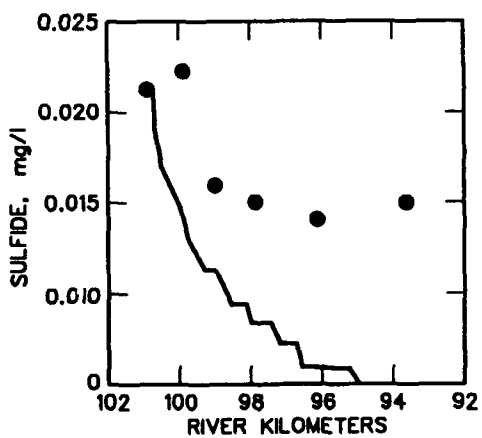
105. The inability to predict the nitrification rate at three of the four sites may be due to the scatter in the data used to develop Equation 27. Nitrification rates also depend upon bacteria and conditions for bacterial growth, thus making prediction of rates difficult. However, the predicted nitrification rates were generally close to the calibrated rates with only slight adjustments required during calibration.

106. Results for organic nitrogen are shown in Figures 7d (Greeson), 8d (Nimrod), and 9d (Rough River). Boundary conditions for organic nitrogen (Table 7) were estimated as the difference between total Kjeldahl nitrogen (TKN) and ammonia nitrogen for each site (Nix et al. 1991). TKN was not measured at Canyon tailwater, so it was not modeled at this site. Default values (Brown and Barnwell 1987) for organic nitrogen hydrolysis and settling were used for all applications (Table 7). Final results for organic nitrogen compared favorably with observed concentrations except at Nimrod, where the concentrations increased downstream instead of decreasing as would be expected. This indicates that there may be a source of organic nitrogen, such as algae, that is not being accounted for in the modeling effort.

107. Results for nitrate nitrogen are shown in Figures 7e (Greeson), 8e (Nimrod), 9e (Rough River), and 10d (Canyon). Initially, TWQM had no mechanism for denitrification, and the results for nitrate nitrogen did not compare favorably with observed values, especially at Rough River (see Figure 12d).

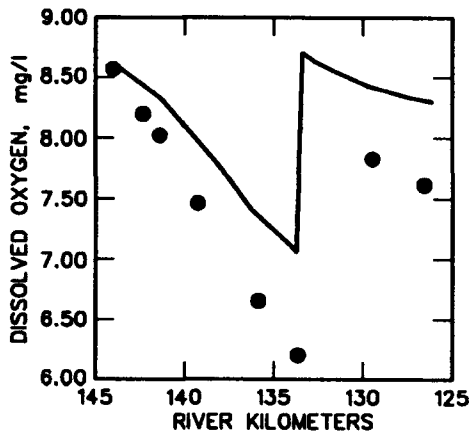


a. Ammonium nitrogen

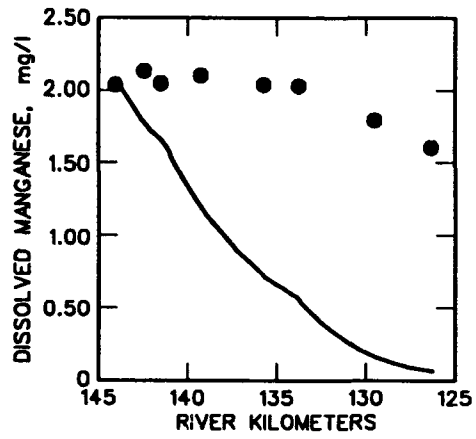


b. Dissolved sulfide

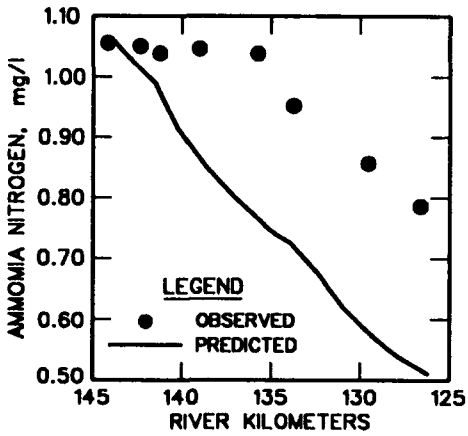
Figure 11. Initial predictions versus observed water quality, Nimrod Dam tailwater



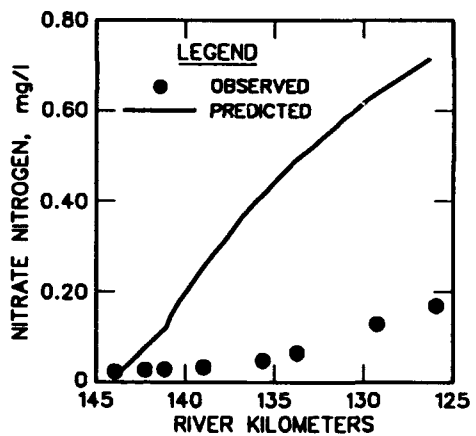
a. Dissolved oxygen



b. Dissolved manganese



c. Ammonium nitrogen



d. Nitrate nitrogen

Figure 12. Initial predictions versus observed water quality, Rough River tailwater

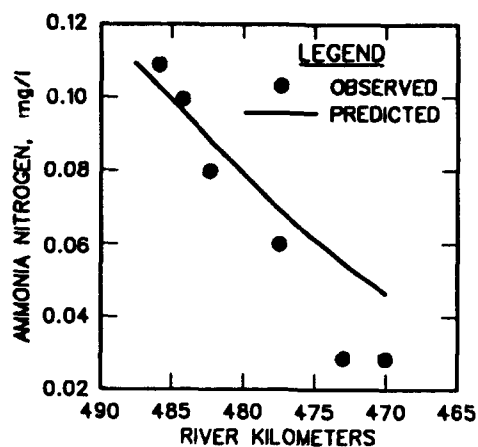


Figure 13. Initial prediction versus observed ammonium nitrogen, Canyon Dam tailwater

Consequently, denitrification was added as a loss mechanism for nitrate nitrogen in TWQM. Once denitrification was included in the model, the final results (Figures 8e, Nimrod, and 9e, Rough River) for nitrate nitrogen were improved from the initial applications. Greeson and Canyon tailwaters did not exhibit denitrification, which could be related to the stream sediment type. Both sites have cobble beds where the anoxic sediment zone necessary for denitrification could be farther below the sediment-water interface. According to Hill and Sanmugadas (1985), denitrification rates are correlated to stream-sediment characteristics.

108. Final results for dissolved sulfide are shown in Figures 8f (Nimrod) and 10e (Canyon). Nimrod and Canyon were the only sites where sulfide was successfully measured, although the odor of sulfide was detectable at the other sites. Initial results for sulfide at Nimrod (Figure 11b) showed sulfide oxidizing too quickly through the model study reach. By reducing the sulfide oxidation rate more than an order of magnitude from the default value (25 day^{-1}), a better comparison to the observed data was obtained (Figure 8f). However, the predicted sulfide approaches zero concentration at the end of the study reach, while the observed data appear to remain at 0.01 mg/l . As mentioned in Part III, the data inferred that the oxidation rate of HS^- at Nimrod was on the low side of reported ranges. Also, most of the sulfide for the pH conditions at Nimrod is H_2S , which volatilizes. Adjustments to the reaeration rate K_2 may have improved sulfide predictions. Sulfide was measured at the first station at Canyon ($40 \text{ } \mu\text{g/l}$) but declined to near zero at the other

stations (Nix et al. 1991). The default value for sulfide oxidation was used at this site, and the results compared favorably with observed data (Figure 10e).

109. Final results for DO are shown in Figures 7a (Greeson), 8a (Nimrod), 9a (Rough River), and 10a (Canyon). The only model source of DO for each application was stream reaeration. Reaeration is especially high at the Greeson site (Figure 7a), where DO releases were low due to this site operating for hydropower. For all applications except the Greeson site, stream reaeration was calculated using the O'Connor-Dobbins (1958) equation option in TWQM. Measured stream reaeration rates at Greeson were obtained by Wilhelms (1987) using a hydrocarbon gas tracer method (Rathbun et al. 1977, 1978). However, the Tsivoglou and Wallace (1972) formulation for reaeration (i.e., the energy dissipation method) was also found to yield good results at Greeson (Dortch and Hamlin 1988).

110. The sinks of DO for all applications included SOD and CBOD. Although Mn^{+2} , Fe^{+2} , sulfide, and ammonia oxidation are also sinks of DO, they had little individual effect on DO concentrations, but their cumulative effect was not negligible. The low individual effects were due to the relatively low release concentrations at all the sites.

111. Boundary conditions for CBOD measurements were estimated from the 10-day BOD studies of in-pool samples conducted by Nix et al. (1991). The deepest in-pool sample was used to estimate release CBOD for all sites. The CBOD was estimated by subtracting accountable oxygen demands (i.e., oxidation of reduced substances) from the total oxygen demand. The decrease in reduced substances and/or the increase in the oxidized forms, such as sulfate, was converted to DO equivalents through stoichiometric relationships. Estimated release concentrations for CBOD at all sites were approximately 1 mg/l except Rough River, which was 2 mg/l. SOD rates were calibrated (Table 7) at Greeson and Canyon; measured SOD values (Nix et al. 1991) were used for Rough River and Nimrod. Zero SOD was used at the Greeson site for all reaches except the last reach due to the rocky, cobble substrate conditions. The last reach is characterized as a slower moving stream with silty substrate and a flatter slope; thus, SOD was specified in this reach.

112. With major sources and sinks of DO accounted for, all the predicted DO measurements compared favorably with the observed data except at Rough River (Figure 12a), where data indicated there may be another sink of DO not accounted for in the modeling effort. Based on examination of the total

and dissolved iron measurements, the data indicated that FeS might be present, especially since sulfate increased in the downstream direction. Sulfate also increased with time in the 10-day BOD studies for Rough River. The decision was made to include FeS as a model variable at this site. The FeS boundary conditions were estimated as the difference between total and dissolved iron, yielding a value for FeS of 2.5 mg/l. Final results of Rough River DO are shown in Figure 9a and compare favorably with observed data. The reaeration through the mill dam is also evident in Figure 9a; this reaeration was modeled using the equation of Gameson (Brown and Barnwell 1987).

113. The other data sets were examined for the possible presence of FeS, but only the Nimrod site, in addition to Rough River, indicated the possible presence of FeS. A substantial difference in total and dissolved iron occurred at Nimrod, which could be attributed to FeS. However, there was no increase in sulfate in the tailwater. If FeS was present, it must have oxidized rapidly as it passed through the release structure and the first 200 m of the tailwater.

114. Dissolved iron (i.e., Fe^{+2}) was modeled for Nimrod and Rough River (Figures 8g and 9f, respectively); very little iron was detected at the Greeson and Canyon sites. The model shows reduced iron decreasing rapidly to values near zero, whereas the data indicate that dissolved iron decreases much more slowly and does not reach zero. Nimrod data actually indicate that dissolved iron does not decrease after traveling through the first few kilometers of tailwater. As discussed earlier, it is suspected that fine particulate iron passed through the filter, thus yielding an inaccurate measurement of dissolved iron.

PART V: CONCLUSIONS AND RECOMMENDATIONS

115. The studies reported herein were an attempt to obtain an improved understanding of water quality processes in reservoir tailwaters. The focus was on DO and the removal and/or oxidation of reduced substances (e.g., dissolved iron and manganese, sulfide, and ammonia) present in deep releases from anoxic reservoir strata. The intent of the analyses was to develop kinetic descriptions and rates for constructing a model of water quality in reservoir tailwaters. An attempt was made to develop relationships to predict kinetic rate coefficients based on ambient stream conditions.

116. Much information was gained from the dissolved manganese and ammonia data collected in this study. It was possible to develop relationships to predict the removal rate of dissolved manganese through adsorption onto the streambed. These relationships are based on the type of streambed (i.e., sediment or cobble) and the stream hydraulic conditions, which affect the diffusive sublayer thickness and the bed/water column mass transfer rate. Similarly, a relationship for the nitrification rate was developed using stream hydraulic conditions. The predictive relationship for nitrification was not as strongly correlated to hydraulic conditions as the relationship for manganese removal. Both relationships were developed from results of four field study sites; thus, only through studies at other sites can the relationships be further improved.

117. Data limitations precluded the development and/or improvement of predictive relationships for reduced iron, sulfide, and iron sulfide oxidation rates. Methods for measuring reduced (i.e., dissolved) iron and dissolved sulfide were not adequate to accurately account for the oxidation and/or removal of these substances from the tailwater. Additionally, the data suggest that iron sulfide was present in the releases at several of the sites, further complicating the studies. A limited amount of data was used to assess existing equations for predicting iron and sulfide oxidation rates. These results, although far from conclusive, did suggest that existing rate equations could be used as a rough estimate for oxidation rates.

118. Future studies should further address the oxidation/removal kinetics of iron, sulfide, and iron sulfide. Proper methods for sampling, handling, and analysis must be prescribed to better quantify concentrations of ferrous and ferric iron and iron sulfide. For example, Nix et al. (1991) recommended that a 0.1- μ (rather than 0.45- μ) filter be used to separate

dissolved and particulate iron. The sulfide analysis technique of Hongzhang (1982), which was used during the latter stages of the field studies by Nix et al. (1991), shows much promise for measuring low concentrations of sulfide. A technique must be identified to distinguish the amount of particulate iron that is iron sulfide versus ferric iron. After prescribing improved sampling and analysis procedures, field studies similar to the ones reported in this study should be undertaken to yield information concerning kinetic rates. Laboratory kinetic rate studies would also greatly expedite the development of general predictive relationships for processes that are not dependent on stream substrate and hydraulics.

119. The results of the 10-day BOD studies (Nix et al. 1991) indicate that little of the oxygen demand of hypolimnetic water is caused by the decomposition of organic carbon. However, these results were not conclusive because of the analytical problems discussed above for iron and sulfide. If future studies are conducted to investigate iron and sulfide, 10-day BOD studies should be conducted to more accurately delineate any DO demand arising from organic carbon synthesis. These studies should be conducted with and without seeded bacteria. Some consideration should also be given to detecting methane and any associated DO demand.

120. The model developed in this work (TWQM) is considered to have performed well for DO, dissolved manganese, nitrogen species, and dissolved sulfide. The relationships for predicting dissolved manganese removal rates are considered to be applicable for tailwaters that have experienced deep releases containing reduced manganese. For sites that do not have such releases but are considering a deep release (such as opening a bottom sluice that is rarely used), it may take some time (on the order of weeks) for the tailwater to acclimate and form a substrate that effectively sorbs dissolved manganese. The predictive equations for manganese removal do not account for any acclimation period.

121. Although the data for hydrogen sulfide were limited, the model should provide reasonable estimates since the formulations are based in part on volatilization, which is fairly well understood. Although the model contains simplistic algorithms for dissolved iron and iron sulfide, the lack of adequate field data prohibited the development of general relationships for kinetic rates or proper evaluation of model results. As discussed above, more work is required to better resolve the kinetics of dissolved iron and iron sulfide.

122. It is recommended that future extensions of the model include the capability to predict pH changes in the tailwater. This could be accomplished by building in CO₂, alkalinity, and carbonate equilibria. The escape of CO₂ through the air-water interface can be modeled like other gas exchange processes, such as reaeration and volatilization of H₂S. As CO₂ escapes, pH increases. Since pH affects other processes, such as the rate of oxidation of reduced iron, incorporating pH would advance the utility of the model.

REFERENCES

- American Public Health Association, American Water Works Association, and Water Pollution Control Federation. 1981. Standard Methods for the Examination of Water and Wastewater, 16th ed., Washington, DC.
- Almgren, T., and Hagstrom, I. 1974. "The Oxidation Rate of Sulfide in Sea Water," Water Research, Vol 8, pp 395-400.
- Avrahami, M., and Golding, R. M. 1968. Journal of the Chem. Society of America, pp 647-651.
- Benefield, L. D., Judkins, J. F., and Weand, B. L. 1982. Process Chemistry for Water and Wastewater Treatment, Prentice-Hall, Englewood Cliffs, NJ.
- Benton, D. J. 1987. "User Guide to TPL0T Generalized Plot Package" (Version 4.4), Norris, TN.
- Berner, R. A. 1980. Early Diagenesis. A Theoretical Approach, Princeton University Press, Princeton, NJ.
- Bohac, C. E., Boyd, J. W., Harshbarger, E. D., and Lewis, A. R. 1983. "Techniques for Reaeration of Hydropower Releases," Technical Report E-83-5, US Army Engineer Waterways Experiment Station, Vicksburg, MS.
- Boudreau, B. P., and Guinasso, N. L., Jr., 1982. "The Influence of a Diffusive Sublayer on Accretion, Dissolution, and Diagenesis at the Sea Floor," The Dynamic Environment of the Ocean Floor, K. A. Fanning and F. T. Manheim, eds., Lexington Books, Lexington, MA.
- Bowie, G. L., Mills, W. B., Porcella, D. B., Campbell, C. L., Pagenkopf, J. R., Gretchen L. R., Johnson, K. M., Chan, P. W. H., Gherini, S. A., and Chamberlin, C. E. 1985. "Rates, Constants, and Kinetics Formulations in Surface Water Quality Modeling," 2d ed., EPA/600/3-85/040, US Environmental Protection Agency, Athens, GA.
- Brown, L. C., and Barnwell, T. O. 1987. "The Enhanced Stream Water Quality Models QUAL2E and QUAL2E-UNCAS: Documentation and User Manual," EPA/600/3-87/007, US Environmental Protection Agency, Athens, GA.
- Chen, K. Y., and Morris, J. C. 1972a. "Oxidation of Aqueous Sulfide by O₂; 1. General Characteristics and Catalytic Influences," Advances in Water Pollution Control Research, S. H. Jenkins, ed., Pergamon Press, New York.
- _____. 1972b. "Kinetics of Oxidation of Aqueous Sulfide by O₂," Environmental Science and Technology, Vol 6, No. 6, pp 529-537.
- Churchill, M. A., Elmore, H. L., and Buckingham, R. A. 1962. "The Prediction of Stream Reaeration Rates," International Journal of Air and Water Pollution, Vol 6, pp 467-504.
- Connell, W. E. 1966. "The Reduction of Sulfate to Sulfide Under Anaerobic Soil Conditions," M.S. thesis, Louisiana State University, Baton Rouge, LA.
- Davis, J. E., Holland, J. P., Schneider, M. L., and Wilhelms, S. C. 1987. "SELECT: A Numerical, One-Dimensional Model for Selective Withdrawal," Instruction Report E-87-2, US Army Engineer Waterways Experiment Station, Vicksburg, MS.

- Dortch, M. S., and Hamlin, D. E. 1988. "Research on Water Quality of Reservoir Tailwaters," WOTS Information Exchange Bulletin, Vol E-88-2, US Army Engineer Waterways Experiment Station, Vicksburg, MS.
- Dortch, M. S., and Martin, J. L. 1989. "Water Quality Modeling of Regulated Streams," Alternatives in Regulated River Management, J. A. Gore and G. E. Petts, eds., CRC Press, Boca Raton, FL.
- Fischer, H. B., List, E. J., Koh, R. C. Y., Imberger, J., and Brooks, N. H. 1979. Mixing in Inland and Coastal Waters, Academic Press, New York.
- Golden Software, Inc. 1988. "GRAPHER Reference Manual," Golden, Co.
- Gordon, J. A. 1983. "Iron, Manganese and Sulfide Mechanics in Streams and Lakes--A Literature Review," Report No. TTU-CE-83-2, Department of Civil Engineering, Tennessee Technical University, Cookeville, TN.
- _____. 1989. "Manganese Oxidation Related to the Releases from Reservoirs," Water Resources Bulletin, Vol 25, No. 1, pp 187-192.
- Gordon, J. A., Bonner, W. P., and Milligan, J. D. 1984. "Iron, Manganese and Sulfides Downstream from Normandy Dam," Lake and Reservoir Management, Report No. 440/5/84-001, US Environmental Protection Agency, pp 58-62.
- Gordon, J. A., and Burr, J. L. 1989. "Treatment of Manganese from Mining Seep Using Packed Columns," Journal of Environmental Engineering, Vol 115, No. 2, pp 386-394.
- Hatcher, K. J. 1986. "Sediment Oxygen Demand: Processes, Modeling, and Measurement," Institute of Natural Resources, University of Georgia, Athens, GA.
- Hess, G. W. 1984. "A Transport Model of Manganese in Rivers," M. S. thesis, Georgia Institute of Technology, Atlanta, GA.
- Hess, G. W., Byung, R. K., and Roberts, P. J. W. 1989. "A Manganese Oxidation Model for Rivers," Water Resources Bulletin, Vol 25, No. 2, pp 359-365.
- Hill, A. R. 1979. "Denitrification in the Nitrogen Budget of a River Ecosystem," Nature, Vol 281, pp 291-292.
- Hill, A. R., and Sanmugadas, K. 1985. "Denitrification Rates in Relation to Stream Sediment Characteristics," Water Research, Vol 19, No. 12, pp 1579-1586.
- Hongzhang, W. 1982. "Visual Mercurimetric Titration Method for the Determination of Hydrogen Sulfide in Air and Water at ppb Levels," Chemical Abstracts, Vol 97, No. 202959h (translated from Chinese by Language Services, Knoxville, TN).
- Hsiung, T. M. 1987. "Manganese Dynamics in the Richard B. Russell Impoundment," M.S. thesis, Clemson University, Clemson, SC.
- Langbien, W. B., and Durum, W. H. 1967. "The Aeration Capacity of Steams," Circular 542, US Geological Survey, Washington, DC.
- Lyman, W. J., Reehl, W. F., and Rosenblatt, D. H. 1982. Handbook of Chemical Property Estimation Methods, McGraw-Hill, New York.
- McCutcheon, S. C. 1989. Water Quality Modeling: Vol I. Transport and Surface Exchange in Rivers, R. H. French, ed., CRC Press, Boca Raton, FL.
- Millero, F. J. 1986. "The Thermodynamics and Kinetics of the Hydrogen Sulfide System in Natural Waters," Marine Chemistry, Vol 18, pp 121-147.

- Morgan, J. J. 1967. "Chemical Equilibria and Kinetic Properties of Manganese in Natural Waters," Principles and Applications of Water Chemistry, S. U. Faust and J. V. Hunter, eds., Wiley & Sons, New York, pp 561-624.
- Nix, J. 1986. "Spatial and Temporal Distribution of Sulfide and Reduced Metals in the Tailwater of Narrows Dam (Lake Greeson), Arkansas," Technical Report E-86-14, US Army Engineer Waterways Experiment Station, Vicksburg, MS.
- Nix, J., Hamlin-Tillman, D. E., Ashby, S. L., and Dortch, M. S. 1991. "Water Quality of Selected Tailwaters," Technical Report W-91-2, US Army Engineer Waterways Experiment Station, Vicksburg, MS.
- Noike, T., Kanji, N., and Jun'ichiro, M. 1983. "Oxidation of Ferrous Iron by Acidophilic Iron-Oxidizing Bacteria from a Stream Receiving Acid Mine Drainage," Water Research, Vol 17, pp 21-27.
- O'Brien, D. J., and Birkner, F. B. 1977. "Kinetics of Oxygenation of Reduced Sulfur Species in Aqueous Solution," Environmental Science and Technology, Vol 11, No. 12, pp 1114-1120.
- O'Connor, D. J., and Dobbins, W. E. 1958. "The Mechanism of Reaeration in Natural Stream," Journal of the Sanitary Engineering Division, American Society of Civil Engineers, Vol 82, pp 1-30.
- Owens, M., Edwards, R. W., and Gibbs, J. W. 1964. "Some Reaeration Studies in Streams," International Journal of Air and Water Pollution, Vol 8, No. 8/9, pp 469-486.
- Paschke, R. A., Hwang, Y. S., and Johnson, D. W. 1977. "Catalytic Oxidation of Sulfide Wastewater from a Cellulose Sponge-Making Operation," Journal of the Water Pollution Control Federation, pp 2445-2452.
- Rathbun, R. E., Shultz, D. J., Stephens, D. W., and Tai, D. Y. 1977. "Experimental Modeling of the Oxygen Absorption Characteristics of Streams and Rivers," Proceedings: Seventeenth Congress of the International Association of Hydraulic Research, 15-19 August, Baden, Federal Republic of Germany.
- Rathbun, R. E., Shultz, D. J., Stephens, D. W., and Tai, D. Y. 1978. "Laboratory Studies of Gas Tracers for Reaeration," Journal of the Environmental Engineering Division, American Society of Civil Engineers, Vol 104, No. EE2, pp 215-229.
- Roache, P. J. 1972. Computational Fluid Dynamics, Hermosa Publishing, Albuquerque, NM.
- Sarikaya, H. Z. 1990. "Contact Aeration for Iron Removal--A Theoretical Assessment," Water Research, Vol 24, No. 3, pp 329-331.
- SAS Institute, Inc. 1988. "SAS/STAT User's Guide," Statistical Analysis System, Inc., Cary, NC.
- Stumm, W., and Morgan, J. J. 1981. Aquatic Chemistry, an Introduction Emphasizing Chemical Equilibria in Natural Waters, 2d ed., Wiley-Interscience, New York.
- Sung, W., and Morgan, J. J. 1980. "Kinetics and Products of Ferrous Iron Oxygenation in Aqueous Systems," Environmental Science and Technology, Vol 14, No. 5, pp 561-568.
- TenEch Environmental Consultants, Inc. 1978 (Jul). "Waste Load Allocation Verification Study: Final Report," prepared for Iowa Department of Environmental Quality.

- Thackston, E. L., and Krenkel, P. A. 1969. "Reaeration Prediction in Natural Streams," Journal of the Sanitary Engineering Division, American Society of Civil Engineers, Vol 95, No. SA1, pp 65-94.
- Thibodeaux, L. J. 1979. Chemodynamics: Environmental Movement of Chemicals in Air, Water, and Soil, Wiley & Sons, New York.
- Thomann, R. V., and Mueller, J. A. 1987. Principles of Surface Water Quality Modeling and Control, Harper & Row, New York.
- Tsivoglou, E. C., and Wallace, J. R. 1972. "Characterization of Stream Reaeration Capacity," EPA-R3-72-012, Ecology Research Service, Office of Research and Monitor, US Environmental Protection Agency, Washington, DC.
- Wetzel, R. G. 1975. Limnology, W. B. Saunders Company, Philadelphia, PA.
- Wilhelms, S. C. 1987. "Results of Reaeration Study on Little Missouri River, Narrows Dam, Arkansas," Memorandum for Record, US Army Engineer Waterways Experiment Station, Vicksburg, MS.
- Wilmot, P. D., Cadee, K., Katinic, J. J., and Kavanagh, B. V. 1988. "Kinetics of Sulfide Oxidation by Dissolved Oxygen," Journal of the Water Pollution Control Federation, Vol 60, No. 7, pp 1264-1270.
- Wilson, W. E. 1980. "Surface and Complexation Effects on the Rate of Mn(II) Oxidation in Natural Waters," Geochimica et Cosmochimica Acta, Vol 44, pp 1311-1317.

APPENDIX A: 1989 NIMROD TAILWATER DATA

Table A1
Lake Nimrod High Flow (200 cfs)

<u>Station</u>	<u>Time</u>	<u>Temp.</u> <u>°C</u>	<u>DO</u> <u>mg/l</u>	<u>pH</u>	<u>Specific</u> <u>Conductance, μS/cm*</u>		
<u>August 23, 1989</u>							
A	1634	26.0	7.0	6.5	51		
B1	1615	27.0	26.2	6.5	48		
B2	1548	25.5	6.8	6.6	48		
B3	1519	27.0	6.7	6.5	48		
C	1443	28.0	6.7	6.5	46		
D	1405	26.5	5.9	6.5	46		
<u>August 24, 1989</u>							
A	1045	29.0	7.0	6.5	49		
B1	1015	29.0	6.7	6.5	50		
B2	955	27.0	6.6	6.5	48		
B3	920	27.0	6.5	6.5	48		
C	815	22.5	6.1	6.5	47		
D	815	21.5	5.8	6.4	46		
<u>Station</u>	<u>Turbidity</u> <u>NTU</u>	<u>Alkalinity</u> <u>mg/l</u>	<u>CO₂</u> <u>mg/l</u>	<u>TOC</u> <u>mg/l</u>	<u>TKN</u> <u>mg/l</u>	<u>NH₄-N</u> <u>mg/l</u>	<u>No₃N</u> <u>mg/l</u>
<u>August 23, 1989</u>							
A	36	16	6	7.	0.6	0.28	0.03
B1	24	19	5	7.	0.5	0.22	0.04
B2	23	14	5	5.	0.6	0.20	0.07
B3	23	14	5	6.	0.6	0.18	0.07
C	22	15	4	6.	0.6	0.14	0.10
D	16	14	6	5.	0.5	0.07	0.14
<u>August 24, 1989</u>							
A	29	16	5	6.	0.7	0.26	0.02
B1	30	16	5	6.	0.8	0.25	0.03
B1 (R)	27	16	6	6.	0.6	0.26	0.04
B2	28	16	5	6.	0.7	0.25	0.08
B3	21	15	6	6.	0.7	0.22	0.08
C	19	15	6	6.	0.5	0.19	0.11
D	18	14	6	5.	0.5	0.10	0.15

(Continued)

* μ S = μ mhos/cm.

Table A1 (Concluded)

<u>Station</u>	<u>S⁻²</u> <u>μg/l</u>	<u>SO₄⁻²</u> <u>mg/l</u>	<u>cl⁻</u> <u>mg/l</u>	<u>Total Fe</u> <u>mg/l</u>	<u>Diss. Fe</u> <u>mg/l</u>	<u>Total Mn</u> <u>mg/l</u>	<u>Diss. Mn</u> <u>mg/l</u>
<u>August 23, 1989</u>							
A	16	2.7	2.0	2.6	1.0	1.30	1.2
B1	17	2.9	1.9	2.1	0.8	1.00	1.0
B2	11	2.9	2.0	1.9	0.7	0.90	0.8
B3	10	3.0	2.1	1.7	0.7	0.88	0.7
C	9	3.2	2.0	1.6	0.7	0.71	0.6
D	10	3.0	2.1	1.3	0.7	0.41	0.3
<u>August 24, 1989</u>							
A	17	2.7	1.9	2.4	0.9	1.20	1.1
B1	12	3.2	2.0	2.2	0.9	1.20	1.1
B1 (R)	11	2.7	2.0	2.2	0.9	1.20	1.1
B2	11	2.8	2.0	2.1	0.8	1.10	1.0
B3	10	1.9	3.0	1.9	0.8	0.95	0.8
C	11	2.9	2.0	1.8	0.8	0.82	0.7
D	10	2.8	2.0	1.4	0.8	0.42	0.3

Note: B1 (R) is a repeated sampling of station B1.

Table A2
Lake Nimrod Profiles

<u>Depth, m</u>	<u>Temperature</u> °C	<u>DO</u> mg/l	<u>pH</u>	<u>Specific</u> <u>Conductance, μs/cm</u>
<u>August 23, 1989, 0745 hr</u>				
0	28.3	5.4	6.7	40
1	28.3	5.3	6.6	40
2	28.1	4.1	6.6	40
3	27.9	3.3	6.6	40
4	27.4	2.2	6.4	41
5	26.6	0.7	6.3	42
6	26.2	0.1	6.2	44
7	26.0	0.0	6.2	47
8	25.9	0.0	6.2	49
9	25.7	0.0	6.2	55
10	25.0	0.0	6.2	64
<u>August 23, 1989, 1845 hr</u>				
0	28.0	6.4	6.8	41
1	28.2	4.4	6.7	41
2	27.6	2.1	6.5	41
3	26.5	0.2	6.4	44
4	26.3	0.1	6.3	46
5	26.2	0.0	6.3	46
6	26.1	0.0	6.2	47
7	26.0	0.0	6.2	52
8	25.7	0.0	6.2	61
9	25.5	0.0	6.2	61
10	24.8	0.0	6.2	71
<u>August 24, 1989, 0650 hr</u>				
0	27.2	3.0	6.4	42
1	27.2	3.1	6.4	42
2	27.2	3.0	6.4	42
3	27.2	2.8	6.3	42
4	26.8	0.6	6.2	42
5	26.2	0.0	6.2	46
6	26.0	0.0	6.2	49
7	25.9	0.0	6.2	50
8	25.8	0.0	6.1	55
9	25.6	0.0	6.1	57
10	24.9	0.0	6.2	67

(Continued)

Table A2 (Concluded)

<u>Depth, m</u>	<u>Temperature</u> <u>°C</u>	<u>DO</u> <u>mg/l</u>	<u>pH</u>	<u>Specific</u> <u>Conductance, μs/cm</u>
<u>August 24, 1989, 1400 hr</u>				
0	31.2	7.0	6.8	41
1	30.9	6.8	6.8	41
2	30.1	6.4	6.7	41
3	28.2	2.9	6.5	42
4	27.8	2.9	6.1	42
5	27.5	0.2	6.1	41
6	26.6	0.0	6.1	47
7	26.4	0.0	6.1	50
8	26.3	0.0	6.1	51
9	26.2	0.0	6.1	53
10	25.7	0.0	6.1	61

Table A3
Lake Nimrod In-pool Water Quality

<u>Sample</u>	<u>Lab pH</u>	<u>Free CO₂ mg/l</u>	<u>Total Fe mg/l</u>	<u>Dissolved Fe mg/l</u>	<u>Total Mn mg/l</u>	<u>Dissolved Mn mg/l</u>	<u>S⁻² μg/l</u>
<u>August 23, 1989</u>							
N-1-0	6.64	4	0.82	0.41	0.09	0.00	6
N-1-1	6.60	4	0.79	0.35	0.09	0.01	7
N-1-2	6.60	6	0.84	0.45	0.10	0.01	7
N-1-3	6.54	7	0.93	0.47	0.12	0.01	6
N-1-4	6.47	8	0.95	0.48	0.14	0.02	8
N-1-5	6.33	10	1.4	0.57	0.45	0.30	9
N-1-5R	6.33	9	1.4	0.55	0.38	0.24	10
N-1-6	6.36	10	1.5	0.57	0.47	0.30	10
N-1-7	6.41	11	2.0	0.48	0.90	0.79	10
N-1-8	6.39	10	2.1	0.43	1.1	1.0	14
N-1-9	6.40	12	2.6	0.90	1.5	1.4	14
N-1-10	6.39	13	3.2	1.4	1.9	1.8	30

<u>Sample</u>	<u>NH₄^{-N} mg/l</u>	<u>NO₃-N mg/l</u>	<u>SO₄⁻² mg/l</u>	<u>c/- mg/l</u>	<u>TOC mg/l</u>	<u>DOC mg/l</u>	<u>TKN mg/l</u>	<u>Alkalinity mg/l</u>	<u>Turbidity NTU</u>
<u>August 23, 1989</u>									
N-1-0	0.02	0.03	3.90	2.2	4.4	3.1	0.4	11	
N-1-1	0.03	0.02	2.89	2.0	4.2	3.0	0.8	11	10.0
N-1-2	0.05	0.03	2.99	2.1	4.2	3.2	0.6	11	11.0
N-1-3	0.08	0.03	3.20	2.2	4.1	3.3	0.6	11	14.0
N-1-4	0.08	0.03	3.36	2.1	5.3	3.3	0.5	11	11.0
N-1-5	0.14	0.03	3.98	2.0	4.4	3.6	0.8	12	20.0
N-1-5R	0.13	0.02	3.64	1.9	4.5	3.4	0.8	12	21.0
N-1-6	0.13	0.02	3.10	2.0	4.1	3.2	0.6	12	21.0
N-1-7	0.20	0.02	2.94	2.0	4.2	3.4	0.7	14	31.0
N-1-8	0.23	0.05	3.54	2.4	3.9	3.8	0.7	14	30.0
N-1-9	0.32	0.04	3.27	2.4	4.0	3.4	0.7	17	35.0
N-1-10	0.42	0.06	2.75	2.5	4.7	3.3	0.08	18	39.0

APPENDIX B: MODEL OPERATION

Introduction

1. The Tailwater Quality Model (TWQM) is a user-friendly, interactive, menu-driven, PC-based model of water quality in reservoir tailwaters. TWQM computes the one-dimensional (1D), longitudinal, steady-state distribution of water quality along the stream axis, beginning at the reservoir release and progressing downstream for any number of miles as specified by the user. The model was developed to evaluate downstream water quality characteristics resulting from reservoir releases. Examples of the types of issues affecting tailwater quality that might be addressed include:

- a. Changes in the reservoir outlet elevation and/or release flow.
- b. Changes in release reaeration characteristics, such as adding hydropower (i.e., add-on hydropower).
- c. Changes in release water quality due to degradation of in-pool water quality.
- d. Changes in the downstream channel, such as reregulation.

TWQM focuses on the problematic water quality variables, such as low dissolved oxygen and reduced substances (e.g., dissolved iron, dissolved manganese, ammonium, and sulfide), but includes biochemical oxygen demand, major nutrients, and algae. The model can also be used to evaluate the downstream distance required for recovery of water quality to some standard. TWQM is designed for ease of application with limited input requirements (due mainly to the steady-state assumption). A first-time user should be able to apply the model within a few days. An experienced user should be able to apply the model within a day, given that all the data are in hand.

2. TWQM is composed of a number of programs (i.e., pre- and post-processor programs and a numerical model) that are menu driven. TAILWTR.FOR is the numerical one-dimensional tailwater model based on the US Environmental Protection Agency riverine water quality model QUAL2E. TAILWTR.FOR predicts estimates of constituent concentrations in a river reach based on the input parameters given. The main batch file that executes all the programs that make up TWQM is TWQB.BAT. Descriptions of each program and its output are given in Table B1. The order in which TWQB.BAT calls these files is shown in Figure B1. The first several programs executed by TWQB are pre-processor programs that assist the user in using TWQM (giving general information and instructions) and also assist the user in creating an input data set for

Table B1
TWQM File Description

File	Description
TWQB.BAT	Batch program that runs all files contained in the Tailwater Quality Model.
TEXPLAIN.FOR	Prints screens containing general information and instructions for TWQM.
TMENU.FOR	Allows the user to select which water quality constituents are to be modeled and input headwater boundary conditions for those constituents selected.
TWQI.FOR	Creates the input data file required by TAILWTR.FOR. Also creates the file containing observed data, OBSERVED.DAT, which is used by K4GRAPH.BAT to graph observed data.
TFIX.FOR	Allows the user to alter an existing input data file.
TAILWTR.FOR	Determines the tailwater quality of dam discharges. Creates a user-named output file, and the files PREDICT.DAT and PREDICT.HYD.
TREFORM.FOR	Reads PREDICT.DAT and PREDICT.HYD and combines them into one file, TPREDICT.DAT.
TPREDICT.DAT	Data file for all graphing (graph viewed on monitor) and plotting (hard copy of graph) files. Contains output for all elements for selected constituents from the last run of TAILWTR.FOR.
TPFILE.FOR and TPFILEPL.FOR	Creates the files used by TPGRAPH.BAT (*.TPL) and TPLOT.BAT (*.PLT) for graphing and plotting TAILWTR.FOR output.
TWGRAPH.BAT and TWPLOT.BAT	Batch files which call the graphing and plotting programs written for GRAPHER software (Golden Software, Inc. 1988). Uses files with AXS, GRF, and PLT extensions.
TPGRAPH.BAT and TPLOT.BAT	Batch files which call graphing and plotting software written for TPLOTT software (Benton 1987). Uses files with TPL and PLT extensions.

TAILWTR.FOR. Output from TAILWTR.FOR is plotted using commercial software such as GRAPHER (Golden Software, Inc. 1988)* or TPLOTT (Benton 1987).

Tailwater Model Input Screens

3. The TWQM is a user-friendly, interactive model. Screens have been developed to assist the user with model operations and to prompt the user for appropriate information. The initial screens contain cautionary comments about the model and input requirements. If the user chooses to create a new input data set for TAILWTR.FOR, he is prompted for the data required. In many instances these screens already contain default values for the data. To select ALL of the default values shown on a screen, answer no (N) when asked if changes need to be made. To select some of the default values shown on the screen and enter new values for the others, enter yes (Y). Enter the new values where desired and press ENTER to go to the next value. To select the default value shown, press ENTER. The TWQM is very specific on how the data are input with respect to integer and real numbers. Unless prompted otherwise, all numerical input should be real. A note to this effect will appear on all screens. In instances where integer input is required, a note will appear indicating so.

4. The user is required to input information in TMENU, TWQI, TFIX, TAILWTR, and the graphics program GRAFMENU.BAT (optional). In all cases the required input will be an answer to a direct question appearing on the screen. Types of entries required by the user are real or integer numbers, yes or no answers, data file names, or a short descriptive text (i.e., river name).

5. In the following section, screens are shown in the order that they appear to the user when explanatory/cautionary comments are required for clarification, or when user input is required. A short description of each screen, along with information concerning the input, is also included.

* See References at the conclusion of the main text.

Screens in TWQI.FOR

12. TWQI is the main interactive program in TWQM and serves as a preprocessor that generates the input data file for TAILWTR. Since TAILWTR was developed using QUAL2E, the data file generated by TWQI is very similar to a QUAL2E input data file.

13. TWQI prompts the user for most input required to generate a data file for TAILWTR. Some data such as evaporation coefficients and certain constants are included in TWQI but are not user definable and will not appear on any menus. There is usually a default value for the data that the user must enter. The notable exceptions are input dealing with flow and location (river mile). A value **MUST** be entered for these before any simulation can be performed even though a default value of 0.0 appears on the screen.

14. TWQI is very specific concerning input format. The importance of reading and following the directions at the bottom of each screen cannot be overemphasized. Most values that are input into TWQI must be real numbers. However, there are certain instances when integer values are required by TWQI. Unless indicated otherwise, all numeric input is to be in real numbers.

15. The first screen of TWQI is the title screen which contains a description of TWQI (Figure B9). Upon pressing RETURN (or ENTER), TWQI prompts the user for the name of the input data file TWQI will generate. This file will be a new file; the name of an existing file must not be used. If the file name of an existing file is used, TWQI will stop. This precaution prevents a user from erroneously writing over an existing data file. The file name must not exceed eight characters and may have an extension of up to three characters.

K₂ Option 3

27. O'Connor and Dobbins (1958) proposed equations based on the turbulence characteristics of a stream. For streams that have low velocities and isotropic conditions, the equation is given as

$$K_{2_{20}} = \frac{(D_m \bar{u})^{0.5}}{d^{1.5}} \quad (B2)$$

28. For streams with higher velocities and nonisotropic conditions, the equation is given as

$$K_{2_{20}} = \frac{480 D_m^{0.5} S_o^{0.25}}{d^{1.25}} 2.31 \quad (B3)$$

where

D_m = molecular diffusion coefficient, ft²/day and is found as
 $D_m = 1.91 \times 10^3 (1.037)^{T-20}$

S_o = slope of the streambed, ft/ft

d = mean stream depth, ft

Equation B2 has been found to be generally applicable to most streams and is the default K_2 option for TAILWTR.

K₂ Option 4

29. Owens, Edwards, and Gibbs (1964) estimated reaeration coefficients for shallow, fast-moving streams based on six streams in England. Combining their work with that of Churchill, Elmore, and Buckingham (1962), they developed an equation for streams having depths of 0.4 to 11.0 ft and velocities of 0.1 to 5.0 ft/sec. Their equation is written as

$$K_{2_{20}} = \frac{9.4 \bar{u}^{0.67}}{d^{1.85}} 2.31 \quad (B4)$$

where

\bar{u} = mean velocity, ft/sec

d = mean depth, ft

K₂ Option 5

30. Thackston and Krenkel (1966) proposed the following equation based on their investigation of several rivers in the Tennessee Valley Authority system.

$$K_{2_{20}} = 10.8 (1 + F^{0.5}) \frac{u_*}{d} 2.31 \quad (B5)$$

where F is the Froude number, which is given by

$$F = \frac{u_*}{\sqrt{gd}} \quad (B6)$$

and u_* is the shear velocity (ft/sec) given by

$$u_* = \sqrt{dS_e g} = \frac{\bar{u} n \sqrt{g}}{1.49 d^{1.167}} \quad (B7)$$

where

d - mean depth, ft

S_e - slope of the energy gradient

g - acceleration of gravity, ft/sec²

\bar{u} - mean velocity, ft/sec

n - Manning's coefficient

K₂ Option 6

31. Langbien and Durum (1967) developed a formula for K₂ at 20 °C:

$$K_{2_{20}} = 3.3 \frac{\bar{u}}{d^{1.33}} 2.31 \quad (B8)$$

where

\bar{u} - mean velocity, ft/sec

d - mean depth, ft

K₂ Option 7

32. Option 7 computes the reaeration coefficient from a power function of flow and is given by

$$K_2 = aQ^b \quad (B9)$$

where

a - coefficient of flow for K₂

Q - flow, ft³/sec

b - exponent on flow for K₂

K₂ Option 8

33. Tsivoglou and Wallace (1972) based their method on the assumption that the reaeration coefficient for a reach is proportional to the change in elevation of the water surface in the reach and inversely proportional to the flow time through the reach. Their equation is written as

$$K_{2,0} = c \frac{\Delta h}{t_f} \quad (B10)$$

where

c - escape coefficient, 1/ft

Δh - change in water surface elevation in reach, ft

t_f - flow time through reach, days

34. Assuming uniform flow, the change in water surface elevation is

$$\Delta h = S_0 \Delta x \quad (B11)$$

where

S₀ - slope of energy gradient, ft/ft

Δx - reach length, ft

and the flow time through the reach is

$$t_f = \frac{\Delta x}{\bar{u}} \quad (\text{B12})$$

where \bar{u} is the mean velocity in the reach (ft/sec).

35. Substituting Equations B11 and B12 into B10 gives

$$K_{2_{20}} = (3,600 \times 24) c S_e \bar{u} \quad (\text{B13})$$

36. Equation B13 is the formula used for Option 8 in TAILWTR.FOR. The constants 3,600 and 24 convert velocity to units of feet per day. The slope is input directly for computing K_2 with this option. The escape coefficient can be estimated based on recommendations of TenEch (1978) using

$$c = 0.054 \text{ ft}^{-1} \text{ (at } 20 \text{ }^\circ\text{C) for } 15 \leq Q \leq 3,000 \text{ ft}^3/\text{sec}$$

$$c = 0.110 \text{ ft}^{-1} \text{ (at } 20 \text{ }^\circ\text{C) for } 1 \leq Q \leq 15 \text{ ft}^3/\text{sec}$$

37. Any of the methods listed can be selected by entering their corresponding number (real number). If K_2 option 1, 7, or 8 is selected, TWQI will prompt the user to input the appropriate coefficients or values.

Screens in TFIX.FOR

48. TFIX allows the user to make changes to an existing TAILWTR input data file. Only certain information entered using TWQI may be altered with TFIX. Data that cannot be changed using TFIX are variables such as the number of reaches and number of point loads, because new lines of data would have to be entered into the input data set. TFIX does not allow lines to be added, only changed. Items such as headwater, initial, or point load conditions, simulation date, and theta values can be changed in TFIX. If the user must add a new reach or point load, then TWQI should be run or the new information manually entered into the input data set.

49. To alter an existing data file using TFIX instead of creating a new one with TWQI, the user types TWQB OLD when beginning the batch program. This causes TWQB to skip TEXPLAIN, TMENU, TWQI, and proceed directly to TFIX. Once TFIX is exited, TAILWTR is run automatically along with the graphics options. If OLD is not specified when TWQB is begun, then TFIX is not run.

50. The first input for TFIX are the names of the existing data file and the name of the new file to be created. Data from the existing file are read, and can be altered if necessary. These data are then stored in the new data file.

52. Each of the first eight options has its own screen. The cursor will go to each item on the screen. The user makes changes by entering the new value when the cursor is in the appropriate place. To accept the value shown, the user presses the ENTER key. None of these screens allows the user to go back and make changes if mistakes were made entering new values. TFIX will have to be rerun to correct a mistake.

Screens in TAILWTR.FOR

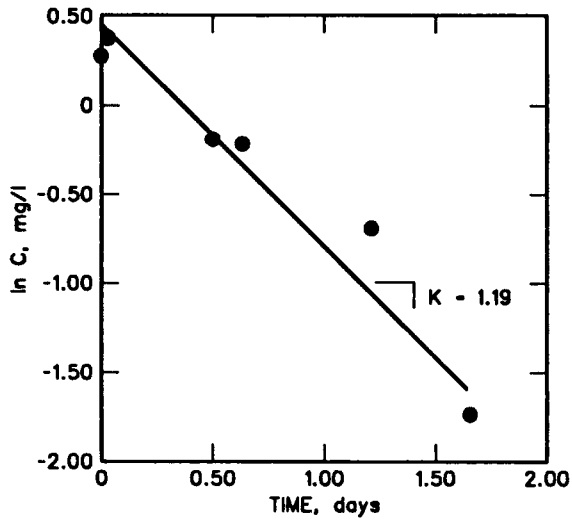
53. TAILWTR requires only the name of the input data file and the name of the output file. The input data file will usually be the data file just created by TWQI. However, the name of any old input data file can be entered. There are three options concerning output. It can be written to the screen, written directly to a printer, or written to a file. The final option is suggested due to the volume of output generated. To have the output written to a file, enter the name of the output file at the prompt concerning the output device. The name of the file can be up to eight characters long with an extension of three characters.

54. When running, TAILWTR will print messages to the screen indicating what tasks are being performed. If desired, these messages can be turned off by answering no (N) when asked about the run time messages.

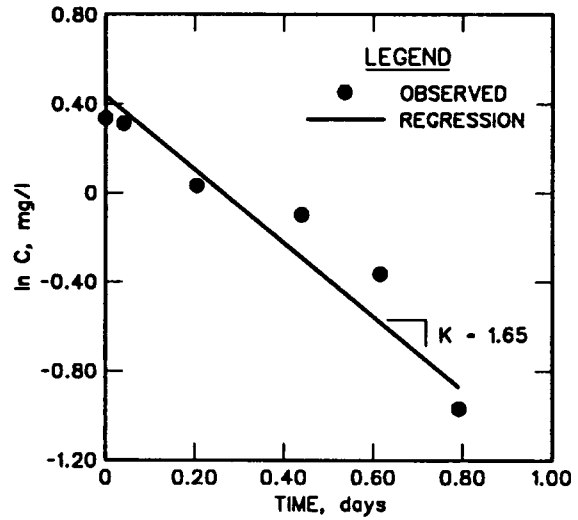
56. When the constituent options menu is exited, the first graphics screen appears and another selection can be made (Figure B33). The user selects E to exit from TWQM.

57. The plotting options for TPLLOT may be selected even if a printer is not attached to the computer. This program creates the plotting files, which are dumped to a printer. One file is created for each graph. These files are: TPTPLOT1.OUT, TPTPLOBS.OUT, FETPLOT1.OUT, MNTPLOT1.OUT, DOTPLOT1.OUT, FETPLOBS.OUT, MNTPLOBS.OUT, and DOTPLOBS.OUT. When the plotting option for TPLLOT is selected, these files are created but not sent to a printer. Once TWQB is complete, these files can be sent to a printer by typing HP2LJET fn.ft if an HP-compatible laser jet II printer is being used (Benton 1987). Other files are included with TPLLOT that allow for other printers to be used. For more information, refer to the TPLLOT user's manual.

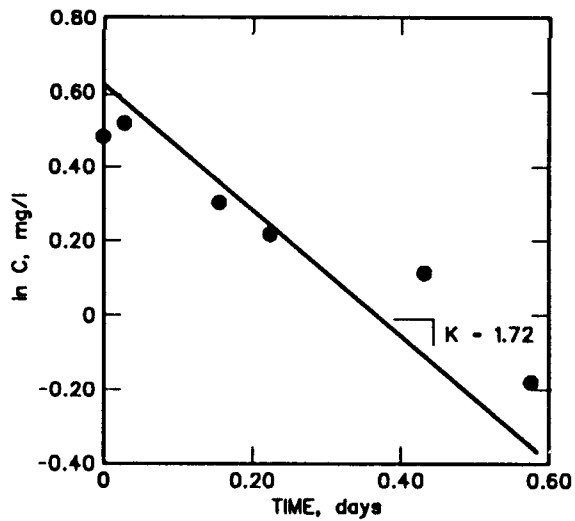
APPENDIX C: KINETIC RATE REGRESSIONS



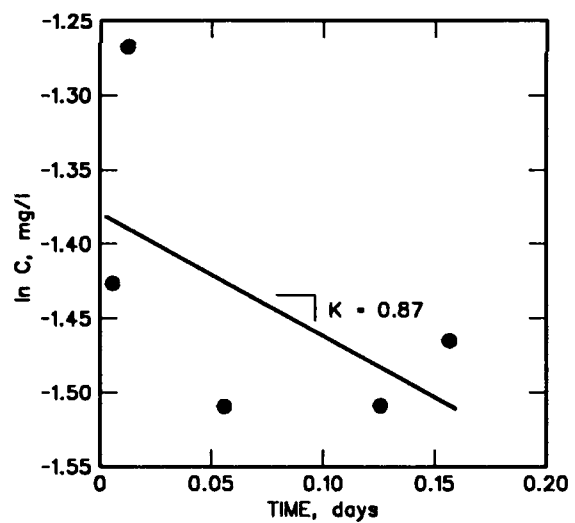
a. Duck River (data set 1), 43 cfs



b. Duck River (data set 2), 119 cfs

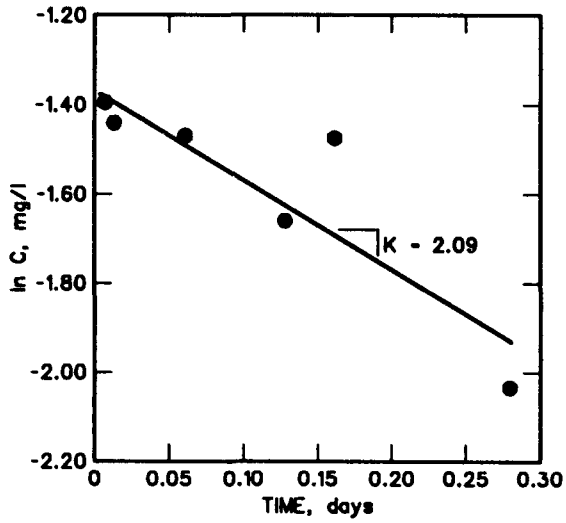


c. Duck River (data set 3), 182 cfs

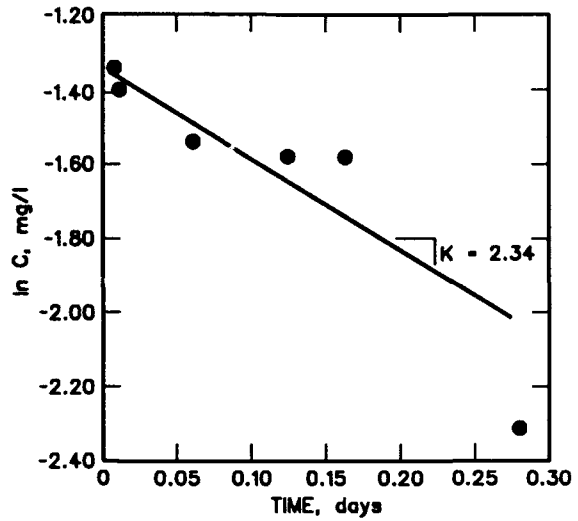


d. Little Missouri River (data set 1), 25 Jul 1983

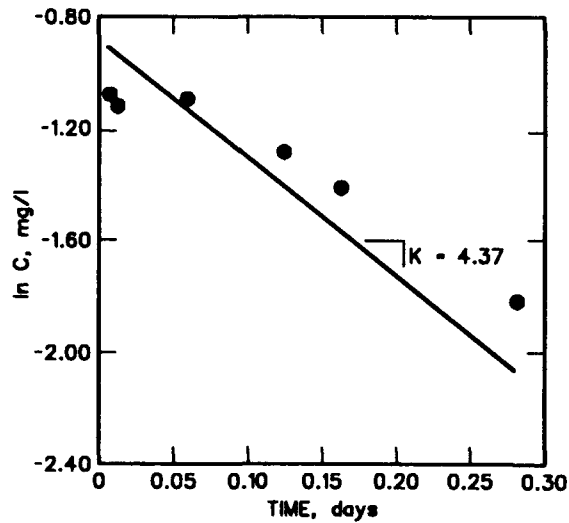
Figure C1. Regressions for dissolved manganese removal rate
(Sheet 1 of 6)



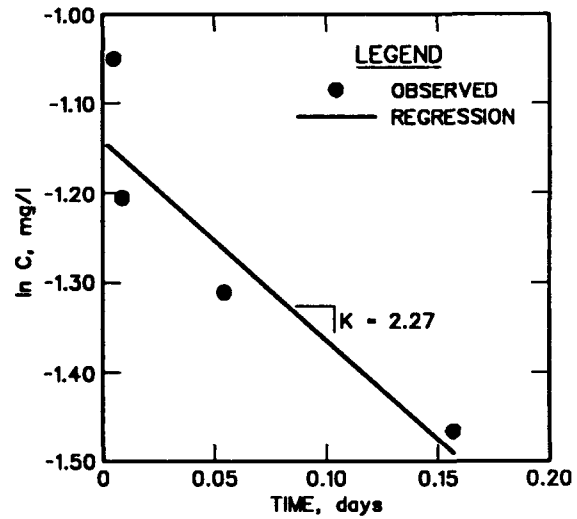
e. Little Missouri River (data set 2), 9 Aug 1983



f. Little Missouri River (data set 3) 17 Aug 1983

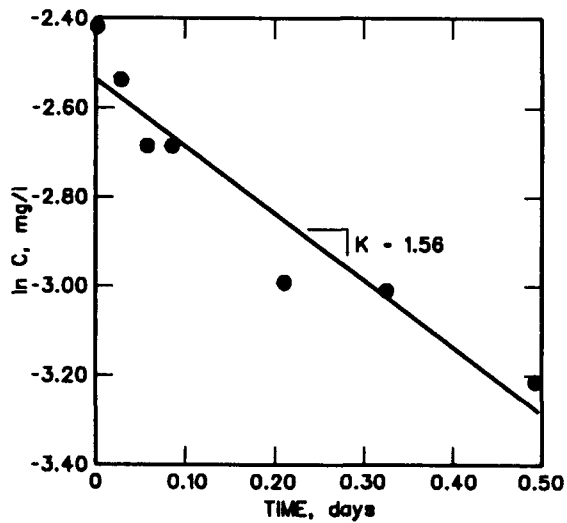


g. Little Missouri River (data set 4), 7 Sep 1983

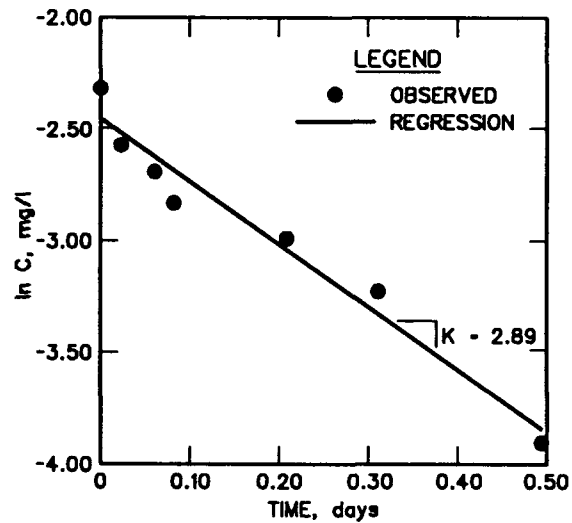


h. Little Missouri River (data set 5) 27 Oct 1983

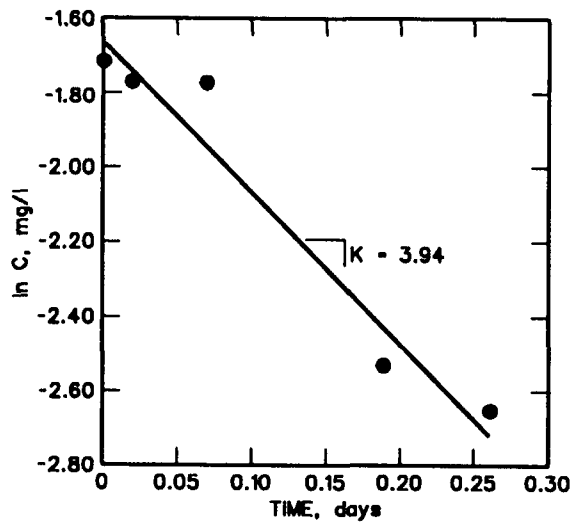
Figure C1. (Sheet 2 of 6)



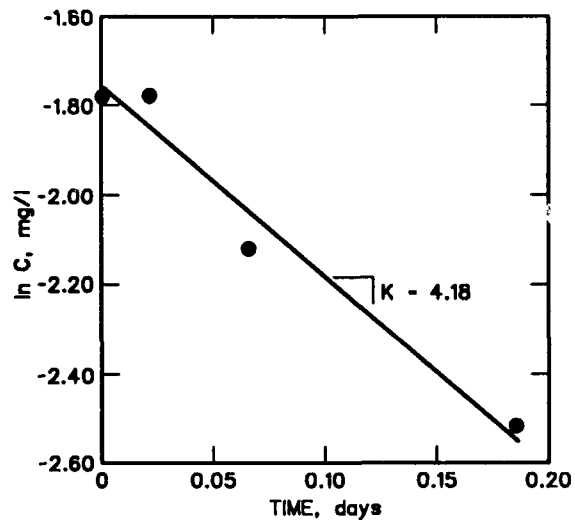
i. Little Missouri River time-of-travel sampling at 500 cfs (data set 6), 12 Sep 1987



j. Little Missouri River steady-state sampling at 500 cfs (data set 7), 12 Sep 1987

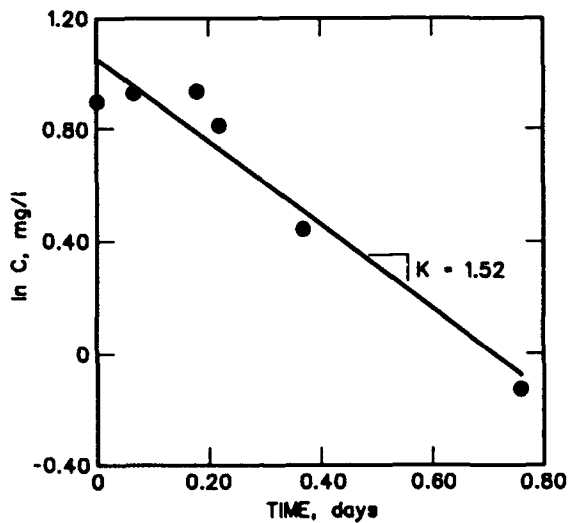


k. Little Missouri River time-of-travel sampling at 500 cfs (data set 8), 14 Oct 1987

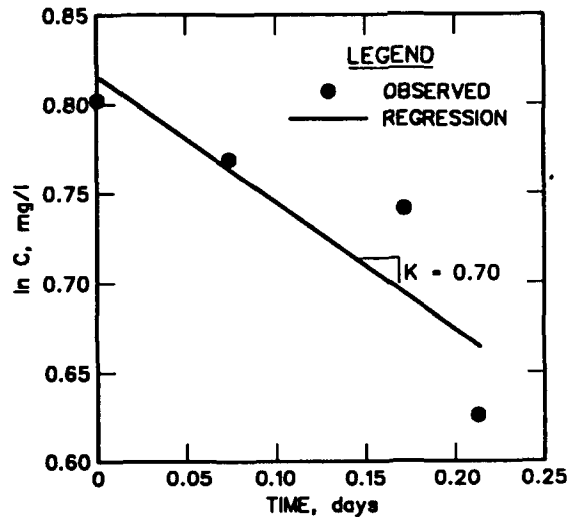


l. Little Missouri River steady-state sampling at 500 cfs (data set 9), 14 Oct 1987

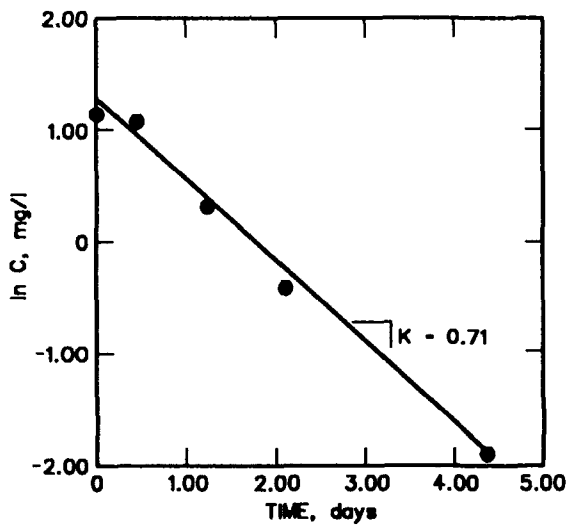
Figure C1. (Sheet 3 of 6)



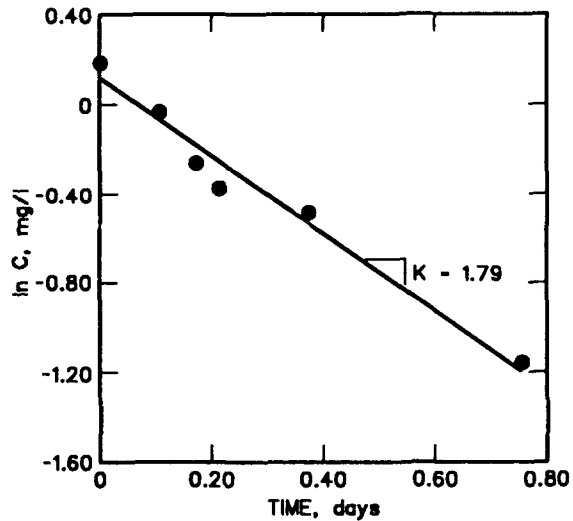
m. Fourche La Fave River steady-state sampling at 200 cfs data set 1), 20 Jul 1988



n. Fourche La Fave River time-of-travel sampling at 200 cfs (data set 2), 20 Jul 1988

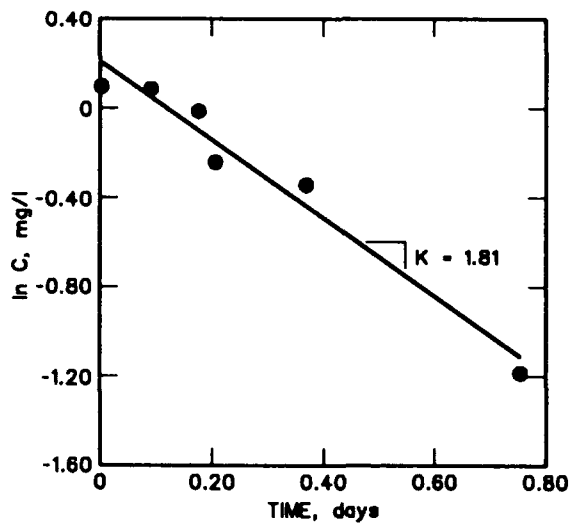


o. Fourche La Fave River low-flow steady-state sampling at 25 cfs (data set 3), 19 Jul 1988

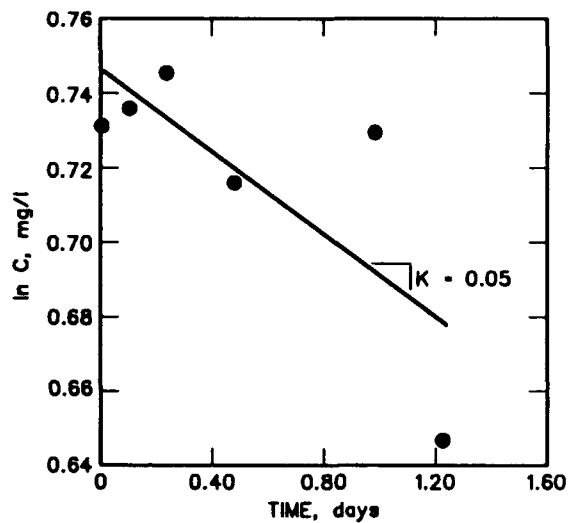


p. Fourche La Fave River steady-state sampling at 200 cfs (data set 4), 23 Aug 1989

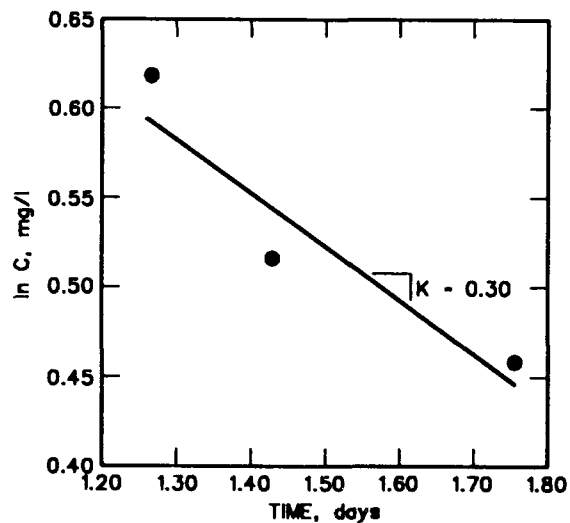
Figure C1. (Sheet 4 of 6)



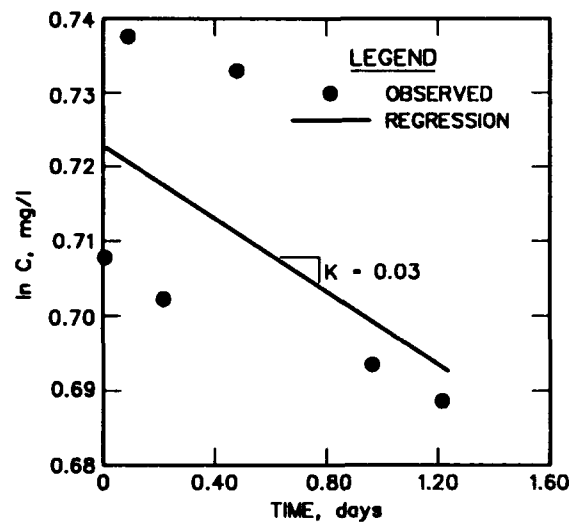
q. Fourche La Fave River steady-state sampling at 200 cfs (data set 5), 24 Aug 1989



r. Rough River upper reach time-of-travel sampling at 200 cfs (data set 1), 17 Aug 1988

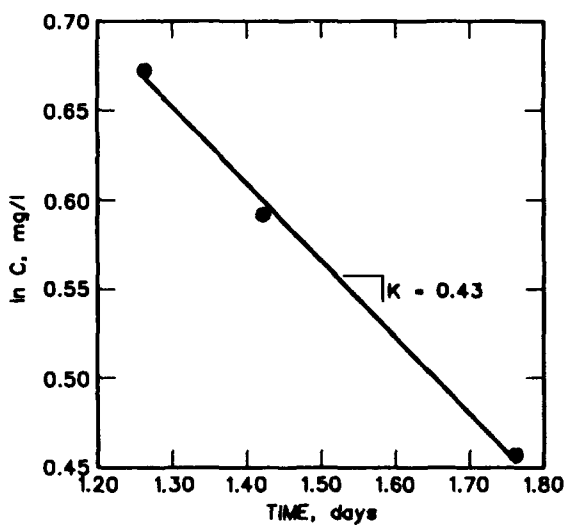


s. Rough River lower reach time-of-travel sampling at 200 cfs (data set 2), 19 Aug 1988

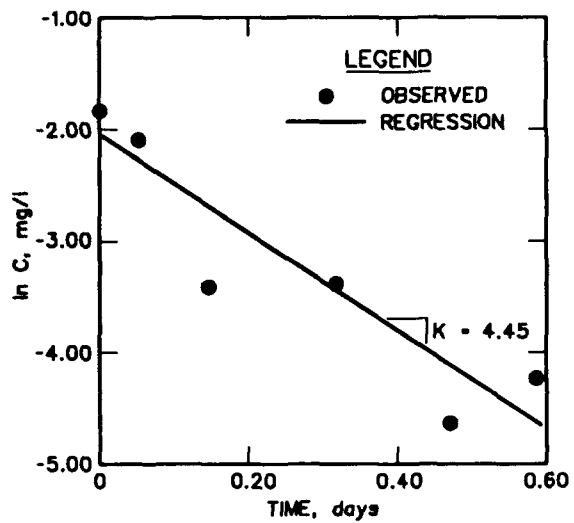


t. Rough River upper reaches steady-state sampling at 200 cfs (data set 3), 18 Aug 1988

Figure C1. (Sheet 5 of 6)

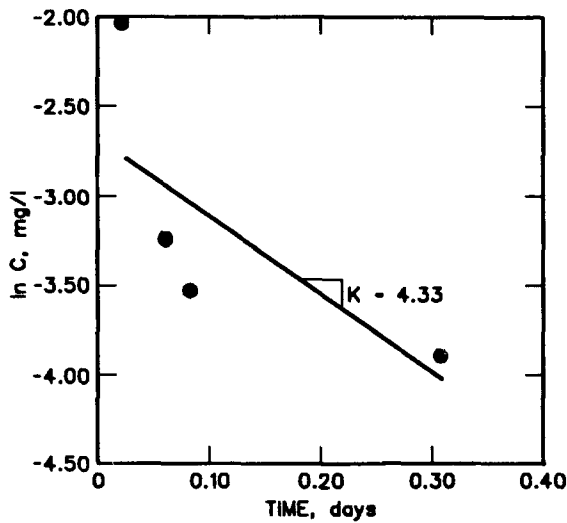


u. Rough River lower reaches steady-state sampling at 200 cfs (data set 4), 18 Aug 1988

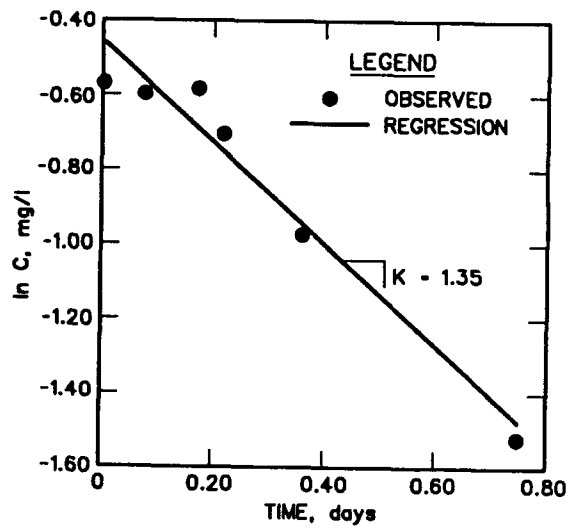


v. Guadalupe River steady-state sampling at 114 cfs, 19 Sep 1988

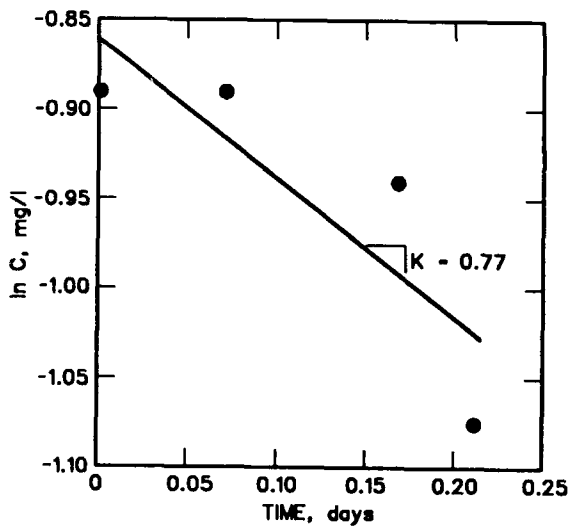
Figure C1. (Sheet 6 of 6)



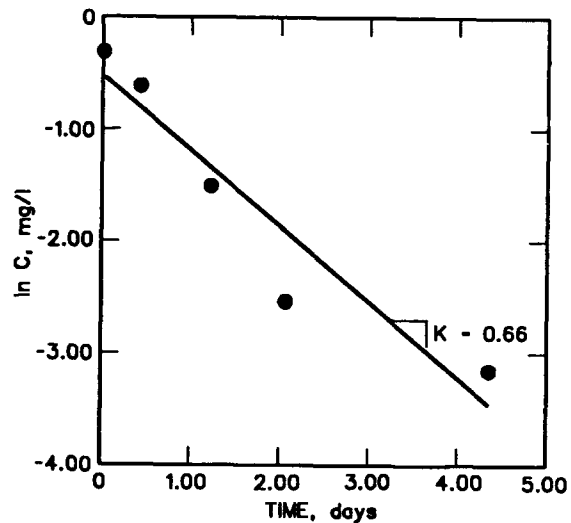
a. Little Missouri River time-of-travel sampling at 500 cfs
12 Sep 1987



b. Fourche La Fave River steady-state sampling at 200 cfs (data set 1), 20 Jul 1988

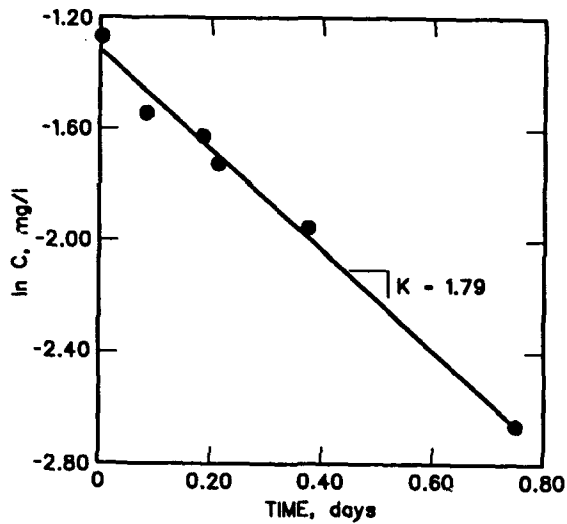


c. Fourche La Fave River time-of-travel sampling at 200 cfs (data set 2), 20 Jul 1988

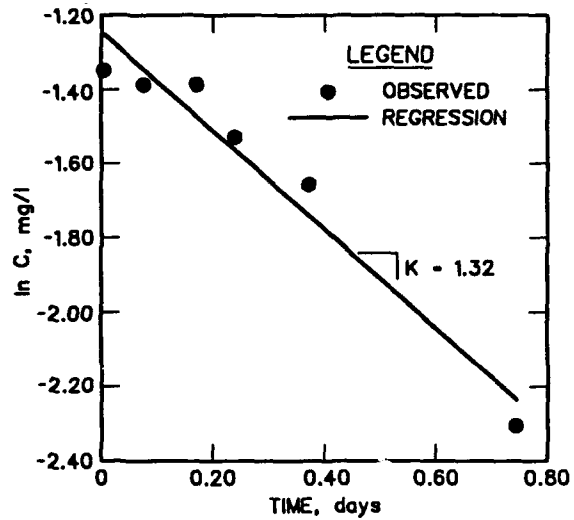


d. Fourche La Fave River steady-state sampling at 20 cfs (data set 3), 19 Jul 1988

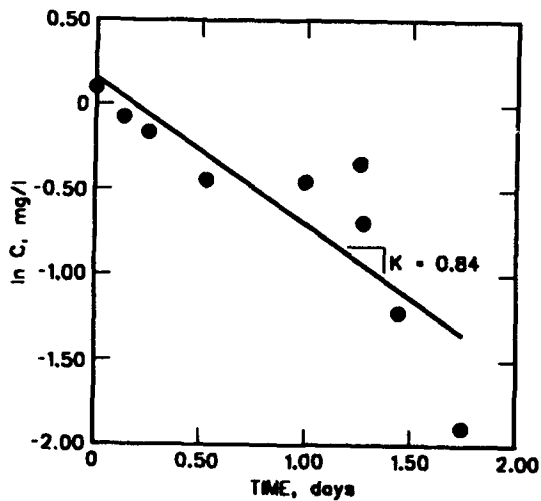
Figure C2. Regressions for ammonia nitrogen removal rate
(Sheet 1 of 3)



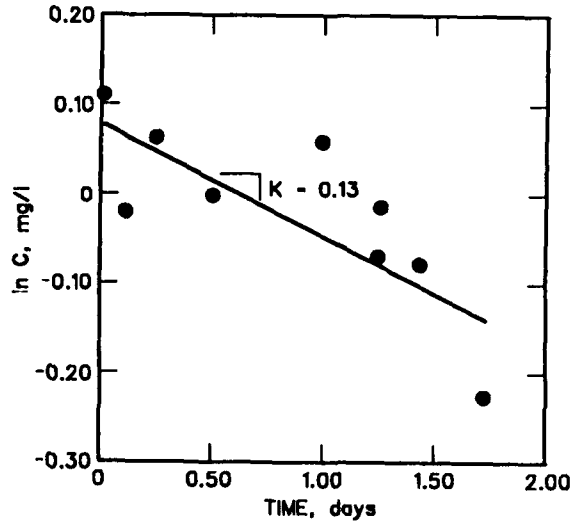
e. Fourche La Fave River steady-state sampling at 200 cfs (data set 4), 24 Aug 1989



f. Fourche La Fave River time-of-travel sampling at 200 cfs (data set 5), 23 Aug 1989

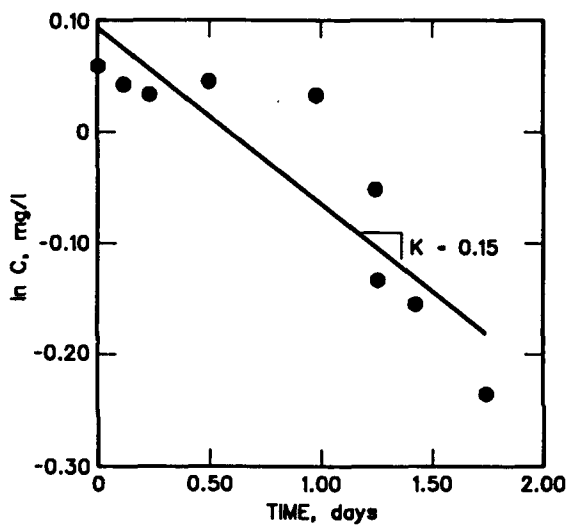


g. Rough River steady-state sampling at 20 cfs (data set 1) 16 Aug 1988

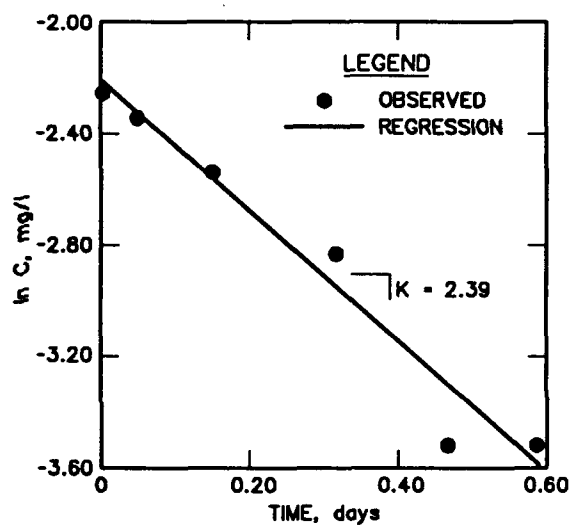


h. Rough River time-of-travel sampling at 200 cfs (data set 2) 17 Aug 1988

Figure C2. (Sheet 2 of 3)



i. Rough River steady-state sampling at 200 cfs (data set 3), 18 Aug 1988



j. Guadalupe River steady-state sampling at 114 cfs, 19 Sep 1989

Figure C2. (Sheet 3 of 3)

APPENDIX D: NOTATION

APPENDIX D: NOTATION

a	Regression coefficient, dimensionless
	Coefficient of flow for K_2
A	Bottom planar area
A_s	Surface area of the bed control volume, m^2
b	Exponent of flow for K_2
c	Escape coefficient, 1/ft
C	Constituent concentration
	Mn^{+2} observed at downstream station, mg/l
C_b	Concentration of reduced manganese or iron sulfide in the bed, mg/l
C_0	Initial (release) Mn^{+2} concentration, mg/l
C_s	Concentration of H_2S in the stream
d	Average stream depth, ft
D	Longitudinal dispersion
$DO_{1/2}$	Dissolved oxygen half-saturation constant, mg/l
DO_{25}	Molecular diffusion coefficient of Mn^{+2} at 25 °C, $6.88 \times 10^{-6} \text{ cm}^2/\text{sec}$
D_m	Molecular diffusion coefficient, ft^2/day
D_n	Numerical dispersion for steady-state conditions, L^2/T
D_s	Stream dispersion, L^2/T
D_T	Molecular diffusion coefficient of Mn^{+2} at stream temperature T, cm^2/sec
D^o	Molecular diffusivity of DO, cm^2/sec
D^s	Molecular diffusivity of H_2S , cm^2/sec
[Fe(II)]	Concentration of ferrous iron, moles/l
(FeS)	Iron sulfide concentration, mg/l
FRACT	Fraction of total dissolved sulfide as H_2S
g	Gravitational acceleration, L/T^2
H	Hydraulic depth, ft/ft
[H^+]	Hydrogen ion concentration, moles/l
J	Volatilization, mg
k	Heterogeneous reaction rate, $day^{-1} (\text{moles}/l)^{-4}$
k_{Fe}	$3.0 \times 10^{-12} \text{ moles}/l \text{ min}^{-1}$ at 20 °C
k_{FeS}	First-order sulfide oxidation rate, day^{-1}
k_s	Sulfide oxidation rate, day^{-1}
$(k_s)_{20}$	Oxidation rate at 20 °C

k_0	Homogeneous reaction rate, $\text{day}^{-1} (\text{moles}/\ell)^{-3}$
K	Reaction coefficient
K_a	Nitrification rate, day^{-1}
K_b	Oxidation rate of reduced manganese or iron sulfide in the bed, 1/day
K_{Fe}	Overall reaction rate for ferrous iron
K_{Mn}	First-order removal rate for Mn^{+2} Mn^{+2} loss rate for a specific field condition, 1/day
K_s	Volatilization rate of H_2S , day^{-1}
K_T	Reaction rate at temperature T
K_2	DO stream reaeration rate, day^{-1}
K_{20}	Reaction rate at 20 °C
Mn	Dissolved (reduced) manganese concentration, mg/ℓ
Mn_b	Reduced manganese concentration in sediment pore water, mg/ℓ
[Mn(II)]	Dissolved (reduced) manganese concentration, moles/ℓ
[Mn(IV)]	Particulate (oxidized) manganese concentration, moles/ℓ
M^o	Molecular weight of DO, g/mole
M^s	Molecular weight of H_2S , g/mole
n	Manning's coefficient
[OH ⁻]	Hydroxide ion concentration, moles/ℓ
P	Point load
P_0	Partial pressure of oxygen, atm
Q	Flow rate
s	Water surface or streambed slope, nondimensional
S	Rate of change in concentration resulting from transformation or chemical reactions
	Sulfide concentration in the form of HS^- , mg/ℓ
Sc	Schmidt number (ν/D), nondimensional
S_e	Slope of energy gradient
S_o	Slope of streambed, ft/ft
t	Travel time to station, days
T	Ambient stream temperature, °C
t_f	Flow time through reach, days
u	Average stream velocity, m/sec
u_*	Shear velocity (\sqrt{gHs}), L/T
U	Stream mean velocity
V	Control volume of fixed volume

V_b	Volume of bed control volume, m^3
V_s	Mass transfer velocity across diffusive sublayer separating water and substrate, L/T
V_{sm}	Measured mass transfer rate, L/T
V_{sc}	Mass transfer coefficient computed with Equation 25, L/T
w	Loading rate (i.e., mass transfer rate or settling rate) to bed, m/day
W	Top width of stream, m Stream withdrawal in TWQM input
W_s	Settling rate of FeS, m/day
x	Distance downstream
X	pH of stream
α	Statistical error bound in analytical solution of 1-D transport Stoichiometric conversion factors
Δh	Change in water surface elevation in reach, ft
ΔSOD	Additional SOD resulting from manganese or iron sulfide oxidation in bed, $g O_2/(m^2/day)$
Δx	Computational element length, m
θ	Temperature correction constant
ν_{25}	Kinematic viscosity of water at 25 °C, $6.88 \times 10^{-6} cm^2/sec$
ν_T	Kinematic viscosity at stream temperature T , cm^2/sec

Waterways Experiment Station Cataloging-in-Publication Data

Dortch, Mark S.

Modeling water quality of reservoir tailwaters / by Mark S. Dortch, Dorothy H. Tillman, Barry W. Bunch ; prepared for Department of the Army, U.S. Army Corps of Engineers.

145 p. : ill. ; 28 cm. — (Technical report ; W-92-1)

Includes bibliographic references.

1. Water quality — Computer programs. 2. Reservoirs — Environmental aspects — Mathematical models. 3. Tailwater ecology. 4. Water — Aeration. I. Title. II. Tillman, Dorothy H. III. Bunch, Barry W. IV. United States. Army. Corps of Engineers. V. U.S. Army Engineer Waterways Experiment Station. VI. Water Quality Research Program. VII. Series: Technical report (U.S. Army Engineer Waterways Experiment Station) ; W-92-1.

TA7 W34 no.W-92-1